Modeling Cl_2 formation from aqueous NaCl particles: Evidence for interfacial reactions and importance of Cl_2 decomposition in alkaline solution

Eladio M. Knipping and Donald Dabdub

Department of Mechanical and Aerospace Engineering, University of California at Irvine, Irvine, California, USA

Received 23 May 2001; revised 14 February 2002; accepted 2 April 2002; published 27 September 2002.

[1] A series of experiments have demonstrated that a significant yield of chlorine gas is produced when mixtures of ozone and sodium chloride particles above their deliquescence point are irradiated at 254 nm. In order to obtain expressions for future modeling studies, a comprehensive model is used to analyze the system and to determine its sensitivity. This work reexamines and expands previous studies [*Knipping et al.*, 2000]. The enhanced model, described in detail herein, reaffirms that current known physical and chemical processes fail to reproduce the observed Cl_2 formation in the experiments. A methodological analysis, proposed as a framework for similar studies, of the physicochemical system supports the accountability of an overall mechanism initiated by the formation of a relatively stable complex of the hydroxyl radical and chloride ions at the gas–liquid interface for the observed chlorine generation. Different potential fates of the $OH\bullet\bullet\bullet Cl^{\bullet-}_{surface}$ intermediate are discussed. A rate expression and kinetic parameters are presented for the overall reaction of the interfacial mechanism. In addition, sensitivity studies underscore the importance of accurately modeling chlorine decomposition processes in alkaline solution—in particular, the reactions of chlorine with hydroxide, carbonate, and basic hydrogen peroxide. Recommended aqueous-phase rate constants for these reactions are drawn from a literature evaluation illustrating the limited availability and lack of agreement of related kinetic data. *INDEX TERMS:* 0305 Atmospheric Composition and Structure: Aerosols and particles (0345, 4801); 0312 Atmospheric Composition and Structure: Air/sea constituent fluxes (3339, 4504); 0317 Atmospheric Composition and Structure: Chemical kinetic and photochemical properties; 0365 Atmospheric Composition and Structure: Troposphere—composition and chemistry

Citation: Knipping, E. M., and D. Dabdub, Modeling Cl_2 formation from aqueous NaCl particles: Evidence for interfacial reactions and importance of Cl_2 decomposition in alkaline solution, *J. Geophys. Res.*, *107*(D18), 4360, doi:10.1029/2001JD000867, 2002.

1. Introduction

[2] The role of chlorine atoms as potential oxidants in the marine boundary layer and coastal urban areas has received a great deal of attention in recent years [*Keene et al.*, 1990, 1996, 1998; *Finlayson-Pitts*, 1993; *Pszenny et al.*, 1993; *Finlayson-Pitts and Pitts*, 2000; *Finlayson-Pitts and Hemminger*, 2001]. Laboratory and modeling studies have shown that photolabile chlorine-containing species are generated from several reactions involving sea salt particles [*Vogt et al.*, 1996; *Sander and Crutzen*, 1996; *Langer et al.*, 1997; *De Haan et al.*, 1999; *Weis and Ewing*, 1999; *Massucci et al.*, 1999; *Regimbal and Mozurkewich*, 2000]. In addition, intriguing evidence from field and laboratory studies indicates that aqueous sea salt particles serve as a potential source of molecular chlorine, Cl_2 [*Spicer et al.*, 1998; *Oum et al.*, 1998].

[3] *Spicer et al.* [1998] have detected concentrations of molecular chlorine in the marine boundary layer at levels higher than those expected from known reactions of sea salt particles. Using an atmospheric pressure chemical ionization mass spectrometer, Spicer et al. measured Cl_2 mixing ratios as high as 150 parts per trillion (ppt) during nighttime at a site off the mid-Atlantic coast of the United States. Using a photochemical box model, the investigators concluded that the observed Cl_2 levels could not be reconciled by known chemistry and inferred the presence of an unrecognized continuous chlorine source averaging up to 330 Cl_2 ppt day^{-1}. Whereas the peak Cl_2 concentrations measured by Spicer et al. are indicative of a nighttime mechanism for Cl_2 build-up, *Oum et al.* [1998] present evidence that could explain a daytime component for Cl_2 release from deliquesced sea salt aerosol.

[4] *Oum et al.* [1998] performed laboratory experiments in a modern aerosol chamber that identify Cl_2 as the product of the photolysis of ozone in the presence of deliquesced sea salt particles. The use of both synthetic sea salt and sodium chloride particles resulted in similar rates of Cl_2 production. The experiments are able to generate Cl_2 only when the particles are above their deliquescence point and the chamber contents are photolyzed; Cl_2 production is not observed

0148-0227/02/2001JD000867$09.00

either when the deliquesced particles and ozone remain in the dark or when the chamber contents are irradiated in the absence of ozone. Oum et al. report a small production of Cl_2 when "dry" sea salt particles are introduced into the chamber, attributed to reactions occurring on films of adsorbed water known to persevere on the surface of the particles. Additional experiments were performed in a clean 70 L Teflon reaction chamber in order to ensure that the observed Cl_2 production was not a consequence of some unknown chamber contaminant or artifact. Cl_2 formation was observed in conditions similar to those of the aerosol chamber.

[5] Oum et al. proposed a mechanism involving $OH^\bullet$ oxidation of the chloride ion, Cl^-, as the potential pathway for the observed Cl_2 production. Although this mechanism includes paths of chlorine production based on known bulk aqueous-phase chemistry, model simulations will show that it fails to reproduce observed Cl_2 values by as much as four orders of magnitude.

[6] There is increasing recognition that aqueous aerosol chemistry is not limited to bulk liquid-phase reactions. Laboratory studies have shown that Cl_2 reacts with bromide ions at aqueous aerosol interfaces, forming a surface complex species $(Cl_2\bullet Br)^-$ and leading to enhanced uptake of the gas [*Hu et al.*, 1995]. Additional experiments uphold similar conclusions for reactions of SO_2 with water at droplet surfaces [*Jayne et al.*, 1990; *Boniface et al.*, 2000]. Second harmonic generation and static surface tension measurements of SO_2 surface coverage support the hypothesis of SO_2 adsorption on liquid surfaces [*Donaldson et al.*, 1995].

[7] There is strong evidence suggesting that the underlying mechanism for the observed Cl_2 production in the aerosol chamber experiments may involve similar reactions occurring at the interface of deliquesced sodium chloride particles. Molecular dynamics simulations illustrate that chloride ions are much more prevalent than sodium ions at the surfaces of concentrated NaCl solutions. Furthermore, quantum chemical calculations predict that these chloride ions will attract reactive gases such as $OH^\bullet$ and O_3 [*Knipping et al.*, 2000; *Jungwirth and Tobias*, 2000]. The probability of these reactions is explored in this research.

[8] Clearly, the formation of molecular chlorine from the reaction of ozone with aqueous sea salt particles involves the simultaneous occurrence of a number of interrelated chemical and physical processes. In order to analyze the experimental results and explore the viability of different chemical reaction mechanisms, a new mathematical model simulating the physical and chemical processes within the experimental chamber used by *Oum et al.* [1998] is presented. The model incorporates a comprehensive mechanism of gas-phase and aqueous-phase chemical reactions in conjunction with a dynamic treatment of gas-phase to aqueous-phase mass transport. Furthermore, the model also considers reactions occurring at the gas–particle interface. Hence, the new model is named Model of Aqueous, Gaseous and Interfacial Chemistry, or MAGIC. Details of the model are presented herein, including the latest revisions.

[9] The results from MAGIC are analyzed in order to test various pathways for the observed Cl_2 formation. Once a suitable rationalization for the phenomena is reached, an appropriate mechanism and overall rate expression are developed. This mechanism should be subjected to further appraisal by complex atmospheric models such as MOCCA [*Sander and Crutzen*, 1996], CAPRAM [*Herrmann et al.*, 2000] and future expanded versions of MAGIC. As chlorine atoms, resulting from the subsequent photolysis of Cl_2, can affect the chemistry of the marine boundary layer and coastal regions, this mechanism will assist models in better determining the significance of chlorine chemistry in these regions. An added goal of this research is to appeal to the scientific community to further investigate alkaline chlorine decomposition processes found essential to the analysis of the physicochemical system at hand through a suite of sensitivity analyses.

2. Model Description

[10] The model developed for the current study simulates the conditions present in the aerosol chamber. A description of the aerosol chamber and experiments is found elsewhere [*De Haan et al.*, 1999; *Knipping et al.*, 2000]. Briefly, sodium chloride aerosol is introduced into a stainless-steel chamber, whose walls are coated with halocarbon wax to render them inert, at a relative humidity above its deliquescence point and at ambient temperature. Ozone is introduced into the chamber and Cl_2 production is measured using an atmospheric pressure ionization mass spectrometer after photolysis of the chamber contents.

[11] The model contains a comprehensive treatment of gas-phase and aqueous-phase chemical reactions, using the most recent kinetic data available, as well as mass transfer of species between the gas phase and the aqueous phase. We refer the reader to the seminal works of *Fuchs and Sutugin* [1971] and *Schwartz* [1986], as well as a recent review by *Sander* [1999], for a detailed overview of the modeling of gas-phase and aqueous-phase interactions.

[12] The steps involved in the dissolution, and subsequent aqueous-phase chemical reaction, of gas-phase species into droplets are well established in the literature [*Schwartz and Freiberg*, 1981; *Schwartz*, 1986; *Kumar*, 1989; *Lelieveld and Crutzen*, 1991]. These processes occur in parallel with chemical reaction in the gas phase and are summarized as follows:

1. Transport of the species from the gas phase toward the droplet gas–liquid interface.
2. Transfer of the species across the interface.
3. Possible hydrolysis and partial ionization of the species in the aqueous phase.
4. Diffusion of the ionic and nonionic species in the droplet.
5. Aqueous-phase chemical reaction.

[13] Steps 1–5 may also proceed in reverse order, potentially generating concentration gradients at the droplet interface that lead to the volatilization of species to the gas phase. In addition, MAGIC also considers reactions on the surface of the aerosol particles. These reactions are also assumed to occur in parallel with the physical and chemical processes described above.

2.1. Gas-Phase Chemistry

[14] The treatment of gas-phase chemical reactions in the model adheres to the recommendations made by the NASA/JPL evaluation panel [*DeMore et al.*, 1997; *Sander et al.*, 2000] which are in general agreement with the recommen-

Table 1. List of Species Included in the Model for Laboratory Simulations

Group	Gas phase	Aqueous phase
HO_x	$O(^1D)$, $O(^3P)$, $\mathbf{O_2}$, $\mathbf{O_3}$, $\mathbf{OH^\bullet}$, $\mathbf{HO_2^\bullet}$, $\mathbf{H_2O_2}$, H_2O	$O(^3P)$, $\mathbf{O_2}$, $\mathbf{O_3}$, $\mathbf{OH^\bullet}/O^{\bullet-}$, $\mathbf{HO_2^\bullet}/O_2^{\bullet-}$, $\mathbf{H_2O_2}/HO_2^-$, $HO_3^\bullet$, $O_3^{\bullet-}$, H^+/OH^-
ClO_x	$\mathbf{Cl_2}$, $\mathbf{Cl^\bullet}$, $\mathbf{HCl}$, $\mathbf{HOCl}$, $\mathbf{Cl_2O}$, $ClO^\bullet$, $OClO^\bullet$, $ClOO^\bullet$, Cl_2O_2	$\mathbf{Cl_2}$, $Cl^\bullet$, $Cl_2^{\bullet-}$, $\mathbf{HCl}/Cl^-$, $\mathbf{HOCl}/ClO^-$, $\mathbf{Cl_2O}$, $HOClH^\bullet$, $HOCl^{\bullet-}$
CO_2	$\mathbf{CO_2}$	$\mathbf{CO_2 \bullet H_2O}/HCO_3^-/CO_3^{2-}$, $HCO_3^\bullet/CO_3^{\bullet-}$
Other	N_2	Na^+

Species in bold are transferred between the aqueous phase and the gas phase.

dations made by the IUPAC panel [*Atkinson et al.*, 1997, 2000]. Table 1 lists the species considered in the gas and aqueous phase during these simulations.

[15] Low-pressure mercury lamps used in the experiments were chosen because their primary emission line, at a wavelength, λ, of 254 nm, photolyzes ozone but not Cl_2. The photolysis rates, j, of the gas-phase species (see Table 2) are evaluated by first experimentally determining the photolysis rate of ozone in the aerosol chamber. The photolysis rates for all other species are then computed by taking the ratio of the absorption cross section of the species with respect to the absorption cross section of ozone at $\lambda = 254$ nm and multiplying the ozone photolysis rate by this value. The relative quantum yields at 254 nm are also considered. Some Cl_2 is observed to photolyze due to weaker emission lines (e.g., 313 and 365 nm). The rate of the resulting Cl_2 photolysis in the chamber is quantified experimentally and included in the model. The kinetic data for gas-phase chemical reactions of interest for the chamber studies are presented in Table 3.

2.2. Activity Coefficients

[16] Long-range and short-range electrostatic forces, or interactions, between ions affect the reactivity of species in concentrated ionic solutions. The ionic strength, I, represents the appropriate measure of the total ion concentration of a solution taking into account these effects,

$$I = \frac{1}{2}\sum_i m_i z_i^2 \tag{1}$$

where m and z are the molality and valence of species i, respectively [*Debye and Hückel*, 1923].

[17] The activity of a solute and its concentration are related by activity coefficients, γ. Several methods exist for calculating activity coefficients in ionic solutions [*Kim et al.*, 1993]. The 1991 Pitzer ion interaction model [*Pitzer*, 1991] is used in this study. The Pitzer interaction model has been validated to calculate activity coefficients in multicomponent solutions with ionic strengths up to 6 mol kg^{-1}. This limit may restrict the modeling of highly concentrated atmospheric aerosol but it does not hinder its applicability in this study as this value is above that for saturation of NaCl in water. The Pitzer model can also be expanded to calculate the activity coefficients of neutral solutes, such as CO_2 and O_2, in ionic solutions [*Clegg and Brimblecombe*, 1990].

[18] Pitzer ion interaction data are available for a limited number of possible solutes, representing the salts most prevalent in atmospheric aerosol. The model calculates activity coefficients explicitly for the species H^+, Na^+, Cl^-, HCO_3^-, CO_3^{2-}, OH^-, CO_2, and O_2. For other species, either a Guggenheim approximation of the Debye–Hückel limiting law [*Pethybridge and Prue*, 1972],

$$-\log \gamma_i = \frac{A z_i^2 I^{1/2}}{1 + I^{1/2}}, \tag{2}$$

is employed, where A is the Debye–Hückel constant for activity coefficient, 0.509 (kg $mol^{-1})^{1/2}$ at 298 K, or, in the case of neutral solutes, activity coefficients are calculated using the approximation [*Moldanova and Ljungstrom*, 2001]:

$$\log \gamma_i = 0.1 I. \tag{3}$$

2.3. Mass Transfer

[19] In order to quantify the limitations to mass transport imposed by these physical processes, the mass transfer coefficient, k_{mt}, developed by *Schwartz* [1986] is employed. The mass transfer coefficient is effectively a first-order rate constant that determines the steady state rate by which a gas enters (or escapes) a droplet in response to (spatially averaged) chemical reaction loss and production within the bulk solution, $\langle R_{aq} \rangle$, namely,

$$k_{mt}\left(C_{g,\infty} - \frac{C_{aq,s}}{H^* \mathrm{R} T}\right) = \langle R_{aq} \rangle \tag{4}$$

where

$$k_{mt} = \left[\frac{R_p^2}{3D_g} + \frac{4R_p}{3\bar{c}\alpha}\right]^{-1} \tag{5}$$

and $C_{g,\infty}$ and $C_{aq,s}$ represent the bulk gas-phase and surface aqueous-phase concentration of the species of interest, H^* is the effective Henry's law constant, R is the universal gas constant and T denotes absolute temperature. The droplet radius is denoted by R_p, while D_g, $\bar{c}$ and α represent the gas-phase diffusivity, mean molecular speed and accommodation coefficient for the species of interest, respectively. The value of droplet radius is found using a quasi-size-dependent approach [*Sander and Crutzen*, 1996]. Mathematically, k_{mt} represents the sum in series of the resistances to uptake due to gas-phase diffusion and interfacial mass transport.

[20] Although Henry's law equilibrium is not imposed in the model, the rate of mass transfer to and from the gas

Table 2. Gas-Phase Photolysis Rates

No.	Reaction	σ ($\lambda = 254$ nm) $\times 10^{20}$ cm^2	Φ	j_{298} s^{-1}
1	$O_3 + h\nu \rightarrow O(^3P) + O_2$	1150	0.1	4.50×10^{-4}
2	$O_3 + h\nu \rightarrow O(^1D) + O_2$	1150	0.9	4.05×10^{-3}
3	$H_2O_2 + h\nu \rightarrow OH^\bullet + OH^\bullet$	6.7	1.0	2.62×10^{-5}
4	$HOCl + h\nu \rightarrow OH^\bullet + Cl^\bullet$	14.6	1.0	5.71×10^{-5}
5	$Cl_2 + h\nu \rightarrow Cl^\bullet + Cl^\bullet$	0.0	–	1.0×10^{-4}[a]
6	$OClO^\bullet + h\nu \rightarrow ClO^\bullet + O(^3P)$	0.0	–	0
7	$Cl_2O_2 + h\nu \rightarrow ClOO^\bullet + Cl^\bullet$	544.5	1.0	2.13×10^{-3}
8	$Cl_2O + h\nu \rightarrow Cl^\bullet + ClO^\bullet$	193	1.0[b]	7.55×10^{-4}

Absorption cross sections: *DeMore et al.* [1997].
[a] Measured in chamber.
[b] Estimated.

Table 3. Gas-Phase Chemical Mechanism

No.	Reaction	Order	A	E/R	k_{298}[2]
9	$O(^1D) + O_2 \rightarrow O(^3P) + O_2$	2	3.2×10^{-11}	−70	4.0×10^{-11}
10	$O(^1D) + O_3 \rightarrow O_2 + O_2$	2	1.2×10^{-10}	0	1.2×10^{-10}
11	$O(^1D) + O_3 \rightarrow O(^3P) + O(^3P) + O_2$	2	1.2×10^{-10}	0	1.2×10^{-10}
12	$O(^1D) + H_2O \rightarrow OH^\bullet + OH^\bullet$	2	2.2×10^{-10}	0	2.2×10^{-10}
13	$O(^1D) + N_2 \rightarrow O(^3P) + N_2$	2	1.8×10^{-11}	−110	2.6×10^{-11}
14	$O(^3P) + O_2 + M \rightarrow O_3 + M$	2			1.5×10^{-14}
15	$O(^3P) + O_3 \rightarrow O_2 + O_2$	2	8.0×10^{-12}	2060	8.0×10^{-15}
16	$O(^3P) + HO_2^\bullet \rightarrow OH^\bullet + O_2$	2	3.0×10^{-11}	−200	5.9×10^{-11}
17	$O(^3P) + H_2O_2 \rightarrow OH^\bullet + HO_2^\bullet$	2	1.4×10^{-12}	2000	1.7×10^{-15}
18	$O_3 + OH^\bullet \rightarrow HO_2^\bullet + O_2$	2	1.6×10^{-12}	940	6.8×10^{-14}
19	$OH^\bullet + OH^\bullet \rightarrow O(^3P) + H_2O$	2	4.2×10^{-12}	240	1.9×10^{-12}
20	$OH^\bullet + OH^\bullet + M \rightarrow H_2O_2 + M$	3			5.9×10^{-12}
21	$OH^\bullet + HO_2^\bullet \rightarrow O_2 + H_2O$	2	4.8×10^{-11}	−250	1.1×10^{-10}
22	$H_2O_2 + OH^\bullet \rightarrow HO_2^\bullet + H_2O$	2	2.9×10^{-12}	160	1.7×10^{-12}
23	$O_3 + HO_2^\bullet \rightarrow OH^\bullet + O_2 + O_2$[2]	2	1.1×10^{-14}	500	2.0×10^{-15}
24	$HO_2^\bullet + HO_2^\bullet \rightarrow H_2O_2 + O_2$[2]	2	2.3×10^{-13}	−600	1.7×10^{-12}
25	$HO_2^\bullet + HO_2^\bullet + M \rightarrow H_2O_2 + O_2 + M$[2]	3	1.7×10^{-33} [M]	−1000	4.9×10^{-32} [M]
26	$O(^3P) + ClO^\bullet \rightarrow Cl^\bullet + O_2$	2	3.0×10^{-11}	−70	3.8×10^{-11}
27	$O(^3P) + OClO^\bullet \rightarrow ClO^\bullet + O_2$	2	2.4×10^{-12}	960	1.0×10^{-13}
28	$O(^3P) + HCl \rightarrow Cl^\bullet + OH^\bullet$	2	1.0×10^{-11}	3300	1.5×10^{-16}
29	$O(^3P) + HOCl \rightarrow ClO^\bullet + OH^\bullet$	2	1.7×10^{-13}	0	1.7×10^{-13}
30	$OH^\bullet + Cl_2 \rightarrow Cl^\bullet + HOCl$	2	1.4×10^{-12}	900	6.7×10^{-14}
31	$OH^\bullet + ClO^\bullet \rightarrow HCl + O_2$	2	1.5×10^{-12}	−120	2.2×10^{-12}
32	$OH^\bullet + ClO^\bullet \rightarrow HO_2^\bullet + Cl^\bullet$	2	9.5×10^{-12}	−120	1.4×10^{-11}
33	$OH^\bullet + OClO^\bullet \rightarrow HOCl + O_2$	2	4.5×10^{-13}	−800	6.8×10^{-12}
34	$OH^\bullet + HCl \rightarrow Cl^\bullet + H_2O$	2	2.6×10^{-12}	350	8.0×10^{-13}
35	$OH^\bullet + HOCl \rightarrow ClO^\bullet + H_2O$	2	3.0×10^{-12}	500	5.0×10^{-13}
36	$HO_2^\bullet + Cl^\bullet \rightarrow HCl + O_2$	2	1.8×10^{-11}	−170	3.2×10^{-11}
37	$HO_2^\bullet + Cl^\bullet \rightarrow OH^\bullet + ClO^\bullet$	2	4.1×10^{-11}	450	9.1×10^{-12}
38	$HO_2^\bullet + ClO^\bullet \rightarrow HOCl + O_2$	2	4.8×10^{-13}	−700	5.0×10^{-12}
39	$O_3 + Cl^\bullet \rightarrow ClO^\bullet + O_2$	2	2.9×10^{-11}	260	1.2×10^{-11}
40	$H_2O_2 + Cl^\bullet \rightarrow HO_2^\bullet + HCl$	2	1.1×10^{-11}	980	4.1×10^{-13}
41	$Cl^\bullet + OClO^\bullet \rightarrow ClO^\bullet + ClO^\bullet$	2	3.4×10^{-11}	−160	5.8×10^{-11}
42	$Cl^\bullet + HOCl \rightarrow OH^\bullet + Cl_2$	2	2.5×10^{-12}	130	1.6×10^{-12}
43	$ClO^\bullet + ClO^\bullet \rightarrow Cl_2 + O_2$	2	1.0×10^{-12}	1590	4.8×10^{-15}
44	$ClO^\bullet + ClO^\bullet \rightarrow ClOO^\bullet + Cl^\bullet$	2	3.0×10^{-11}	2450	8.0×10^{-15}
45	$ClO^\bullet + ClO^\bullet \rightarrow Cl^\bullet + Cl^\bullet + O_2$	2	3.5×10^{-13}	1370	3.5×10^{-15}
46	$ClO^\bullet + ClO^\bullet + M \rightarrow Cl_2O_2 + M$	3	See notes		3.4×10^{-13}
47	$Cl^\bullet + O_2 + M \rightarrow ClOO^\bullet + M$	3	See notes		6.7×10^{-14}
48	$Cl^\bullet + ClOO^\bullet \rightarrow Cl_2 + O_2$	2	2.3×10^{-10}	0	2.3×10^{-10}
49	$Cl^\bullet + ClOO^\bullet \rightarrow ClO^\bullet + ClO^\bullet$	2	1.2×10^{-11}	0	1.2×10^{-11}
50	$Cl_2O_2 + M \rightarrow ClO^\bullet + ClO^\bullet + M$	2	See notes		47
51	$ClOO^\bullet + M \rightarrow Cl^\bullet + O_2 + M$[3]	2	See notes		2.7×10^{7}
52	$ClO^\bullet + O_3 \rightarrow ClOO^\bullet + O_2$	2			$<1.4 \times 10^{-17}$
53	$ClO^\bullet + O_3 \rightarrow OClO^\bullet + O_2$[3]	2			$<1.0 \times 10^{-18}$
54	$Cl_2O + H_2O \rightarrow HOCl + HOCl$[3]	2			$<4.5 \times 10^{-23}$
55	$HOCl + HOCl \rightarrow Cl_2O + H_2O$[3]	2			$<5.5 \times 10^{-22}$
56	$Cl_2O + Cl^\bullet \rightarrow Cl_2 + ClO^\bullet$	2	6.2×10^{-11}	−130	9.6×10^{-11}
57	$Cl_2O + O(^3P) \rightarrow ClO^\bullet + ClO^\bullet$	2	2.7×10^{-11}	530	4.6×10^{-12}
58	$Cl_2O + ClO^\bullet \rightarrow Cl_2 + ClOO^\bullet$	2			4.3×10^{-16}
59	$Cl_2O + ClO^\bullet \rightarrow Cl_2 + Cl^\bullet + O_2$	2			2.7×10^{-15}
60	Cl_2 + Wall → Loss	1			1.0×10^{-4}
61	HOCl + Wall → Loss	1			1.0×10^{-3}

Adapted from the works of *DeMore et al.* [1997] and *Sander et al.* [2000], except for (54)–(55) [*Knauth et al.*, 1979], (58)–(59) [*Basco and Dogra*, 1971], and (60)–(61) measured directly in the chamber. k_{54} was measured at 323 K. $k_{55} = k_{54}/K_{Cl_2O+H_2O}$ at 298 K. $K_{Cl_2O+H_2O}$ at 298 K = 0.082 [*Knauth et al.*, 1979]. [M] represents the number of molecules cm^{-3} of air. The rate constants for bimolecular reactions are given by $k = A \exp(-E/RT)$, where A is the Arrhenius factor in cm^3 $molecule^{-1}$ s^{-1} and E/R is the "activation temperature" in K. The rate constants for termolecular reactions (except for (25)) and thermal decomposition are calculated using the methods described by *DeMore et al.* [1997]. (1) The tabulated rate constants for termolecular reactions are the effective second-order rate constants assuming air at 1 atm as the third body. The photolysis and thermal decomposition rates (reactions (1)–(8) and (50)–(51)) are given in s^{-1}. (2) The overall rate constant for the reaction of self reaction of $HO_2^\bullet$ is given by the sum of rates (24) and (25) multiplied by the factor: $1 + 1.4 \times 10^{-21}$ $[H_2O] \exp(2200/T)$. (3) The rate constants for (52)–(55) are taken to match the upper limits.

phase and aqueous phase is determined in effect by the deviation from Henry's law at the surface with respect to the bulk gas-phase concentration. Given that the concentration of an electrolytic species and its dissociation products are tracked by the model's algorithm as a single entity, the overall (effective) Henry's law constant is used in the rate equations for mass transfer for the acid/base groups.

[21] In concentrated solutions, the activity of neutral species must also be considered when evaluating Henry's law constants. Calculation of a Henry's law constant for nonelectrolytes transported between the gas phase and

Table 4. Physical Solubility (Henry's Law) Constants and Accommodation Coefficients

Species	H_{298}	$-\Delta H/R$	Reference	α	Reference
	M atm^{-1}	K			
O_3	0.011	2300	*Kozak-Channing and Heltz* [1983]	0.002	*DeMore et al.* [1997]
O_2	1.3×10^{-3}	1500	*Wilhelm et al.* [1977]	0.01	*Sander and Crutzen* [1996]$^{(E)}$
$OH^{\bullet}$	30	4500	*Hanson et al.* [1992]	0.1	*Takami et al.* [1998]
$HO_2^{\bullet}$	2.0×10^3		*Schwartz* [1984]	0.1	*Hanson et al.* [1992]
H_2O_2	1.0×10^5	6300	*Lind and Kok* [1994]	0.1	*DeMore et al.* [1997]
HCl	1.1	2000	*Marsh and McElroy* [1985]	0.064	*DeMore et al.* [1997]
HOCl	930		*Blatchley et al.* [1992]	0.056	*Sander and Crutzen* [1996]$^{(E)}$
Cl_2	0.091	2500	*Wilhelm et al.* [1977]	0.07	*Hu et al.* [1995]
Cl_2O	17	1800	*Wilhelm et al.* [1977]	0.1	Estimated
CO_2	0.034	2400	*Sillen and Martell* [1964]	0.01	Estimated

The temperature dependence for the Henry's law equilibrium constants is given by $H(T) = H_{298}\exp[(1/298 - 1/T) \times \Delta H/R]$ where ΔH is the enthalpy of dissolution. $^{(E)}$: estimated value.

aqueous phase is equivalent to determining the extent of salting-out as described in other environmental disciplines by Sechenow coefficients. Thus, for a nonelectrolytic species, the effective Henry's law constant is simply,

$$H^* = \left\{\frac{1}{\gamma_A}\right\}H. \tag{6}$$

For a monoprotic electrolyte, the overall solubility of the gas-phase species HA is given by

$$H^* = \left\{\frac{1}{\gamma_{HA}} + \frac{K_a}{\gamma_{A^-}\gamma_{H^+}[H^+]}\right\}H \tag{7}$$

where K_a is the association/dissociation equilibrium constant. A similar expression can be derived for diprotic acids that dissociate sequentially in solution. A complete overview on the application of Henry's law coefficients in multiphase models is offered by *Sander* [1999].

[22] The accommodation coefficient, α, represents the probability of a collision of a gas-phase species with a droplet leading to successful transfer of the species from the gas phase to the aqueous phase. In general, the accommodation coefficient cannot be measured explicitly in the laboratory; rather, the overall uptake coefficient, also denoted by γ, is measured. The accommodation coefficient is decoupled from the other resistances to the overall uptake by applying models based on electrical circuit analogy [*Jayne et al.*, 1990; *Hu et al.*, 1995; *Davidovits et al.*, 1995; *Hanson*, 1997]. These uptake resistance models, as well as the treatment of mass transfer processes in MAGIC, have a similar basis as the work of *Schwartz* [1986]. The reader is referred elsewhere for further discussion on accommodation and uptake coefficients [*DeMore et al.*, 1997; *Finlayson-Pitts and Pitts*, 2000]. Table 4 provides values of the physical Henry's law constants and accommodation coefficients used in the present study.

2.4 Aqueous-Phase Chemistry

[23] The rates of aqueous-phase chemical reactions are selected from a compilation of the most recent kinetic data available. An initial mechanism is developed from the NIST database of solution-phase chemistry [*Ross et al.*, 1998] and aqueous-phase inorganic radical chemistry reviews [*Buxton et al.*, 1988; *Neta et al.*, 1988]. Significant hydrogen peroxide concentrations are expected in the system, thus aqueous H_2O_2 photochemistry and thermal/H_2O_2-initiated ozone decomposition mechanisms, including carbonate ion inhibition effects, were evaluated [*Gonzalez and Martire*, 1997; *Sehested et al.*, 1991, 1998; *Nemes et al.*, 2000]. Recently published aqueous chlorine free radical mechanisms are also considered [*Buxton et al.*, 1998, 2000; *Alegre et al.*, 2000], but aside from Cl_2 hydrolysis, nonradical chlorine chemistry is generally absent from available mechanisms. Finally, unfavorable kinetics and equilibria eliminate the necessity of including higher oxidation chlorine solutes, i.e., ClO_m^- and $ClO_{m-1}^{\bullet}$ where $m > 1$.

[24] Table 5 provides the rate constants for aqueous-phase chemical reactions relevant to the experimental conditions. Temperature dependences of many aqueous-phase reactions are not well established. Consequently, data are only provided for rate constants at 298 K. This does not pose any significant source of error since all experiments were performed near this temperature.

[25] Calculations of the light intensity in droplets based on Mie theory provide evidence that the actinic flux in aqueous particles may be enhanced, with respect to intensity, on average by a factor of two compared to the surrounding gas [*Madronich*, 1987; *Ruggaber et al.*, 1997]. Such an enhancement would affect the photolysis rates inside the droplets. However, this effect is deemed of minimal importance in this study as the photolysis of O_3 occurs predominantly in the gas phase due to its low solubility. As confirmation, the photolysis rate of ozone in the presence of nonreactive sodium sulfate (Na_2SO_4) droplets measured in the experimental chamber was indeed equal to the photolysis rate in humid air alone. Therefore, the photolysis rates of aqueous-phase species are assumed equal to those of the corresponding gas-phase species.

[26] Acidic species included in the model possess electrolytic properties when transported into an aqueous medium. Other species, such as CO_2, can hydrolyze to form products that also dissociate in solution. For aqueous-phase reactions of atmospheric and laboratory systems, the timescale for ionization equilibrium is less than the timescale for chemical reaction [*Schwartz and Freiberg*, 1981]. Thus, it is assumed that electrolytic species and their dissociation products diffuse and react while preserving equilibrium and overall electroneutrality. Table 6 provides values for the equilibrium expressions used in this study.

2.5. Kinetic Salt Effect

[27] Although atmospheric models consider medium or salt effects in equilibrium/solubility expressions [*Sander*

Table 5. Aqueous-Phase Chemical Mechanism

No.	Reaction	O[a]	k_{298}[b]	Reference(s)
1001	$H_2O_2 + h\nu \rightarrow 2\ OH^\bullet$	1	Photo	
1002	$O_3 + h\nu + H_2O \rightarrow H_2O_2 + O_2$	1	Photo	
1003	$O_3 + h\nu \rightarrow O(^3P) + O_2$	1	Photo	
1004	$O_3 \rightarrow O(^3P) + O_2$	1	3.0×10^{-6}	*Sehested et al.* [1992]
1005	$OH^\bullet + OH^\bullet \rightarrow H_2O_2$	2	5.5×10^{9}	*Buxton et al.* [1988, 2000]
1006	$OH^\bullet + HO_2^\bullet \rightarrow O_2 + H_2O$	2	1.0×10^{10}	*Elliot and Buxton* [1992]
1007	$OH^\bullet + O_2^{\bullet-} \rightarrow OH^- + O_2$	2	1.0×10^{10}	*Elliot and Buxton* [1992]
1008	$OH^\bullet + H_2O_2 \rightarrow HO_2^\bullet + H_2O$	2	2.7×10^{7}	*Buxton et al.* [1988]
1009	$OH^\bullet + HO_2^- \rightarrow HO_2^\bullet + OH^-$	2	7.5×10^{9}	*Buxton et al.* [1988]
1010	$OH^\bullet + O_3 \rightarrow HO_2^\bullet + O_2$	2	1.1×10^{8}	*Neta et al.* [1988]
1011	$OH^\bullet + O_3^{\bullet-} \rightarrow O_2^{\bullet-} + HO_2^\bullet$	2	5.9×10^{9}	*Buxton et al.* [1988]
1012	$OH^\bullet + O_3^{\bullet-} \rightarrow O_3 + OH^-$	2	2.6×10^{9}	*Buxton et al.* [1988]
1013	$O^{\bullet-} + O_2 \rightarrow O_3^{\bullet-}$	2	3.6×10^{9}	*Buxton et al.* [1988]
1014	$O^{\bullet-} + HO_2^- \rightarrow O_2^{\bullet-} + OH^-$	2	4.0×10^{8}	*Buxton et al.* [1988]
1015	$O^{\bullet-} + O_2^{\bullet-} + H_2O \rightarrow 2\ OH^- + O_2$	2	6.0×10^{8}	*Buxton et al.* [1988]
1016	$O^{\bullet-} + OH^\bullet \rightarrow HO_2^-$	2	$\leq 2.0 \times 10^{10}$	*Buxton et al.* [1988]
1017	$O^{\bullet-} + O^{\bullet-} + H_2O \rightarrow HO_2^- + OH^-$	2	1.0×10^{9}	*Buxton et al.* [1988]
1018	$O^{\bullet-} + O_3 \rightarrow O_2^{\bullet-} + O_2$	2	1.0×10^{8}	*Gonzalez and Martire* [1997]
1019	$O^{\bullet-} + O_3^{\bullet-} \rightarrow 2\ O_2^{\bullet-}$	2	7.0×10^{8}	*Buxton et al.* [1988]
1020	$HO_2^\bullet + HO_2^\bullet \rightarrow H_2O_2 + O_2$	2	8.3×10^{5}	*Bielski* [1978]
1021	$HO_2^\bullet + O_2^{\bullet-} \rightarrow HO_2^- + O_2$	2	1.0×10^{8}	*Bielski* [1978]
1022	$HO_2^\bullet + H_2O_2 \rightarrow OH^\bullet + O_2 + H_2O$	2	0.5	*Weinstein and Bielski* [1979]
1023	$HO_2^\bullet + O_3 \rightarrow OH^\bullet + 2\ O_2$	2	$<1.0 \times 10^{4}$	*Sehested et al.* [1984b]
1024	$O_2^{\bullet-} + O_2^{\bullet-} + 2\ H_2O \rightarrow H_2O_2 + 2\ OH^- + O_2$	2	<0.3	*Bielski* [1978]
1025	$O_2^{\bullet-} + H_2O_2 \rightarrow OH^\bullet + OH^- + O_2$	2	0.13	*Weinstein and Bielski* [1979]
1026	$O_2^{\bullet-} + O_3 \rightarrow O_3^{\bullet-} + O_2$	2	1.5×10^{9}	*Sehested et al.* [1983]
1027	$O_2^{\bullet-} + O_3^{\bullet-} \rightarrow 2\ OH^- + 2\ O_2$	2	5.0×10^{4}	*Gonzalez and Martire* [1997]
1028	$O_3^{\bullet-} \rightarrow O^{\bullet-} + O_2$	1	5.0×10^{3}	*Neta et al.* [1988]
1029	$O_3^{\bullet-} + H^+ \rightarrow OH^\bullet + O_2$	2	9.0×10^{9}	*Sehested et al.* [1984a]
1030	$O_3^{\bullet-} + H^+ \rightarrow HO_3^\bullet$	2	5.0×10^{10}	*Neta et al.* [1988]
1031	$HO_3^\bullet \rightarrow OH^\bullet + O_2$	1	1.0×10^{5}	*Neta et al.* [1988]
1032	$HO_3^\bullet \rightarrow O_3^{\bullet-} + H^+$	1	3.7×10^{4}	*Bühler et al.* [1984]
1033	$O_3 + OH^- \rightarrow HO_2^- + O_2$	2	48	*Neta et al.* [1988]
1034	$O_3 + OH^- \rightarrow HO_2^\bullet + O_2^{\bullet-}$	2	70	*Neta et al.* [1988]
1035	$O_3 + H_2O_2 \rightarrow OH^\bullet + HO_2^\bullet + O_2$	2	0.025	*Sehested et al.* [1992]
1036	$O_3 + HO_2^- \rightarrow HO_3^\bullet + O_2^{\bullet-}$	2	5.5×10^{6}	*Neta et al.* [1988]
1037	$O(^3P) + O_2 \rightarrow O_3$	2	4.0×10^{9}	*Klaening et al.* [1984]
1038	$O(^3P) + OH^- \rightarrow HO_2^-$	2	4.2×10^{8}	*Sauer et al.* [1984]
1039	$O(^3P) + H_2O_2 \rightarrow OH^\bullet + HO_2^\bullet$	2	1.6×10^{9}	*Sauer et al.* [1984]
1040	$O(^3P) + HO_2^- \rightarrow OH^\bullet + O_2^{\bullet-}$	2	5.3×10^{9}	*Sauer et al.* [1984]
1041	$O^{\bullet-} + H_2O_2 \rightarrow O_2^{\bullet-} + H_2O$	2	$\leq 5.0 \times 10^{8}$	*Buxton et al.* [1988]
1101	$HOCl + h\nu \rightarrow OH^\bullet + Cl^\bullet$	1	Photo	
1102	$ClO^- + h\nu \rightarrow Cl^- + O(^3P)$	1	Photo	
1103	$ClO^- + h\nu \rightarrow Cl^\bullet + O^{\bullet-}$	1	Photo	
1104	$ClO^- + h\nu + H_2O \rightarrow Cl^- + H_2O_2$	1	Photo	
1105	$Cl_2 + h\nu \rightarrow 2\ Cl^\bullet$	1	Photo	
1106	$Cl^\bullet + Cl^- \rightarrow Cl_2^{\bullet-}$	2	8.5×10^{9}	*Buxton et al.* [1998]
1107	$Cl_2^{\bullet-} \rightarrow Cl^\bullet + Cl^-$	1	6.0×10^{4}	*Buxton et al.* [1998]
1108	$OH^\bullet + Cl^- \rightarrow HOCl^{\bullet-}$	2	4.3×10^{9}	*Jayson et al.* [1973]
1109	$HOCl^{\bullet-} \rightarrow OH^\bullet + Cl^-$	1	6.1×10^{9}	*Jayson et al.* [1973]
1110	$Cl_2^{\bullet-} + H_2O \rightarrow HOClH^\bullet + Cl^-$	1	1.3×10^{3}	*Buxton et al.* [1998]
1111	$HOClH^\bullet + Cl^- \rightarrow Cl_2^{\bullet-} + H_2O$	2	8.0×10^{9}	*Alegre et al.* [2000]
1112	$Cl^\bullet + H_2O \rightarrow HOClH^\bullet$	1	2.5×10^{5}	*Buxton et al.* [1998]
1113	$HOClH^\bullet \rightarrow Cl^\bullet + H_2O$	1	5.0×10^{4}	*Alegre et al.* [2000]
1114	$HOCl^{\bullet-} + H^+ \rightarrow HOClH^\bullet$	2	3.0×10^{10}	*Alegre et al.* [2000]; *Jayson et al.* [1973]
1115	$HOClH^\bullet \rightarrow HOCl^{\bullet-} + H^+$	1	1.0×10^{8}	*Alegre et al.* [2000]; *McElroy* [1990]
1116	$Cl_2^{\bullet-} + Cl_2^{\bullet-} \rightarrow Cl_2 + 2\ Cl^-$	2	1.8×10^{9}	*Jacobi et al.* [1999]
1117	$Cl_2^{\bullet-} + OH^- \rightarrow HOCl^{\bullet-} + Cl^-$	2	4.0×10^{6}	*Jacobi et al.* [1997]
1118	$HOCl^{\bullet-} + Cl^- \rightarrow Cl_2^{\bullet-} + OH^-$	2	1.0×10^{4}	*Grigor'ev et al.* [1987]
1119	$Cl_2^{\bullet-} + HO_2^\bullet \rightarrow 2\ Cl^- + H^+ + O_2$	2	1.0×10^{9}	*Navaratnam et al.* [1980]
1120	$Cl_2^{\bullet-} + O_2^{\bullet-} \rightarrow 2\ Cl^- + O_2$	2	1.0×10^{9}	*Neta et al.* [1988]
1121	$Cl_2^{\bullet-} + H_2O_2 \rightarrow 2\ Cl^- + HO_2^\bullet + H^+$	2	5.0×10^{4}	*Elliot* [1989]
1122	$Cl_2^{\bullet-} + OH^\bullet \rightarrow HOCl + Cl^-$	2	1.0×10^{9}	*Wagner et al.* [1986]; *Buxton et al.* [2000]
1123	$Cl_2^{\bullet-} + O_3 \rightarrow ClO^- + Cl + O_2$	2	9.0×10^{7}	*Bielski* [1993]
1124	$Cl^\bullet + Cl^\bullet \rightarrow Cl_2$	2	8.8×10^{7}	*Neta et al.* [1988]
1125	$Cl^\bullet + OH^- \rightarrow HOCl^{\bullet-}$	2	1.8×10^{10}	*Neta et al.* [1988]
1126	$Cl^\bullet + HO_2^\bullet \rightarrow Cl^- + H^+ + O_2$	2	3.1×10^{9}	*Graedel and Goldberg* [1983]
1127	$Cl^\bullet + H_2O_2 \rightarrow Cl^- + HO_2^\bullet + H^+$	2	4.1×10^{7}	*Graedel and Goldberg* [1983]
1128	$Cl_2 + HO_2^\bullet \rightarrow Cl_2^{\bullet-} + H^+ + O_2$	2	1.0×10^{9}	*Bjergbakke et al.* [1981]
1129	$HOCl + O_2^{\bullet-} \rightarrow Cl^- + OH^\bullet + O_2$	2	7.5×10^{6}	*Long and Bielski* [1980]
1130	$Cl^- + O_3 \rightarrow ClO^- + O_2$	2	2.0×10^{-3}	*Neta et al.* [1988]
1131	$ClO^- + O_3 \rightarrow Cl^- + 2\ O_2$	2	110	*Neta et al.* [1988]
1132	$Cl_2 + H_2O \rightarrow HOCl + Cl^- + H^+$	1	22	*Wang and Margerum* [1994]

Table 5. (continued)

No.	Reaction	O^a	k_{298}[b]	Reference(s)
1133	$HOCl + Cl^- + H^+ \rightarrow Cl_2 + H_2O$	3	2.1×10^4	*Wang and Margerum* [1994]
1134	$Cl_2 + OH^- \rightarrow HOCl + Cl^-$	2	1.0×10^8	Estimate, this work (see sections 4.1 and 4.2)
1135	$HOCl + Cl^- \rightarrow Cl_2 + OH^-$	2	2.0×10^{-3}	Estimate, this work (using k_{1134} and equilibrium constants)
1136	$Cl_2 + H_2O_2 \rightarrow 2\ Cl^- + 2\ H^+ + O_2$	2	See notes	*Held et al.* [1978]; *Connick* [1947]; *Makower and Bray* [1933]
1137	$Cl_2 + HO_2^- \rightarrow 2\ Cl^- + H^+ + O_2$	2	1.1×10^8	*Davis et al.* [1992]; *Ruiz-Ibanez and Sandall* [1991]
1138	$HOCl + HO_2^- \rightarrow Cl^- + O_2 + H_2O$	2	4.4×10^7	*Held et al.* [1978]
1139	$Cl^- + H_2O_2 \rightarrow ClO^- + H_2O$	2	1.8×10^{-9}	*Hansen and Espenson* [1995]; *Mohammad and Liebhafsky* [1934]
1140	$Cl^- + H_2O_2 + H^+ \rightarrow HOCl + H_2O$	3	8.3×10^{-7}	*Hansen and Espenson* [1995]; *Mohammad and Liebhafsky* [1934]
1141	$Cl_2O + H_2O \rightarrow 2\ HOCl$	1	7.0	*Beach and Margerum* [1990]
1142	$HOCl + HOCl \rightarrow Cl_2O + H_2O$	2	0.08	*Beach and Margerum* [1990]
1143	$Cl_2O + H^+ + H_2O \rightarrow HOCl + HOCl + H^+$	2	270	*Beach and Margerum* [1990]; *Swain and Crist* [1972]
1144	$HOCl + HOCl + H^+ \rightarrow Cl_2O + H^+ + H_2O$	3	3.1	*Swain and Crist* [1972]
1145	$Cl_2O + h\nu \rightarrow 2\ HCl + O_2$	1	Photo	*Johnsson et al.* [1993]
1201	$HCO_3^- + OH^\bullet \rightarrow CO_3^{\bullet-} + H_2O$	2	8.5×10^6	*Buxton et al.* [1988]
1202	$CO_3^{2-} + OH^\bullet \rightarrow CO_3^{\bullet-} + OH^-$	2	3.9×10^8	*Buxton et al.* [1988]
1203	$HCO_3^- + O_2^{\bullet-} \rightarrow CO_3^{\bullet-} + HO_2^-$	2	1.5×10^6	*Schmidt* [1972]
1204	$CO_3^{2-} + O^{\bullet-} \rightarrow CO_3^{\bullet-} + 2\ OH^-$	2	$<5.0 \times 10^5$	*Gonzalez and Martire* [1997]
1205	$CO_3^{\bullet-} + H_2O_2 \rightarrow HCO_3^- + HO_2^\bullet$	2	4.3×10^5	*Draganić et al.* [1991]
1206	$CO_3^{\bullet-} + HO_2^- \rightarrow CO_3^{2-} + HO_2^\bullet$	2	3.0×10^7	*Gonzalez and Martire* [1997]
1207	$CO_3^{\bullet-} + HO_2^\bullet \rightarrow HCO_3^- + O_2$	2	5.6×10^7	*Behar et al.* [1970]
1208	$CO_3^{\bullet-} + O_2^{\bullet-} \rightarrow CO_3^{2-} + O_2$	2	6.5×10^8	*Ericksen et al.* [1985]
1209	$CO_3^{\bullet-} + O_3^{\bullet-} \rightarrow CO_3^{2-} + O_3$	2	6.0×10^7	*Holcman et al.* [1982]
1210	$CO_3^{\bullet-} + CO_3^{\bullet-} + O_2 + 2\ H_2O \rightarrow 2\ CO_2{\bullet}H_2O + 2\ O_2^{\bullet-}$	2	2.2×10^6	*Huie and Clifton* [1990]
1211	$HCO_3^- + Cl^\bullet \rightarrow CO_3^{\bullet-} + Cl^- + H^+$	2	2.2×10^8	*Mertens and von Sonntag* [1995]
1212	$CO_3^{2-} + Cl^\bullet \rightarrow CO_3^{\bullet-} + Cl^-$	2	5.0×10^8	*Mertens and von Sonntag* [1995]
1213	$CO_3^{2-} + Cl_2^{\bullet-} \rightarrow CO_3^{\bullet-} + 2\ Cl^-$	2	2.7×10^6	Estimate, *Herrmann et al.* [2000]
1214	$Cl_2 + HCO_3^- + H_2O \rightarrow HOCl + Cl^- + CO_2{\bullet}H_2O$	2	3.2×10^3	Estimate, this work (see sections 4.1 and 4.2)
1215	$Cl_2 + CO_3^{2-} + H_2O \rightarrow HOCl + Cl^- + HCO_3^-$	2	1.4×10^5	Estimate, this work (see sections 4.1 and 4.2)
1216	$HOCl + Cl^- + CO_2{\bullet}H_2O \rightarrow Cl_2 + HCO_3^- + H_2O$	3	2.7	Estimate, this work (using k_{1214} and equilibrium constants)
1217	$HOCl + Cl^- + HCO_3^- \rightarrow Cl_2 + CO_3^{2-} + H_2O$	3	0.012	Estimate, this work (using k_{1215} and equilibrium constants)
1218	$CO_2{\bullet}H_2O + OH^\bullet \rightarrow CO_3^{\bullet-} + H^+ + H_2O$	2	$\geq 7.0 \times 10^4$	*Czapski et al.* [1999]

$k_{1136} = 183.3/(2.27[H^+][Cl^-] + 1)$.
[a] Reaction order.
[b] Units in $M^{(1-O)}\ s^{-1}$.

and Crutzen, 1996; *Moldanova and Ljungstrom*, 2001], kinetic salt effects are also warranted in the calculation of the rate constants of aqueous-phase reactions. The historical and theoretical background of the kinetic salt effect is found in classic review articles [*Rochester*, 1971; *Perlmutter-Hayman*, 1971; *Pethybridge and Prue*, 1972]. Briefly, the kinetics of a reaction between two (or more) solution-phase reactants is dictated by the formation of an activated complex, X, in accordance with transition state theory, as shown in equation (8) for the case of a bimolecular reaction between A and B.

$$A + B \rightleftharpoons X \rightarrow \text{Products} \tag{8}$$

[28] Bronsted and Bjerrum independently proposed that the rate of aqueous-phase chemical reactions depends not only on the activities of the reactants, but also on the activity of a "critical complex," i.e., the activated complex. The rate constant for an aqueous-phase chemical reaction is determined by the so-called Bronsted–Bjerrum relation:

$$k = k^\circ F = k^\circ \frac{\gamma_A \gamma_B}{\gamma_X} \tag{9}$$

where k^o is the rate constant at infinite dilution while γ_A, γ_B, and γ_X denote the activity coefficients of the reactants and the activated complex, respectively. The ratio of the activity coefficients, F, is the kinetic activity factor.

[29] From simple application of the Debye limiting law, the Bronsted–Bjerrum relation becomes

$$\log k = \log k^\circ + A\Delta z^2 \sqrt{I} \tag{10}$$

Table 6. Aqueous-Phase Acid/Base Equilibrium Expressions

Equilibrium reaction	K_{a298} (M)	$-\Delta H/R$ (K)	Reference
$H_2O \rightleftharpoons; H^+ + OH^-$	1.00×10^{-14}	6710	*Smith and Martell* [1976]
$H_2O_2 \rightleftharpoons; H^+ + HO_2^-$	2.50×10^{-12}		*Sauer et al.* [1984]
$HO_2^\bullet \rightleftharpoons; H^+ + O_2^{\bullet-}$	2.05×10^{-5}		*Bielski* [1978]; *Bielski et al.* [1985]
$OH^\bullet \rightleftharpoons; H^+ + O^{\bullet-}$	1.26×10^{-12}		*Buxton et al.* [1988]
$HCl \rightleftharpoons; H^+ + Cl^-$	1.70×10^6	6896	*Marsh and McElroy* [1985]
$HOCl \rightleftharpoons; H^+ + ClO^-$	2.80×10^{-8}		*Huthwelker et al.* [1995]
$CO_2{\bullet}H_2O \rightleftharpoons; H^+ + HCO_3^-$	4.30×10^{-7}	920	*Sillén and Martell* [1964]
$HCO_3^- \rightleftharpoons; H^+ + CO_3^{2-}$	4.30×10^{-11}	1786	*Sillén and Martell* [1964]
$HCO_3^\bullet \rightleftharpoons; H^+ + CO_3^{\bullet-}$	$\gg 1$		*Czapski et al.* [1999]

The temperature dependence for the equilibrium constants is given by $K_a(T) = K_{a298} \exp[(1/298 - 1/T) \times \Delta H/R]$ where and ΔH is the enthalpy of reaction.

where

$$\Delta z^2 = z_X^2 - z_A^2 - z_B^2 - \dots \quad (11)$$

In the above equations, z represents the charge of the species, A is the Debye parameter, and I is the ionic strength of the solution. Equation (10), commonly known as the Debye–Bronsted equation, simplifies in the case of a bimolecular reaction to

$$\log k = \log k^\circ + 2Az_Az_B\sqrt{I} \quad (12)$$

[30] The validity of equation (12) at ionic strengths below 0.1 M is manifest by the Livingston diagram [*Benson*, 1960; *Finlayson-Pitts and Pitts*, 2000]. The range of ionic strength is enhanced using the extended Debye–Huckel limiting law, yielding the Debye–Huckel–Bronsted equation:

$$\log k = \log k^\circ + \frac{A\Delta z^2\sqrt{I}}{1+\sqrt{I}} \quad (13)$$

[31] A revised Livingston diagram shows that equation (13) yields good agreement for $I \leq 0.5$ M [*Pethybridge and Prue*, 1972]. However, at relative humidities near the deliquescence point, marine aerosol can be expected to reach ionic strengths near 6 M. Some progress, at least in experimental settings, can be made by further extending the Debye–Huckel limiting law as proposed by Guggenheim and incorporating it into the Bronsted–Bjerrum relation yielding

$$\log k = \log k^\circ + \frac{A\Delta z^2\sqrt{I}}{1+\sqrt{I}} + \sum_i B_{A,i}C_i + \sum_j B_{B,j}C_j - \sum_k B_{X,k}C_k \quad (14)$$

where $B_{m,n}$ are specific interaction coefficients between ion m and all ions of opposite charge n having concentration C_n. This expression can be simplified if the relative ionic concentrations remain fairly unchanged in a series of experiments into

$$\log k = \log k^\circ + \frac{A\Delta z^2\sqrt{I}}{1+\sqrt{I}} + BI \quad (15)$$

where the empirical kinetic salt effect parameter B is separated into the individual contributions B_A, B_B and B_X due to the reactants and the activated complex:

$$B = B_A + B_B - B_X \quad (16)$$

Equation (15) is also known as the Debye–Huckel–Bronsted–Davies equation when B is substituted by an equivalent parameter b' that is written at times with an opposite sign:

$$\log k = \log k^\circ + \frac{A\Delta z^2\sqrt{I}}{1+\sqrt{I}} - b'I \quad (17)$$

The range of B (or $-b'$) varies greatly with reported values reaching as high and positive as 0.74 [*Kumar et al.*, 1986] and as large and negative as −0.86 [*Pethybridge and Prue*, 1972]. An important corollary of the theory above is that for neutral–neutral or neutral–ion reactions equation (15) reduces to

$$\log k = \log k^\circ + BI \quad (18)$$

implying that, at sufficiently high ionic strengths, a kinetic salt effect may also be present.

[32] Unfortunately, the determination of the kinetic salt effect in atmospheric modeling applications is cumbersome due primarily to the following physical processes: (1) Changes in relative humidity alter the overall concentration and ionic strength of an aqueous aerosol particle. (2) Absorption and volatilization of constituents from and to the gas phase affect the relative concentrations of ionic species with respect to each other. (3) Chemical reactions within the droplet (or at the surface of the droplet) also affect the overall composition of the aerosol.

[33] At best, atmospheric models can only attempt to estimate the kinetic salt effect. This can be done by several methods. First, the kinetic activity factor, F, may be evaluated directly through calculation of individual activity coefficients. However, the activities of many organic species, inorganic constituents at atypical oxidation states, and radical ions cannot be calculated with current activity coefficient models thus leading to their estimation by extended Debye–Huckel expressions [*Sander and Crutzen*, 1996; *Moldanova and Ljungstrom*, 2001]. In addition, the activity of the activated complex must also be estimated.

[34] Second, the effective rate constant may be determined via Debye–Huckel–Bronsted equations. The advantage, simplicity, is easily overshadowed by the disadvantage, lack of validity beyond ionic strengths of 0.5 M. Nonetheless, if insight of the importance of various processes, not absolute values, is the desired output from the modeling studies, such a method may prove sufficient and attractive. With the understanding of this important caveat, this is the method employed in the current implementation of MAGIC.

[35] Finally, the effective rate constant may be determined via Debye–Huckel–Bronsted–Guggenheim—or the similar Debye–Huckel–Bronsted–Davies—equations. Considering equation (14) in an experimental context, the determination of the specific interaction parameters $B_{m,n}$—primarily for the activated complexes and radical ions—could be an unapproachably difficult task. Instead, determination of an overall kinetic salt effect parameter, B, is more advantageous. Experimental studies shall determine whether this parameter is chosen as a constant coefficient to ionic strength, or adjusted as a function of the concentrations of the primary ions in solution.

[36] If a compilation of aqueous-phase chemical data for atmospheric modeling is commissioned [*Jacob*, 2000], the selection of a common method for determining the kinetic salt effect should be included and suggestions to quantify such effects conveyed accordingly.

2.6. Aqueous-Phase Diffusion

[37] Only species actively transported between the gas phase and aqueous phase, and their hydrolysis and/or dissociation products, need to be considered as presenting

spatial gradients within the droplets [*Jacob*, 1986]. For these species, a concentration value at the surface must be determined in order to calculate volatilization fluxes and another average bulk concentration value must be determined to calculate the overall rate of aqueous-phase reactions within the droplet. All other species are assumed well mixed throughout the droplet.

[38] The temporal and spatial dependence of the concentration of species undergoing diffusion and irreversible reaction inside a spherically symmetrical droplet is governed by the equations

$$\frac{dC_j(r,t)}{dt} = D_{aq,j}\frac{1}{r^2}\frac{d}{dr}\left(r^2\frac{dC_j(r,t)}{dr}\right) - k_{L,j}(r,t)C_j(r,t) + P_j(r,t). \tag{19}$$

where r is the distance from the center of the droplet; t is the temporal variable; $D_{aq,j}$ and $C_j(r, t)$ are the aqueous-phase diffusivity and concentration of species j, respectively; and $R(r, t)$ is the aqueous-phase reaction rate. Equation (19) also contain two chemical reaction terms: an effective global first-order loss rate constant $k_{L,j}$ (s^{-1}) for species j and a global production rate P_j (M s^{-1}) by aqueous-phase reactions both of which may depend on other species that present radial dependencies on concentration, i.e., other species transported to and from the gas phase.

[39] In the extreme situation of a droplet suddenly exposed to a gas-phase reagent whose concentration remains constant at the surface (in the absence of any aqueous-phase production), the rate of uptake into the droplet calculated from the steady state solution does not greatly exceed the rate calculated from the time dependent solution [*Schwartz and Freiberg*, 1981]. Accordingly, through application of the steady state solution, equation (19) become

$$D_{aq,j}\frac{1}{r^2}\frac{d}{dr}\left(r^2\frac{dC_j(r)}{dr}\right) - k_{L,j}(r)C_j(r) + P_j(r) = 0, \tag{20}$$

subject to the boundary conditions

$$\left(\frac{dC_j(r)}{dr}\right)_{r=0} = 0 \tag{21}$$

$$C_j(R_p) = C_j^*, \tag{22}$$

where C_j^* is the concentration at the droplet surface. After mathematical manipulation of equations (20)–(22), the average bulk concentrations of aqueous-phase species are determined by solving a system of closely coupled nonlinear equations given by:

$$\langle C_j\rangle = QC_j^* + (1-Q)\frac{P_j}{k_{L,j}}. \tag{24}$$

where

$$Q = 3\left(\frac{\coth q_j}{q_j} - \frac{1}{q_j^2}\right) \tag{25}$$

and

$$q_j = R_p\left(\frac{k_{L,j}}{D_{aq,j}}\right)^{1/2}. \tag{26}$$

2.7. Interfacial Reactions

[40] The rates of gas-phase reactions may be enhanced by the presence of liquid or solid surfaces [*Ravishankara*, 1997]. A thorough analysis of the data (see results section) shows that in the experimental system at hand, the prospect of a surface reaction involving chloride ions and hydroxyl radicals is a fully reasonable deduction. A brief description of the modeling of the surface mechanism follows.

[41] Results by *Knipping et al.* [2000] suggest that chloride ions present at aqueous surface hold a high affinity for gas-phase $OH^\bullet$ radicals, thereby enhancing scavenging of the gas at the surface and leading to the formation of a surface complex species, $OH\bullet\bullet\bullet Cl^{\bullet-}_{surface}$,

$$OH^\bullet_g + Cl^-_{aq,surface} \rightarrow OH\bullet\bullet\bullet Cl^{\bullet-}_{surface}. \tag{27}$$

Recalling the equation for the molecular collision rate per surface area, the formation of $OH\bullet\bullet\bullet Cl^-_{surface}$ is determined by

$$R_{27} = \gamma_s\frac{\bar{c}}{4}A[OH^\bullet]_g, \tag{28}$$

where γ_s is the overall probability of Reaction 27 occurring once an $OH^\bullet$ molecule strikes the droplet surface and A is the total particle surface area. The probability, γ_s, is a function of the availability of chloride ions at the surface and the likelihood of complexation. Molecular dynamic simulations [*Jungwirth and Tobias*, 2000] suggest that the fraction of the droplet surface covered by chloride ions can be estimated as $0.02[Cl^-]$, where $[Cl^-]$ is the concentration of chloride expressed in M (mol L^{-1}), and the numerical constant has units of M^{-1}. The probability is therefore be expressed as

$$\gamma_s = 0.02\ \gamma'_s[Cl^-], \tag{29}$$

where γ'_s is a fitting parameter incorporating the probability of an $OH^\bullet$ radical forming the complex. The value of the γ'_s term is explored in the results section.

[42] In contrast to earlier studies of the same system [*Knipping et al.*, 2000], instead of attempting to speculate the specific fate of $OH\bullet\bullet\bullet Cl^{\bullet-}_{surface}$ and the kinetics of the individual reactions thereof, the present study is limited to finding an overall rate expression on the premise that the formation of the chloride–hydroxyl complex is the rate limiting step of an overall reaction given by

$$OH^\bullet_g + Cl^-_{aq,surface} \rightarrow \frac{1}{2}Cl_{2,g} + OH^-_{aq}. \tag{30}$$

This assumption agrees with initial modeling studies and offers several important advantages: (1) an ability to focus solely on the leading hypothesis: a surface enhanced mechanism determines the rate of chlorine formation; (2) provides a straightforward expression amenable to inclusion by other models; and (3) underscores the possibility of

several, not necessarily exclusive, reactions in the interfacial region involving the initially formed $OH\bullet\bullet\bullet Cl^{\bullet-}_{surface}$.

2.8. Governing Equations

[43] Applying the results obtained from mass transfer theory of *Schwartz* [1986] in combination with terms for bulk gas-phase chemical reaction, R_g, and interfacial reactions, R_{int}, the temporal variations of the concentrations of gas-phase and aqueous-phase species are described by

$$\frac{dC_g}{dt} = -k_{mt} w_L C_g + \frac{k_{mt}}{HRT} C_{aq} w_L + R_g \pm R_{int} \tag{31}$$

$$\frac{dC_{aq}}{dt} = k_{mt} C_g - \frac{k_{mt}}{HRT} C_{aq} + \langle R_{aq} \rangle \mp \frac{R_{int}}{w_L}, \tag{32}$$

where R_{int} is the overall rate of the interfacial mechanism as expressed in equation (28).

2.9. Methodology of Mechanism Validation

[44] An extensive literature search performed in order to assemble the chemical mechanism for the "relatively simple" system of interest, resulted in nearly 200 parameters including aqueous-phase and gas-phase rate constants, Henry's law constants, accommodation coefficients and acid/base equilibrium constants. Although many of these parameters are well known, the potential for error is explored through sensitivity studies.

[45] The strategy developed in collaboration with our experimental and theoretical chemistry associates in order to clarify the mechanism for Cl_2 production is as follows:

1. Create a model that attempts to reproduce the experimental results using the best known data and representation of the physical and chemical processes of the experiments.

If the model cannot duplicate, within reasonable error, the levels of chlorine detected in the experimental chamber the ensuing steps were taken:

2. Study the sensitivity of the system in order to determine which reactions are significant and evaluate whether the uncertainty of these reactions can explain the Cl_2 production.
3. Investigate whether error in model ino5g (initial conditions and aerosol or chamber parameters) can justify for the level of discrepancy.
4. Investigate whether any unknown, yet rational, chemical reaction or physical process solely in the aqueous phase or gas phase can account for the Cl_2 formation.

It is only upon complete failure of all three tests (2–4) above that the likelihood for chemical reaction(s) at the interface is (are) considered. The burgeoning evidence for these types of reactions suggests that a similar reaction is plausible in our system (see section 1). The methodology invoked in the mechanism's analysis proceeds by performing the following tests:

5. Determine which of the reactive gas concentrations, in combination with the amount of surface area available, correlates better with the observed rates of Cl_2 formation.
6. Confirm the likelihood of the participation of the preferred gas-phase species using theoretical and thermodynamic considerations.

[46] If the above tests yield a potential candidate for a surface reaction, then a surface mechanism can be reasonably inferred. Given the level of complexity involved in determining such a mechanism from limited laboratory data, it is preferable to determine a kinetic expression for the overall rate of Cl_2 production. Nevertheless, in order to support such a hypothesis, at least one compatible and reasonable mechanism must be presented in a qualitative fashion. Two such mechanisms that are chemically sound given the present level of understanding of interfacial processes on aqueous sodium chloride surfaces are presented.

[47] Finally, once an overall rate expression is obtained, this "interface model" is subjected to the same rigorous tests as the "noninterface model." In this case, we wish not only to see whether any reasonable discrepancy between the model results and experimental data can be explained by variations in model input and/or parameters, but also to guarantee that the level of modeled Cl_2 production is not attributable to some fortuitous combination of highly sensitive parameters.

[48] Given the vanguard nature of these combined theoretical, experimental and kinetic modeling efforts, the results presented here are intended to serve as a springboard to further investigate a promising area in aerosol reactions in the atmosphere, i.e., reactions at the air–water interface.

3. Experimental Modeling

3.1. Established Chemical Mechanisms

[49] In order to clarify the mechanism for the observed Cl_2 production in the chamber experiments, different pathways are evaluated by performing simulations using MAGIC and comparing the results to the experimental data. Table 7 contains the parametric data of three principal experimental scenarios. The experiments are denoted as the low, middle and high O_3 experiments according to their initial ozone concentration. The model, in correspondence with experimental procedure, runs for 12 min in the dark, allowing the system to approach an initial equilibrium state. Determination of Cl_2 levels in the chamber after each 2-min photolysis period (10 total) requires flowing some of the contents through the atmospheric pressure ionization mass spectrometer (API-MS) during a 6-min dark sampling period, effectively diluting the chamber. In order to reproduce the chamber conditions, this effect is modeled as a first-order loss resulting in a decrease in gas-phase concentrations in the proportion given by the dilution factor on Table 7. The first-order dilution rate constant is given by

$$k_{dilution} = -\frac{\log(\textit{dilution factor})}{t_{API\ Sampling}} \tag{33}$$

[50] Modeled Cl_2 and O_3 time series (Figures 2–7) exhibit a sawtooth shape indicative of API gas-phase dilution; experimental Cl_2 measurements are shown as 6-min bars corresponding to the average concentration measured during sampling, whereas experimental O_3 measurements are shown as instantaneous points measured at the onset of the API dark sampling period.

[51] O_2, N_2 and H_2O concentrations do not change during the sampling period due to the addition of humid ultrapure air. The aerosol particle concentration, i.e., the mass of aerosol particles per unit volume in the chamber, also does not change during the simulation. The count and measurement of the aerosol population is performed twice before

Table 7. Model Parameters for Sequence of Experiments Varying Initial O_3 Concentration

Parameter	Units	Simulation		
		High ozone	Middle ozone	Low ozone
$[O_3]_0$	molecule cm^{-3}	3.37×10^{14}	2.44×10^{14}	6.31×10^{13}
$[CO_2]_0$	ppm	17.7	16.6	16.9
$[NaCl]_0$	M	4.30	4.30	4.28
Dilution factor		0.945	0.940	0.956
RH	%	81.8	81.8	81.9
Temperature	K	298	298	298
Number	cm^{-3}	1.86×10^5	1.43×10^5	1.09×10^5
Median diameter	nm	224	227	209
Mass transfer radius	nm	396	353	353
Geometric standard deviation	–	1.93	1.97	2.09
Area	nm^2/cm^3	8.16×10^{10}	5.79×10^{10}	4.42×10^{10}
Volume	nm^3/cm^3	9.74×10^{12}	6.92×10^{12}	5.95×10^{12}

The mass transfer radius is the effective radius used in the quasi-size-dependent calculation of the mass transfer rate coefficient, k_{mt}, and is derived by integrating over the droplet population [*Schwartz*, 1986; *Sander and Crutzen*, 1996].

initiating the experiments and twice after completing the final API sampling. An average aerosol distribution is used throughout the model simulation; the error associated with this assumption is treated later in this discussion.

[52] Evaluation of the full mechanism based on known gas-phase and aqueous-phase chemistry is equivalent to an evaluation of the reaction pathway proposed by *Oum et al.* [1998] (see Figure 1). Minor differences reflect the current understanding regarding the equilibria formed by the oxidation of Cl^- by $OH^\bullet$ in aqueous solution and the reactions of $Cl^\bullet/Cl_2^{\bullet-}$ with water [*Jayson et al.*, 1973; *Wagner et al.*, 1986; *McElroy*, 1990; *Buxton et al.*, 1998; *Alegre et al.*, 2000]. The source of this mechanism begins with the photolysis of ozone and subsequent reaction of excited oxygen atoms, $O(^1D)$, with water, leading to hydroxyl radical generation in the gas phase. $OH^\bullet$ is then taken up by the particles and oxidation of the chloride ion eventually leads to Cl_2 release into the gas phase. These simulations based on established chemistry and mass transfer parameters are designated as "base case" simulations.

[53] Figure 2 shows base case modeling results, corresponding to the middle ozone experiment, using only established gas-phase and aqueous-phase chemical reactions and mass transfer processes pertinent to the simulated system—no interfacial reactions have been modeled. Although the ozone decay is in agreement with experimental data (as expected since the photolysis rate was measured independently and input directly into the model), the amount of Cl_2 predicted is more than three orders of magnitude lower than observed. Similar or greater discrepancies are found for the other experimental conditions.

[54] A full sensitivity analysis is performed on the model in order to determine the nature of the feedback expected by perturbations to model parameters, e.g., reaction rate constants, with respect to Cl_2 formation. A full Jacobian matrix indicating change in concentrations versus change in parameters was generated for the system. Table 8 shows the response normalized as a percent change of the Cl_2 concentration due to a +1% change in the corresponding parameter. The results of the sensitivity analysis provide much insight while bearing in mind the caveat that any *local derivative*, such as those calculated here, should not be wildly extrapolated.

[55] The Cl_2 formation due to known chemical reactions is explained by an alternative yet similar mechanism to the one proposed earlier by *Oum et al.* [1998],

$$OH^\bullet + Cl^- \rightleftharpoons HOCl^{\bullet-} \tag{34}$$

$$HOCl^{\bullet-} + Cl^- \rightleftharpoons Cl_2^{\bullet-} + OH^- \tag{35}$$

$$OH^- + H^+ \rightleftharpoons H_2O \tag{36}$$

$$Cl_2^{\bullet-} + Cl_2^{\bullet-} \rightarrow Cl_2 + 2\ Cl^- \tag{37}$$

with the critical steps given by the formation of the $HOCl^{\bullet-}$ radical ion that may then react with the abundant chloride ions to form the chlorine radical ion, $Cl_2^{\bullet-}$. In the model, the pH of the droplets begins at equilibrium with the chamber CO_2 at a value near 6.6 and quickly reaches a value of 8.7, tapering to 9 by the end of the experimental simulation, due to the formation of hydroxide ions in (35). Consequently,

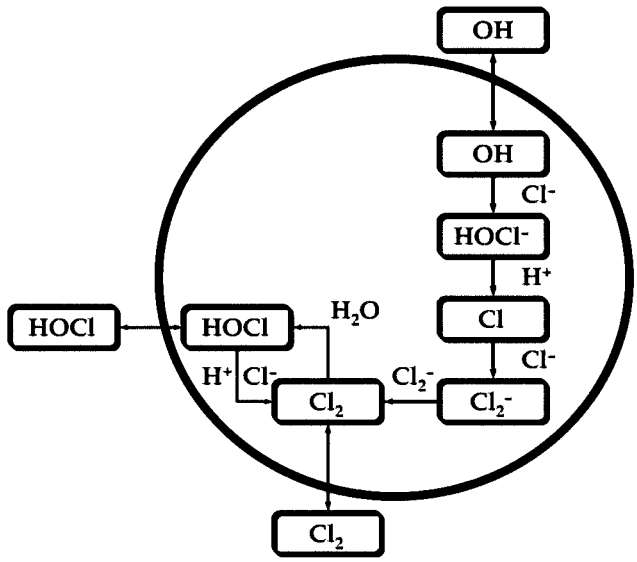

Figure 1. Graphical representation of known aqueous-phase chemical reactions potentially responsible for observed Cl_2.

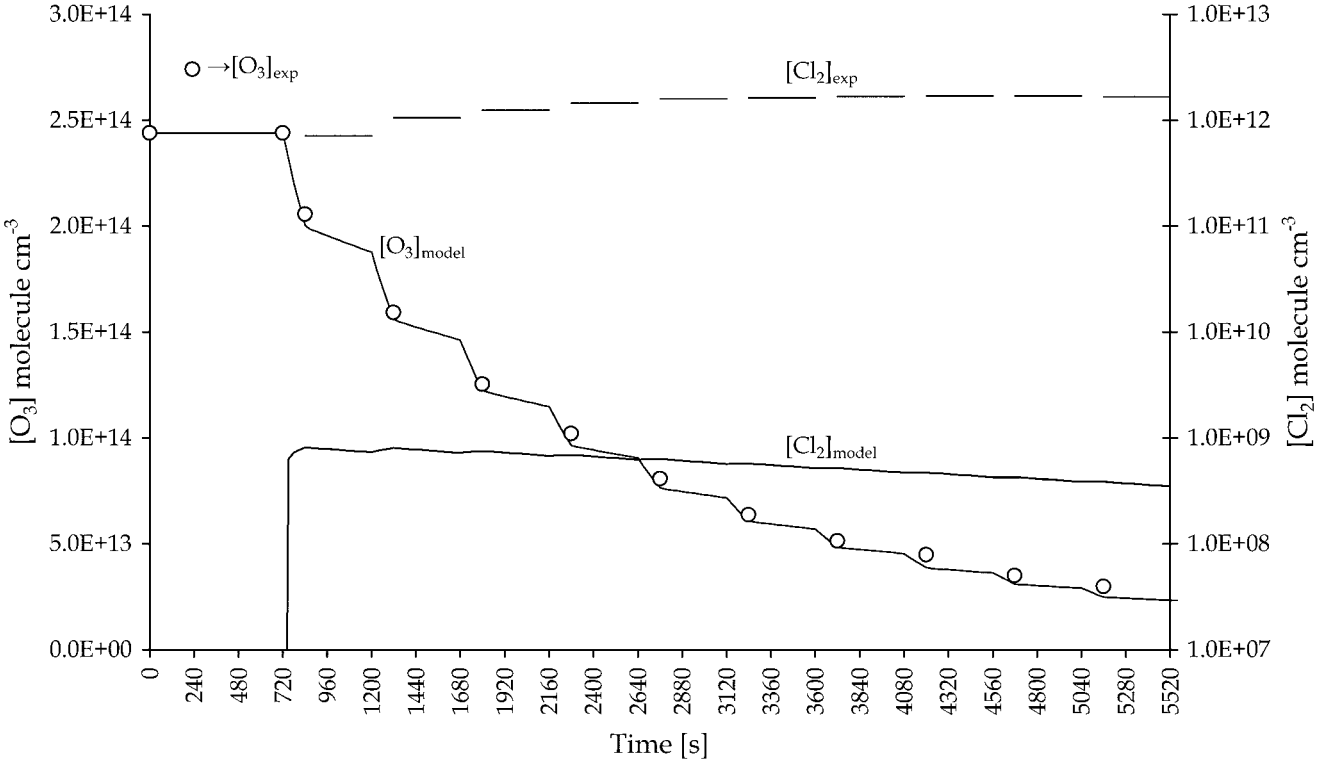

Figure 2. Results of aerosol chamber modeling (middle O_3 experiment) using all known aqueous-phase and gas-phase chemical reactions (base case scenario). Cl_2 concentrations are shown on a logarithmic scale to better illustrate the discrepancy between observations and predictions using known chemistry.

the reaction of the $HOCl^{\bullet-}$ intermediate with H^+ is progressively slower compared to the reaction with Cl^- and throughout the simulation.

[56] The decay in the Cl_2 concentration is attributable to the combined effect of reaction with $OH^\bullet$ in the gas phase, photolysis, loss to the walls of the experimental chamber, and dilution during API-MS sampling. The most important, albeit of lesser overall impact, loss routes in the aqueous phase are reaction with OH^- and HO_2^-. HO_x radicals are removed from the system forming O_2 and H_2O mainly by gas-phase reactions resulting in a net removal of radicals or potential radical-forming species: $O_3 + OH^\bullet$, $OH^\bullet + HO_2^\bullet$, $H_2O_2 + OH^\bullet$ and $O_3 + HO_2^\bullet$.

[57] The confidence level for the rate constant values of the most significant reactions leading to chlorine formation is high, particularly for the gas-phase reactions. Some mass transfer parameters are not as well known but their uncertainty still cannot justify the larger than three order-of-magnitude discrepancy between the model results and experimental observations. For instance, variation of the $OH^\bullet$ and $HO_2^\bullet$ accommodation coefficients within their range of uncertainty, 0.01–1.0 [*Hanson et al.*, 1992; *Takami et al.*, 1998], results in little appreciable Cl_2 increase compared to the chamber measurements. Furthermore, any realistic error regarding the aerosol population, initial concentrations or model formulation cannot result in a 1000-fold increase in chlorine concentrations.

[58] Is there an unknown chemical reaction or physical process that could account for the Cl_2 formation? In view that the droplet pH is a paramount factor in the production of chlorine, a series of simulations are executed in order to evaluate the effect of acidity. A series of model simulations specifying a constant droplet pH starting with five and lowering to one are performed. Figure 3 shows that only at a constant droplet pH of 1.5 do model results match experimental observations. Sensitivity studies (Table 8) and analysis of this simulation show that the chlorine formation process that prevailed in the base case simulation is overwhelmed by a chlorine formation route initiated by hydrochloric acid displacement,

$$H^+ + Cl^- \rightleftharpoons HCl_{aq} \rightleftharpoons HCl_g \tag{38}$$

$$HCl + OH^\bullet \rightarrow Cl^\bullet + H_2O \tag{39}$$

$$Cl^\bullet + O_3 \rightarrow ClO^\bullet + O_2 \tag{40}$$

$$ClO^\bullet + HO_2^\bullet \rightarrow HOCl + O_2 \tag{41}$$

$$HOCl_g \rightleftharpoons HOCl_{aq} \tag{42}$$

$$HOCl + Cl^- + H^+ \rightleftharpoons Cl_2 + H_2O \tag{43}$$

followed by a chain of reactions in the gas phase forming hypochlorous acid. HOCl is subsequently taken up by the droplets and forms Cl_2 via the reverse hydrolysis reaction.

[59] There is no apparent reason why the droplets would become so acidic, and a constant pH is even less sensible. Nonetheless, two possibilities are examined. First, a series of simulations explore the effect of lowering the initial pH

Table 8. Local Sensitivity of Final Cl_2 Concentrations to Model Parameters

Parameter		Simulation		
		Base case	pH = 1.5	Interface
LWC		0.99%	0.99%	−0.11%
Surface area				0.54%
R (mass transfer)		−0.60%	−0.70%	0.03%
R (aq. diffusion)			−0.01%	0.32%
$[NaCl]_0$		−1.74%	−0.45%	1.24%
$[O_3]_0$		0.03%	0.21%	0.19%
$[CO_2]_0$		0.22%		0.08%
γ_s'				0.54%
RH		0.17%	0.28%	0.13%
Dilution factor		9.19%	5.94%	5.53%
k_2	$O_3 + h\nu \rightarrow O(^3P) + O_2$	0.20%	0.35%	0.15%
k_5	$Cl_2 + h\nu \rightarrow Cl^\bullet + Cl^\bullet$	−0.04%	−0.03%	−0.03%
k_9	$O(^1D) + O_2 \rightarrow O(^3P) + O_2$	−0.05%	−0.09%	−0.04%
k_{12}	$O(^1D) + H_2O \rightarrow OH^\bullet + OH^\bullet$	0.17%	0.29%	0.12%
k_{13}	$O(^1D) + N_2 \rightarrow O(^3P) + N_2$	−0.12%	−0.21%	−0.09%
k_{18}	$O_3 + OH^\bullet \rightarrow HO_2^\bullet + O_2$	−0.23%	−0.41%	−0.26%
k_{21}	$OH^\bullet + HO_2^\bullet \rightarrow O_2 + H_2O$	*	−0.05%	−0.05%
k_{23}	$O_3 + HO_2^\bullet \rightarrow OH^\bullet + O_2 + O_2$	*	0.03%	−0.02%
k_{30}	$OH^\bullet + Cl_2 \rightarrow Cl^\bullet + HOCl$	−0.22%	−0.13%	−0.15%
k_{31}	$OH^\bullet + ClO^\bullet \rightarrow HCl + O_2$		−0.06%	
k_{32}	$OH^\bullet + ClO^\bullet \rightarrow HO_2^\bullet + Cl^\bullet$		−0.07%	−0.03%
k_{34}	$OH^\bullet + HCl \rightarrow Cl^\bullet + H_2O$		0.24%	
k_{35}	$OH^\bullet + HOCl \rightarrow ClO^\bullet + H_2O$		−0.07%	
k_{38}	$HO_2^\bullet + ClO^\bullet \rightarrow HOCl + O_2$		0.12%	0.02%
k_{60}	$Cl_2 + Wall \rightarrow Loss$	−0.33%	−0.20%	−0.15%
k_{1009}	$OH^\bullet + HO_2^- \rightarrow HO_2^\bullet + OH^-$	*		
k_{1036}	$O_3 + HO_2^- \rightarrow HO_3^\bullet + O_2^{\bullet-}$			*
k_{1108}	$OH^\bullet + Cl^- \rightarrow HOCl^{\bullet-}$	0.04%	0.03%	
k_{1109}	$HOCl^{\bullet-} \rightarrow OH^\bullet + Cl^-$	−0.03%	−0.02%	
k_{1114}	$HOCl^{\bullet-} + H^+ \rightarrow HOClH^\bullet$		0.02%	
k_{1116}	$Cl_2^{\bullet-} + Cl_2^{\bullet-} \rightarrow Cl_2 + 2\ Cl^-$	0.25%	0.03%	
k_{1118}	$HOCl^{\bullet-} + Cl^- \rightarrow HOCl^{\bullet-} + Cl^-$	0.03%	*	
k_{1119}	$Cl_2^{\bullet-} + HO_2^\bullet \rightarrow 2\ Cl^- + H^+ + O_2$		−0.06%	
k_{1120}	$Cl_2^{\bullet-} + O_2^{\bullet-} \rightarrow 2\ Cl^- + O_2$	*	*	
k_{1133}	$HOCl + Cl^- + H^+ \rightarrow Cl_2 + H_2O$		0.35%	
k_{1134}	$Cl_2 + OH^- \rightarrow HOCl + Cl^-$	−0.02%		−0.15%
k_{1137}	$Cl_2 + HO_2^- \rightarrow 2\ Cl^- + H^+ + O_2$	*		*−0.10%**
k_{1138}	$HOCl + HO_2^- \rightarrow Cl^- + O_2 + H_2O$	0.02%		0.01%
k_{1213}	$CO_3^{2-} + Cl_2^{\bullet-} \rightarrow CO_3^{\bullet-} + 2\ Cl^-$	−0.50%		
k_{1215}	$Cl_2 + CO_3^{2-} + H_2O \rightarrow HOCl + Cl^- + HCO_3^-$			−0.12%
α_{OH}		0.33%	0.38%	−0.03%
α_{HO_2}				0.02%
H_{O_3}				*
H_{OH}		0.03%	0.03%	*
H_{HO_2}			−0.07%	
$H_{H_2O_2}$		*	*	*−0.08%**
H_{HCl}			−0.23%	
H_{HOCl}		*	0.36%	0.01%
H_{Cl_2}		*		−0.43%
H_{CO_2}		0.22%		0.08%
K_{H_2O}		*		−0.15%
$K_{H_2O_2}$		*		*−0.08%**
K_{HO_2}			*	
K_{HCl}			−0.23%	
K_{CO_2}		0.22%		0.08%
$K_{HCO_3^-}$		−0.24%		0.07%

Sensitivity shown when the absolute value of the normalized Jacobian terms, $J_{i,\,j}$, are greater than 0.01%, i.e., $|(\partial C_i/\partial P_j) \times (\partial P_j/C_{i,\,test})| > 0.01\%$. For the above table, C_i is the final $[Cl_2]$, $C_{i,test}$ is the final $[Cl_2]$ under the normal simulation, and P_j represents the parameters tested with $\partial P_j = 0.01\ P_j$. Sensitivities of Cl_2 concentrations to the above parameters are invariably higher during the earlier portions of the experimental simulations. Asterisks (*) denote moderately appreciable Cl_2 Sensitivity, normalized $|J_{[Cl_2],\,j}| > 0.01\%$, found during earlier periods of the simulation. Early moderate sensitivity is also found in general for reactions gas-phase reactions 20, 22, 24, and 25. Maximum values shown in italics for sensitivity to three H_2O_2/HO_2^--related parameters in interfacial mechanism simulation. An increase in the dilution factor equals a reduction in overall dilution.

of the droplets beyond expected values. This would account for the incidence of an unknown phenomenon that could potentially bring the droplets to a lower initial pH, such as sequestering of sodium cations during particle generation or some unexplained generation of hydrochloric acid. Figure 4 shows that in the scenario that matches the initial rate of formation, the droplets have lost 25% of their sodium cations. This is tantamount to having an initial hydrochloric acid concentration of 1.08 M and pH of −0.4, quickly equilibrated during the preliminary 12-min dark period to a

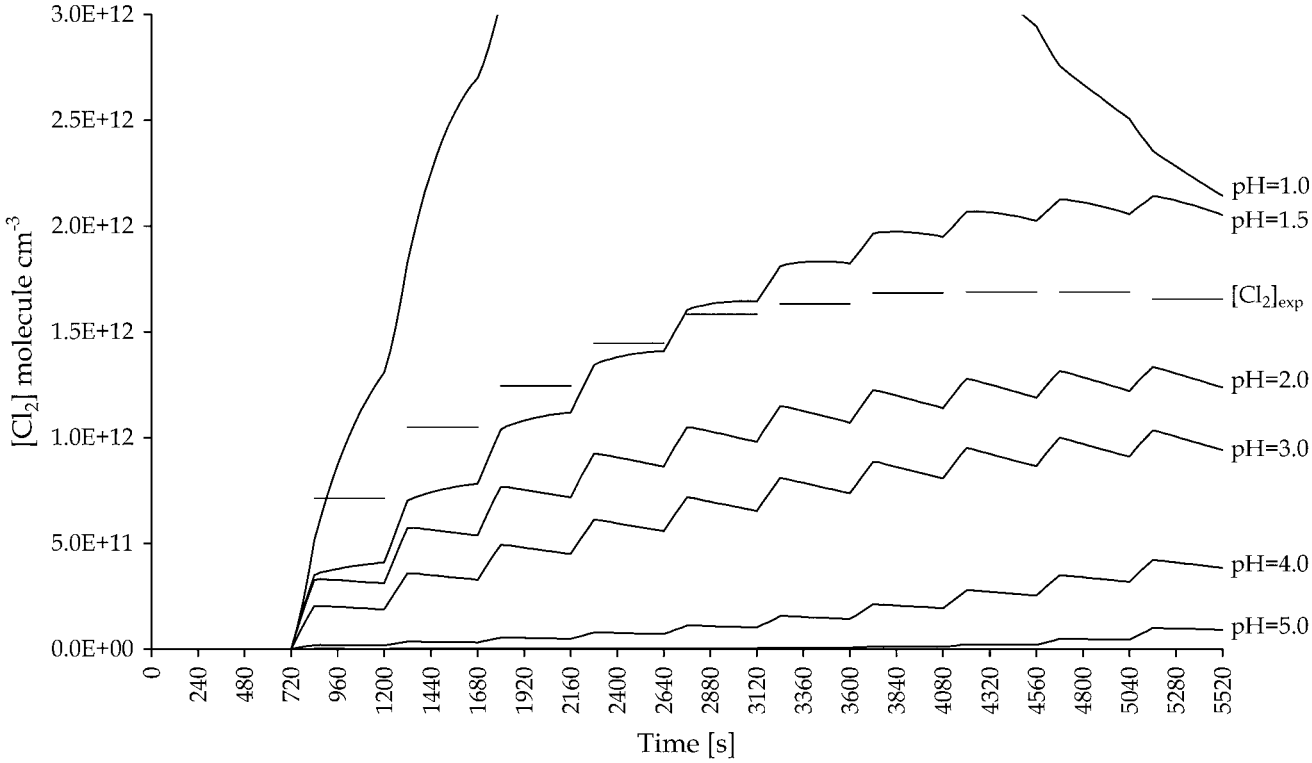

Figure 3. Results of aerosol chamber modeling (middle O_3 experiment) at fixed pH values. The ozone time series are all similar to the ozone time series shown on Figure 2.

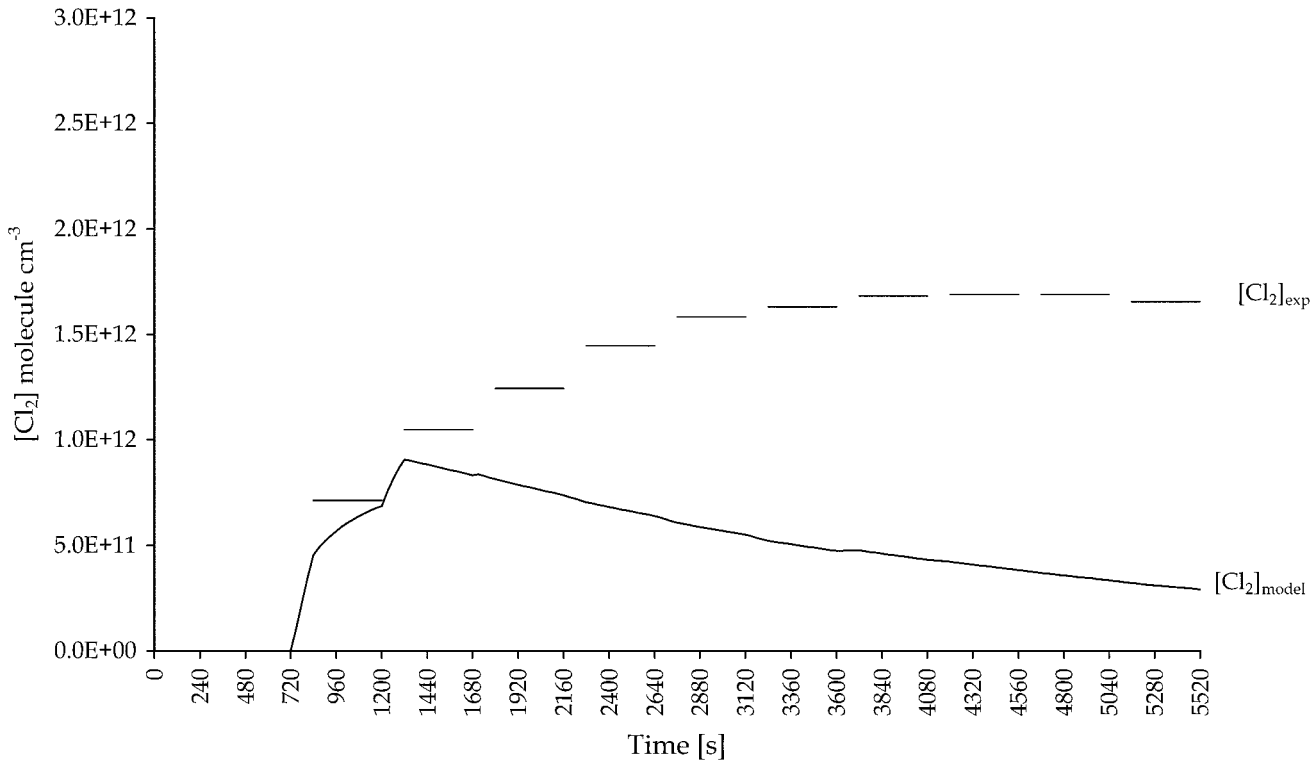

Figure 4. Results of aerosol chamber modeling where 25% initial NaCl substituted by HCl. The ozone time series is similar to the ozone time series shown on Figure 2.

pH of 0.88. Not only is this case highly improbable, it also fails to reproduce the data adequately.

[60] An additional modeling run is performed adding the dissociation of $HOCl^{\bullet-}$, i.e.,

$$HOCl^{\bullet-} \rightleftharpoons ClO^{\bullet 2-} + H^+ \tag{44}$$

to provide a channel for acidification of the particles. *Jayson et al.* [1973] propose such a reaction but the model demonstrates that a considerable rate of Cl_2 formation is obtained only if $HOCl^{\bullet-}$ is found an infinitely strong acid, i.e., $pK_a \ll 0$. This is highly improbable given that the pK_a of $HOClH^{\bullet}$ is ~2.5; the pK_a of $HOCl^{\bullet-}$ should be indicative of the second deprotonation, thus higher than the pK_a of $HOClH^{\bullet}$ and accordingly much higher than zero.

[61] Finally, consideration of chamber wall reactions as the source of the molecular chlorine is safely eliminated. *Oum et al.* [1998] detail the precautionary measures taken in order to minimize any effect of the chamber walls during the experiments and exclusion of the walls as a potential source. Furthermore, the chamber walls are found to be considerable sinks of Cl_2 and HOCl. These effects are modeled as irreversible losses reflecting the current knowledge of the system.

3.2. Interfacial Chemical Mechanisms

[62] Clearly, the observed Cl_2 formation cannot be reconciled by established chemical mechanisms—the disagreement between the experimental and model results is entirely too large. However, as expressed earlier, the gas–liquid interface does provide a sound platform for hitherto investigated chemical reactions to occur between a reactive gas-phase species and available surface chloride.

[63] Two observations are presented before proceeding. First, the values of the gas-phase concentrations of O_3, $HO_2^{\bullet}$ and $OH^{\bullet}$ are not affected significantly by reactions in the aqueous phase or with liberated chlorine species throughout the span of the experimental simulations—an assumption found correct by a posteriori analyses. This assumption is not satisfied for H_2O_2 in any model simulation including surface chemistry mechanisms as described below.

[64] Second, the determination of the surface area and volume of the aerosol population is subject to significant error. In all three of the experiments presented in this paper, careful attempts are made to introduce equivalent aerosol populations using the same laboratory procedures. The aerosol population is counted by a condensation particle counter and measured by a differential mobility analyzer (DMA) twice before and twice after the experiment. In order to minimize error in volume and surface area calculations, each output from the DMA (cutoff radius ~0.5 μm) is fit to a lognormal distribution, integrated over all droplet radii and an average over the four measurements is obtained due to the complexities associated with particle coagulation, loss during API-MS sampling and condensation to chamber walls. There is a +60% difference in aerosol volume and +85% difference in surface area when comparing the low ozone and high ozone experiments. Even though the variations appear genuine, the extent to which these differences could be attributable to errors in aerosol measurement or to the lognormal assumption is unclear—at best, the four-sample averaged lognormal fit can only estimate and not affirm the dimensions of the particles in the region $R_p \geq 0.5$ μm, and it does not consider particle volume adhered to the chamber walls. These possible "errors" cannot justify the thousand fold discrepancy in Cl_2 concentrations in base case model simulations, but should be considered when evaluating the suitability of a potential surface mechanism. In all simulations, the values for surface area and volume, as well as the radius used in the mass transfer and aqueous-phase diffusion equations, are determined using the four sample averaged log normal fit parameters.

[65] The initial rate of Cl_2 formation, calculated from the concentration after 2 min of photolysis, if resultant from a surface reaction is expected adhere to an expression given by:

$$R = \gamma_s \frac{\bar{c}}{4} A[\mathrm{G}]. \tag{45}$$

where [G] is the average concentration of the reacting species and all other variables are as defined in section 2.7. For all experiments, estimates of the initial Cl_2 production rate fall in the narrow range of $4.2–5.9 \times 10^9$ molecule cm^{-3} s^{-1} correlating better with the prediction of a narrow range of initial (averaged over the first 2 min) $OH^{\bullet}$ concentrations, $1.1–1.3 \times 10^{10}$ molecule cm^{-3}, than with the prediction of much wider ranges of initial $[HO_2^{\bullet}]$, $2.3–8.1 \times 10^{10}$ molecule cm^{-3}, and initial $[O_3]$, $0.6–3.0 \times 10^{14}$ molecule cm^{-3}. The middle and high initial O_3 experiments showed remarkably similar Cl_2 formation rates (within 3%) even though aerosol measurements yield 40% more surface area in the latter experiment. Considering the product of gas concentration and surface area, the results are still more consistent with $OH^{\bullet}$ as the reactive species both considering and neglecting the potential errors of aerosol measurement.

[66] The overall surface mechanism proposed is equation (30). The overall enthalpy change of the reaction is calculated at -230.6 kJ mol^{-1} [*Lide*, 1998]; the proposed surface mechanism is exothermic and thermodynamically favorable. The formation of a chloride–hydroxyl complex is assumed to be the rate determining step of the overall reaction (30); the possible fates of the $OH{\bullet\bullet\bullet}Cl^{\bullet-}_{surface}$ species are discussed subsequently. The overall rate of Cl_2 formation is calculated according to equations (28) and (29) from section 2.7. An optimal value of 2 for γ_s' is obtained by fitting Cl_2 predictions to the results of the middle ozone experiments.

[67] Figures 5, 6, and 7 illustrate that for all experiments, including the higher and lower initial ozone concentration experiments, the correspondence of the model results to the experimental data (given the level of uncertainties inherent to the model and in the experiments) is quite good; the modeled Cl_2 concentration profiles are essentially correct with maximum deviations bounded by 2/3 and 1 2/3 multiples of the experimental data. Regardless of the details of the elementary reactions, the model results support the theory of a surface-enhanced Cl_2 generation mechanism.

[68] The present authors in joint investigation with theoretical and experimental chemical researchers [*Knipping et al.*, 2000] presented as a primary hypothesis that the product of the initial reaction between the approaching gas-phase hydroxyl radical and the exposed surface chloride ions is a relatively stable surface complex, $OH{\bullet\bullet\bullet}Cl^{\bullet-}_{surface}$ (equation (27)). No experiments have proven the existence of $OH{\bullet\bullet\bullet}Cl^{\bullet-}_{surface}$; this postulate is offered above all to inspire

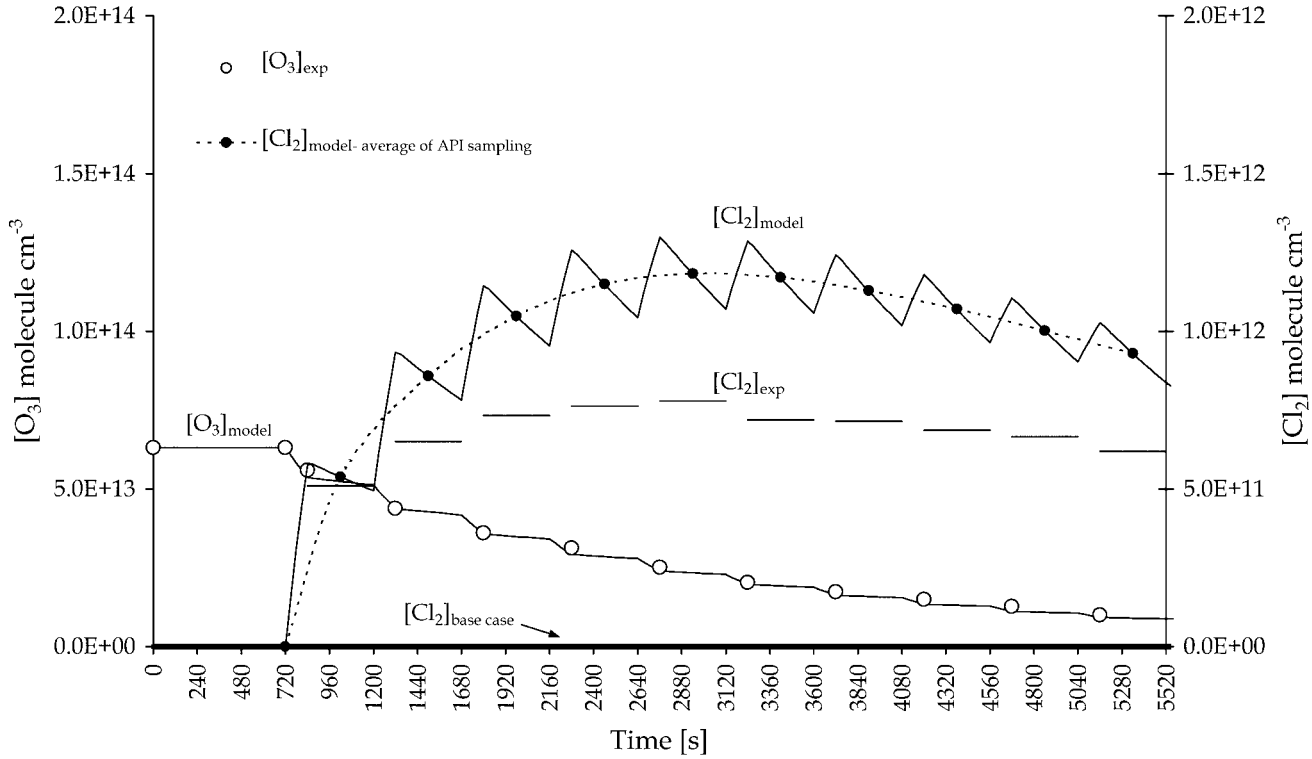

Figure 5. Experimental and model Cl_2 time series using proposed interfacial mechanism: low ozone experiment.

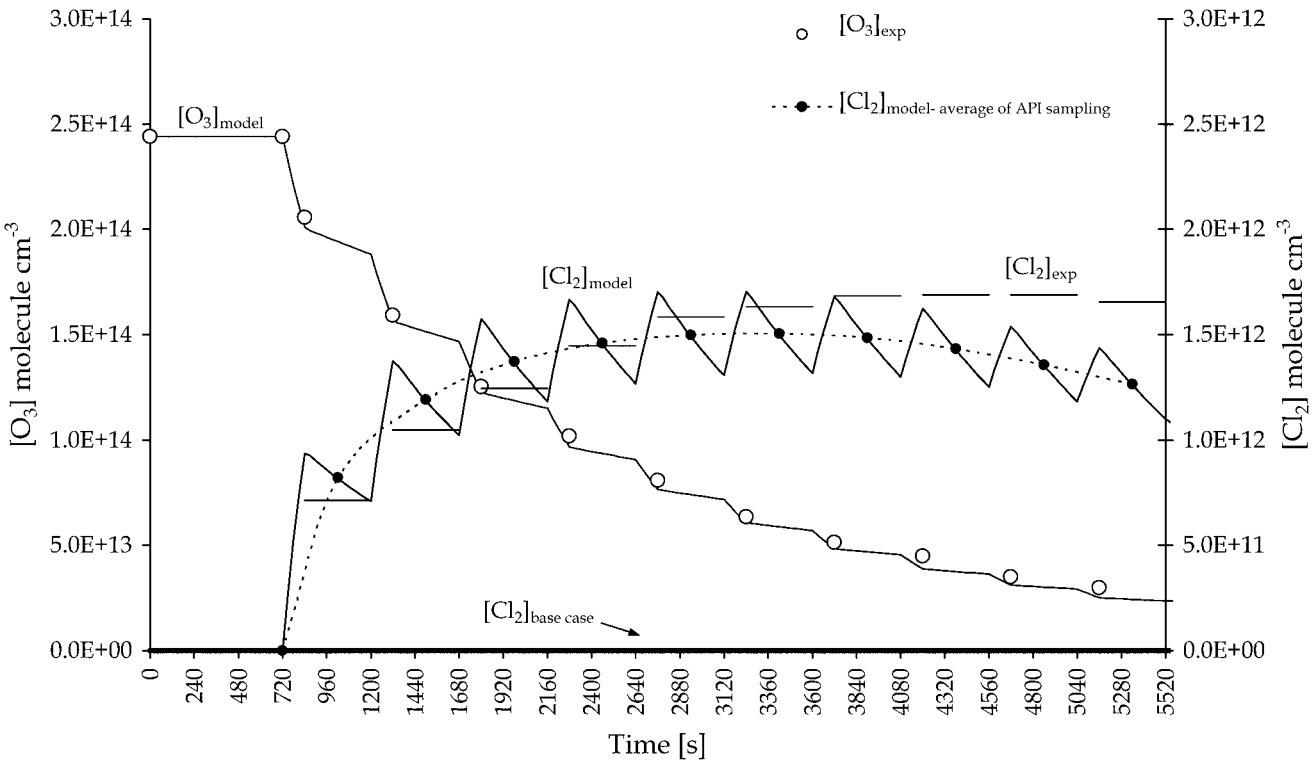

Figure 6. Experimental and model Cl_2 time series using proposed interfacial mechanism: middle ozone experiment.

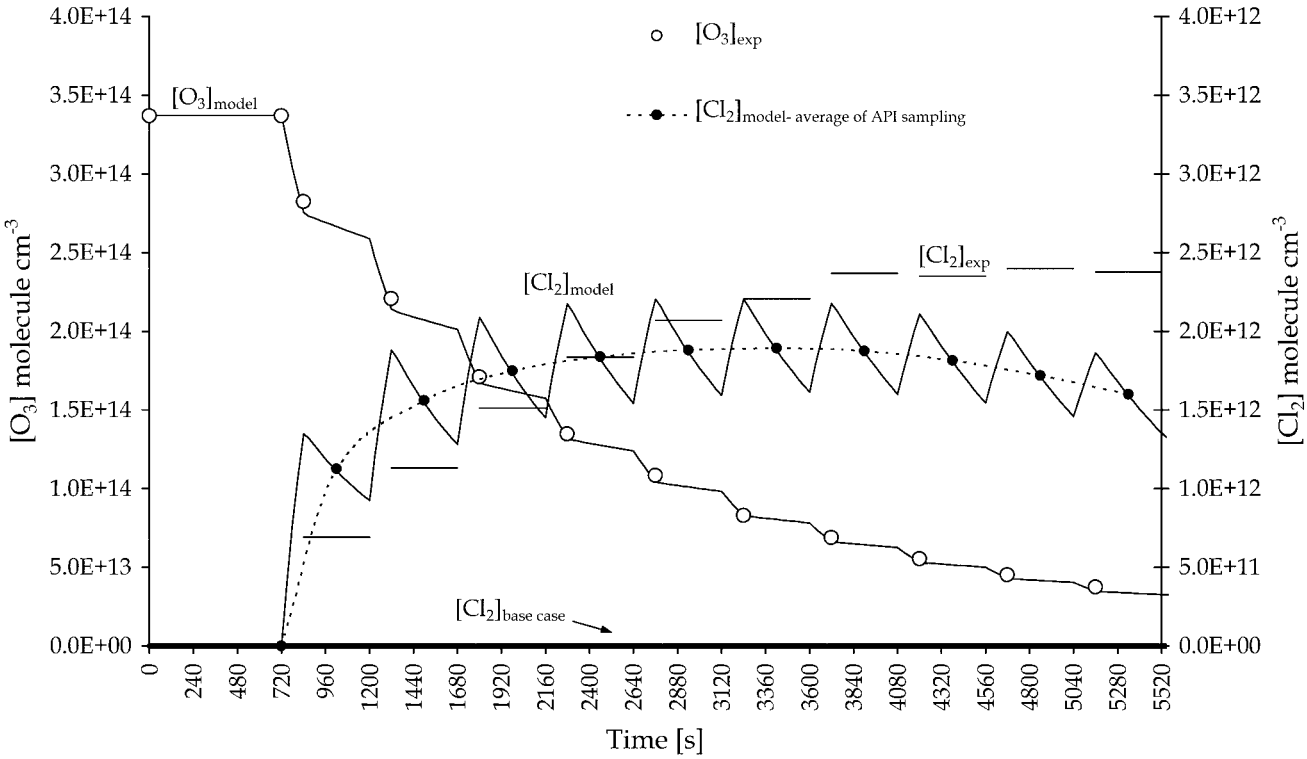

Figure 7. Experimental and model Cl_2 time series using proposed interfacial mechanism: high ozone experiment.

the search for evidence/counterevidence and arouse insightful feedback. Still, the adequacy of the overall rate expression is not dependent on the existence of the chloride–hydroxyl complex even though the basis is motivated by the formation of such a species.

[69] Two fates of the proposed surface chloride–hydroxyl radical ion have been considered. In both cases the bound complex, $OH\bullet\bullet\bullet Cl^-_{surface}$, is assumed to remain in a 1 nm shell (~6 × the ionic radius of Cl^-, 1.81 Å) on the exterior of the droplet, as suggested by density profiles of sodium, chloride and oxygen atoms in water slabs [*Jungwirth and Tobias*, 2000]. The species should be only somewhat stable and therefore undergo decomposition back to reactants

$$OH \bullet\bullet\bullet Cl^{\bullet-}_{surface} \rightarrow OH^{\bullet}_{g} + Cl^-_{aq,surface} \qquad (46)$$

[70] The first prospective fate of the bound complex, illustrated in Figure 8, is the self-reaction

$$OH \bullet\bullet\bullet Cl^{\bullet-}_{surface} + OH \bullet\bullet\bullet Cl^{\bullet-}_{surface} \rightarrow Cl_{2,g} + 2\ OH^-_{aq}. \qquad (47)$$

Due to similarity with the $Cl_2^{\bullet-}$ radical ion, the rate constant of reaction 47 can be estimated from $Cl_2^{\bullet-}$ recombination at $1.8 \times 10^9\ M^{-1}\ s^{-1}$ [*Jacobi et al.*, 1999]. Alternatively, $OH\bullet\bullet\bullet Cl^{\bullet-}_{surface}$ may react directly with surface chloride ions to form $Cl_2^{\bullet-}$ and OH^-. The rate constant for this reaction is matched to the rate constant for the reaction of $HOCl^{\bullet-}$ and Cl^-, i.e., $1 \times 10^4\ M^{-1}\ s^{-1}$ [*Grigor'ev et al.*, 1987]. The $Cl_2^{\bullet-}$ radical anion is assumed to stabilize at the interface where it may build-up in concentration and self-react to form Cl_2 and two chloride ions, or react with another $OH\bullet\bullet\bullet Cl^-_{surface}$ to form Cl_2 and separate chloride and hydroxide ions; preliminary molecular dynamic simulations indicate that $Cl_2^{\bullet-}$, once formed, could indeed remain anchored at the surface of concentrated aqueous particles (P. Jungwirth, personal communication). In both cases, the rate of $OH\bullet\bullet\bullet Cl^{\bullet-}_{surface}$ decomposition must be regulated to $\sim 10^4\ s^{-1}$ in order to guarantee formation of $OH\bullet\bullet\bullet Cl^{\bullet-}_{surface}$ as the rate-limiting step in Cl_2 generation.

[71] An unbiased assessment of the overall mechanism of chlorine production (30) leads to the proposal of a debatably more straightforward product during the reaction of $OH^{\bullet}$ and Cl^-, the $HOCl^{\bullet-}$ species originally reported by *Jayson et al.* [1973]. The differences between the surface complex $OH\bullet\bullet\bullet Cl^{\bullet-}_{surface}$ and the bulk species $HOCl^{\bullet-}$ may or may not be subtle and further research is warranted. *Jayson et al.* [1973] calculated an absorption spectrum for a species in solution they denoted as $HOCl^{\bullet-}$. Aqueous-phase radical chemistry mechanisms based on this species are still undergoing much investigation [*McElroy*, 1990; *Buxton et al.*, 1998; *Alegre et al.*, 2000]. However, in studies of the transition state of the reaction

$$O(^3P) + HCl \rightarrow OH^{\bullet} + Cl^{\bullet}, \qquad (48)$$

Davis et al. [1994] concluded that an $OHCl^-$ ion formed in the gas phase by electron impact of a mixture of HCl and N_2O is best represented as $OH\bullet\bullet\bullet Cl^-$ and calculated a photodetachment spectrum for the species. Electron spin resonance (ESR) studies of Cl^- in frozen aqueous solution and molecular orbital theory calculations by *Sevilla et al.* [1997] support the existence of a Cl-H_2O adduct in solution

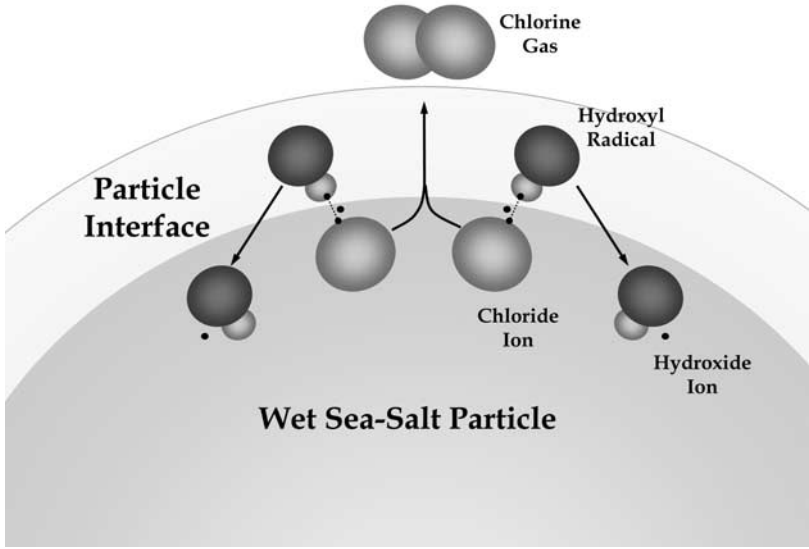

Figure 8. Potential mechanism for Cl_2 production.

rather than Cl-OH$^-$. These studies showed ion–dipole interactions between the hydrogen of OH$^\bullet$ and chloride ion could generate an OH•••Cl$^-$ complex, but it also determined that the bond strength of a Cl$^-$•••HO(H_2O)*n* structure decreased as the number of hydrating waters, *n*, increased. The evidence suggests that the presence of an OH•••Cl$^{\bullet-}$ complex is likely only at gas–liquid interfaces, while the structure of the bulk HOCl$^{\bullet-}$ species could be better represented as Cl(H_2O)-OH$^{\bullet-}$. At any rate, model simulations performed where HOCl$^{\bullet-}$ is produced at the interface, followed by diffusion and reaction in the bulk of the droplet, predict low Cl_2 levels similar to the results of the base case simulation.

[72] Other fates of the OH•••Cl$^{\bullet-}_{surface}$ complex or surface anchored $Cl_2^{\bullet-}$ have been explored without success (e.g., if Cl_2 is generated by electron photodetachment of $Cl_2^{\bullet-}$ within the droplet, using $\sigma = 200 \times 10^{-20}$ cm^2 at 254 nm [*Adams et al.*, 1995], significant induction times and incorrect peak [Cl_2] values are predicted). The viability of the principal mechanisms presented here underscores the importance of further investigating concentrated salt aerosol interfaces.

3.3. Sensitivity Studies of the Overall Interfacial Mechanisms

[73] The sensitivities of Cl_2 formation with respect to model parameters for simulations incorporating the overall interfacial mechanism (30) and kinetic rate expression (28) are presented as normalized Jacobian terms shown on Table 8. There is no evidence that the observed Cl_2 formation in these model simulations can be drastically (on the scale of orders of magnitude) altered by small perturbations of the listed parameters, but the sensitivity results, together with a thorough inspection of the simulation output, do indicate that there are several parameters that could significantly affect the intensity and temporal behavior of the modeled Cl_2 production.

[74] The principal source of Cl_2 in these simulations is the reaction at the interface. This interfacial mechanism produces hydroxide ions in solution thus increasing pH. After the first 2 min of photolysis, the model predicts that particle pH levels rise to ~10.5 and gradually reach a value near 10.8 at the end of the simulation. Any contributions from the reactions of HOCl with Cl$^-$, in the presence and absence of H$^+$, as well as the recombination of $Cl_2^{\bullet-}$ in bulk solution are negligible. Due to the increased alkalinity of the droplets, Cl_2 decomposition reactions with OH$^-$, HO_2^- and CO_3^{2-} become major loss routes for Cl_2. The rate of chlorine loss due to these aqueous-phase reactions is greater than the effect of dilution and wall loss, but the importance of the latter pair is heightened by their ability remove available chlorine from the modeled system. The sensitivity results show that as total particle surface area is increased, the final levels of Cl_2 increase due to the enhancement of the surface reaction. However, as the liquid water content of the aerosol increases, final Cl_2 levels decrease due to the efficient loss processes for dissolved chlorine in alkaline aqueous solution. These two results alone indicate that optimal Cl_2 is likely when the surface to volume ratio is maximized, i.e., smaller particles. (As expected, in simulations where the pH of the particles remains low and the interfacial mechanism is excluded, an increase of aerosol volume increases the final [Cl_2] in an essentially linear fashion.)

[75] The sensitivity of Cl_2 formation to particle size, independent of overall volume and surface area, is intriguing. The chlorine production is insensitive to the radius of the particles used in determining the mass transfer terms, k_{mt}, but is moderately sensitive to the radius of the particles used in determining the spatially averaged aqueous-phase reactions rates, i.e., the radius used in determining the extent of the aqueous-phase diffusion limitation. In the current model, these two radii are equivalent, but the sensitivities are determined separately in order to distinguish between the two limitations to mass transfer. Whereas the sensitivity to the liquid water content and surface area indicates that smaller particles, i.e., large surface to volume ratios, are most favorable to chlorine production, the sensitivity to the

mass transfer and aqueous-phase diffusion limitations indicate that larger particles are better Cl_2 generators.

[76] These results suggest the existence in the chamber, and possibly the atmosphere, of an ideal particle size for Cl_2 activation; however, the value of this optimal size is not explored. (The equations interrelating relative humidity to particle size and salt concentration [*Pruppacher and Klett*, 1997] are complex. A study to determine how the singular effects contributing and limiting Cl_2 production change with increasing particle size would yield an optimization problem with many interdependent parameters.) The sensitivity studies presented here are performed with all variables independent of each other. For example, both the droplet radius (and thus surface area and volume) and the initial sodium chloride concentration are expected to depend on relative humidity, yet all these parameters were explored individually. The advantage of this uncoupled analysis is manifest in the sensitivity (recalling that the sensitivity is a local derivative calculated at normal unperturbed conditions) to initial [NaCl]: in the base case, an increase in initial concentration causes a decrease in final $[Cl_2]$ due to the increase in ionic strength and the consequent kinetic salt effect enhancement of k_{1213} (which is much more pronounced than the enhancement on k_{1116}); while in the constant pH simulation, an increase in ionic strength causes a decrease in final $[Cl_2]$ due to a kinetic salt effect interference on k_{1133}; in both simulations, variations in the ionic strength also cause modifications in the calculation of effective Henry's law constants and acid/base equilibrium constants that ultimately result in an impediment to Cl_2 formation. On the other hand, in the interfacial mechanism, higher initial concentrations of sodium chloride are very effective in generating an increase in Cl_2 due to the amplification of the surface reaction.

[77] Indeed, the interfacial sensitivity studies show that higher salt concentrations are more effective in increasing chlorine production than are higher concentrations of O_3 or CO_2. Nonetheless, the effect of CO_2 is rather considerable in the system. While the interfacial mechanism does not require a contribution of H^+ for Cl_2 production, the chlorine decomposition rate, as discussed earlier, is highly dependent on the droplet pH. The presence of carbon dioxide provides sufficient buffering and keeps modeled pH values in the range of 10.5–10.8, whereas if no CO_2 were present the droplets would reach modeled pH values of $\sim$13 and Cl_2 production would be greatly restricted. (Although the presence of CO_3^{2-} does add another aqueous-phase loss for Cl_2, lowering the effectiveness of the reaction with hydroxide ion is much more effective for maintaining higher Cl_2 values.) CO_2 is present in the chamber at concentrations near 17 ppm. Model evaluations determine that Cl_2 production due to the proposed mechanism is insensitive to the exact value of $[CO_2]$ when initial concentrations are above 10 ppm. However, a significant drop in peak $[Cl_2]$ is revealed for lesser initial carbon dioxide concentrations, and a sharp decline is evident when $[CO_2]_0$ decreases below $\sim$1 ppm. The role of CO_2 with respect to chlorine generation has been indicated recently in studies of the thermal decomposition of ozone in sodium chloride solutions [*Levanov et al.*, 2000].

[78] In the kinetic expression of the overall interfacial mechanism, the magnitude of the free variable, γ_s', is adjusted in order to obtain an optimal match to the production rate and peak values of chlorine in the laboratory chamber. Model evaluations yield an optimum value $\gamma_s' = 2$. Although it is not immediately intuitive that γ_s' should posses a value greater than unity, there are arguments in support of higher values. (However, the condition $\gamma_s \leq 1$ must be constantly upheld.) Practically converged quantum chemical calculations suggest that surface chloride ions in effect attract approaching hydroxyl radicals [*Knipping et al.*, 2000], thus enhancing the rate of scavenging. Such an enhancement due to attractive forces is analogous to the increase of reaction rates beyond the predicted aqueous-phase diffusion-controlled limit exhibited by proton transfer reactions [*Benson*, 1960]. Furthermore, there are indications that $OH^\bullet$ radicals could "roll" on aqueous surfaces. As a result, γ_s' may have a functional form different than a simple constant value and an alternative model for the overall interfacial mechanism rate could be better suited. The sensitivity of Cl_2 levels to γ_s' is high and further studies should be performed in order to better determine the character of this variable.

[79] Figure 9 shows time series depicting the rate of Cl_2 production and loss corresponding to the major chemical and physical processes. Although the rate of reaction of Cl_2 with $OH^\bullet$ in the gas phase is considerable, the formation of chlorine via the proposed interfacial mechanism is an order of magnitude higher resulting in an overall net production effect for $OH^\bullet$. The effects of experimental processes such as the small amount of Cl_2 photolysis, irreversible losses to the walls and dilution during API-MS sampling, are quite significant. (The uncertainty of the dilution factor is much less than one percent thus lowering the impact of its high sensitivity.) Nonetheless, the rate of Cl_2 production is predominated by production at the interface and losses in the aqueous phase. The uncertainties associated with the rate constants for the three main alkaline Cl_2 decomposition processes—reaction with OH^-, HO_2^- and CO_3^{2-}—are rather high, amplifying their sensitivity and hence their importance in developing mathematical chemistry models capable of accurately reproducing Cl_2 concentrations for variable conditions. Due to the importance and uncertainty of these alkaline chlorine decomposition reactions, a brief review of their study and the basis for selecting rate constants is provided in the following sections. In addition, Table 9 illustrates the sensitivity of peak and final model Cl_2 concentration values, expressed as the average concentration measured during the corresponding API dark sampling period, to order-of-magnitude changes in the selected rate constants for these alkaline Cl_2 decomposition processes within the limits reported in the scientific literature.

[80] The uncertainties regarding the geometric parameters (e.g., surface area and liquid water content) of the experimental aerosol populations were discussed in the previous section. Together with the results of these sensitivity analyses, especially given the uncertainties with respect to alkaline Cl_2 decomposition processes, the discrepancies between the lower and higher ozone model results and the experimental data can be explained by variations in model input and/or parameters. These sensitivity studies conclude a methodological analysis of the chemical system. The complete analysis strongly corroborates the suggestion of

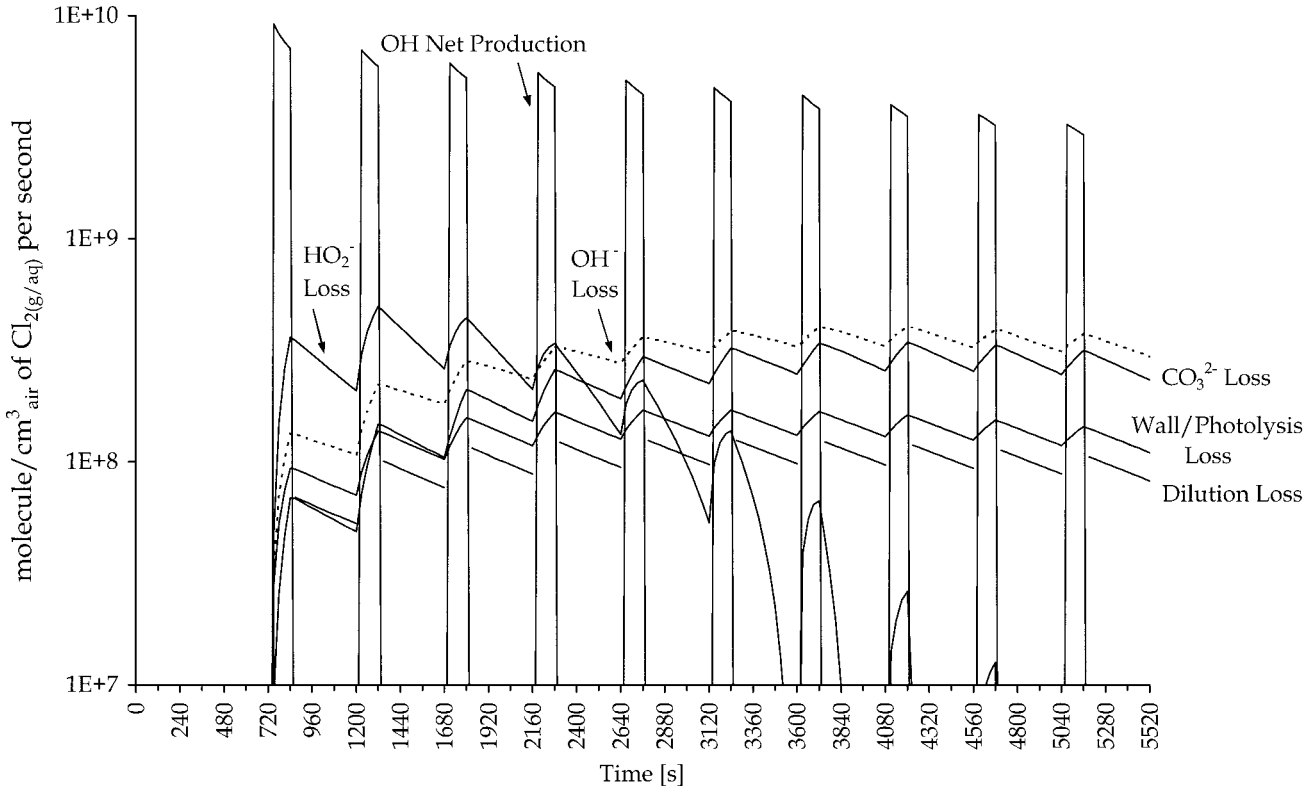

Figure 9. Rates of major Cl_2 production and loss routes.

a Cl_2 production mechanism initiated and limited by the reaction of Cl^- and $OH^\bullet$ at aqueous interfaces.

4. Decomposition of Chlorine in Alkaline Solution

[81] The most significant sink for molecular chlorine in the experimental chamber, according to the interfacial modeling results, is its reaction with hydroxide within the droplets. This aqueous-phase reaction may of modest concern in the real atmosphere as marine aerosol pH values alkalinity most commonly remain below 8 [*Keene et al.*, 1998; *Keene and Savoie*, 1998, 1999; *Erickson et al.*, 1999; *Fridlind and Jacobson*, 2000] with a few exceptions such as within crustal dust plumes over marine regions. However, this reaction is of paramount importance in these experimental studies where model predicted pH values approach 11. Given its vital impact to these findings, a review of this reaction is warranted. In particular, the methods previously used to estimate the rate constant for the reaction of Cl_2 and OH^- are examined and the basis for selecting a value for use in the aqueous-phase chemical mechanism of MAGIC is presented. In addition, the other major alkaline chlorine decomposition processes, reaction with CO_3^{2-} and HO_2^-, are also examined.

4.1. Linear Free Energy Relations

[82] In the analyses of the reaction of chlorine with hydroxide, and chlorine hydrolysis in general, two topics commonly arise: the application of linear free energy relations and the pursuit of evidence regarding the composition of the intermediate species. Linear free energy relations include the Bronsted–Pedersen relations for acid or

Table 9. Sensitivity of Peak and Final Cl_2 Concentrations Within Limits of Key Reaction Rate Constants

k_{1134}	k_{1135}	k_{1137}	k_{1215}	k_{1217}	$[Cl_2]_{peak}$	$[Cl_2]_{final}$
$M^{-1}\ s^{-1}$	$M^{-1}\ s^{-1}$	$M^{-1}\ s^{-1}$	$M^{-1}\ s^{-1}$	$M^{-1}\ s^{-1}$	molecule cm^{-3}	molecule cm^{-3}
1.0×10^8	**2.0×10^{-3}**	**1.1×10^8**	**1.4×10^5**	**0.012**	1.50×10^{12}	1.26×10^{12}
1.0×10^6	2.0×10^{-5}				1.68×10^{12}	1.51×10^{12}
1.0×10^7	2.0×10^{-4}				1.66×10^{12}	1.48×10^{12}
1.0×10^9	2.0×10^{-2}				1.02×10^{12}	6.85×10^{11}
1.0×10^{10}	2.0×10^{-1}				5.05×10^{11}	2.60×10^{11}
		1.1×10^6			1.60×10^{12}	1.26×10^{12}
		1.1×10^7			1.62×10^{12}	1.26×10^{12}
		1.1×10^9			1.27×10^{12}	1.25×10^{12}
			1.4×10^3	1.2×10^{-4}	1.62×10^{12}	1.44×10^{12}
			1.4×10^4	1.2×10^{-3}	1.64×10^{12}	1.47×10^{12}
			1.4×10^6	0.12	1.13×10^{12}	7.84×10^{11}

Bold values on first line are as listed on Table 5. Only values changed in the sensitivity runs are listed on other lines.

Table 10. Summary of Bronsted–Pedersen Relationship Parameters for Base-Assisted Cl_2 Hydrolysis ($Cl_2 + H_2O + A^- \rightleftharpoons HOCl + Cl^- + HA$)[a]

HA	A^-	p	q	pK_a	$k_{\rightarrow}$, M^{-1} s^{-1}	$\log(K_a q/p)$	$\log(k_{\rightarrow}/q)$	Residuals fit with H_3O^+[b]	Residuals fit w/o H_3O^+[c]	Comments
H_3O^+	H_2O	3	2	−1.74	1.6×10^{-1}	1.56	−1.10	0.084		
HSO_4^-	SO_4^{2-}	1	4	1.27	3.2×10^1	−0.67	0.90	0.166	0.005	
$CHCl_2COOH$	$CHCl_2COO^-$	1	2	1.30	2.7×10^1	−1.00	1.13	0.198	0.024	d
H_3PO_4	$H_2PO_4^-$	3	2	1.75	4.5×10^1	−1.93	1.35	0.015	0.001	
$CH_3ClCOOH$	CH_3ClCOO^-	1	2	2.81	9.7×10^1	−2.51	1.69	0.014	0.002	
HCOOH	$HCOO^-$	1	2	3.72	1.2×10^2	−3.42	1.78	0.104	0.068	
CH_3COOH	CH_3COO^-	1	2	4.76	9.4×10^2	−4.46	2.67	0.001	0.032	
								ΣRes. = 0.582	ΣRes. = 0.131	
								$r^2 = 0.932$	$r^2 = 0.937$	e
								$\chi^2 = 0.116$	$\chi^2 = 0.033$	e
Extrapolated points										
$CO_2 \bullet H_2O$	HCO_3^-	2	2	6.08	3.2×10^3	−6.08	3.21			f
HCO_3^-	CO_3^{2-}	1	3	9.90	1.4×10^5	−9.42	4.67			f
H_2O_2	HO_2^{2-}	2	3	11.60	1.1×10^6	−11.43	5.55			f,g
H_2O	OH^-	2	3	15.74	6.9×10^7	−15.56	7.36			f

[a] Data obtained from the work of *Wang and Margerum* [1994] and references therein at $T = 15°C$ and $I = 0.5$ M.
[b] $\beta = 0.583$, $G_B = 0.541$.
[c] $\beta = 0.483$, $G_B = 0.106$.
[d] Obtained from the work of *Lifshitz and Perlmutter-Hayman* [1962] and corrected for temperature and ionic strength effects. Point not used in derivation of fits (thus, results are comparable to fit by *Wang and Margerum* [1994]) but included in r-squared and chi-squared calculations.
[e] $r^2 = 0.953$, $\chi^2 = 0.096$ (with H_3O^+) and $r^2 = 0.937$, $\chi^2 = 0.036$ (without H_3O^+) if $CHCl_2COOH$ point omitted from statistical calculations.
[f] $k_{\rightarrow}$ values calculated using Bronsted–Pedersen fit without H_3O^+.
[g] Direct reaction with HO_2^- to form HOOCl and Cl^- overwhelms potential contribution via base-assisted mechanism (see section 4.2).

base catalyzed reactions [*Benson*, 1960; *Bell*, 1973] and the Swain–Scott relation [*Swain and Scott*, 1953]. In the case of chlorine hydrolysis, studies have shown clear evidence for a base-assisted forward reaction and acid-assisted reverse reaction [*Lifshitz and Perlmutter-Hayman*, 1961, 1962; *Wang and Margerum*, 1994]. *Wang and Margerum* [1994] present a general hydrolysis mechanism consisting of Cl^+ and proton transfers between the reactants and the transition state, as shown by

$$A^- \cdots H - \overset{\overset{\displaystyle H}{|}}{O} \cdots Cl - Cl \rightleftharpoons \left[A^- \cdots H^+ \cdots \overset{\overset{\displaystyle H}{|}}{O^-} \cdots Cl^+ - Cl^- \right]^{\neq} \rightleftharpoons AH \cdots \overset{\overset{\displaystyle H}{|}}{O} - Cl \cdots Cl^- \tag{49}$$

Whereas the nature of the actual intermediate(s) formed during these reactions is still a subject of much debate, the rate constants for the overall reactions,

$$Cl_2 + H_2O + A^- \rightleftharpoons HOCl + Cl^- + HA, \tag{50}$$

are found proportional to the acid–base strength of the catalyst, in agreement with the Bronsted–Pedersen equations,

$$\log\left(\frac{k_{\rightarrow}}{q}\right) = \log G_B - \beta \log\left(\frac{K_a q}{p}\right) \tag{51}$$

$$\log\left(\frac{k_{\leftarrow}}{p}\right) = \log G_A + \alpha \log\left(\frac{K_a q}{p}\right) \tag{52}$$

where K_a is the acid dissociation constant of HA, p is the number of dissociable equally bound protons (equivalent protons) on HA, and q is the number of positions that can attach a proton (equivalent basic sites) on the conjugate base A^-. The constants α and β are measures of the amount of free energy change of ionization attributed to the formation of the transition state and theoretically add up to unity, while G_A and G_B are proportionality constants. Table 10 lists the literature values of $k_{\rightarrow}$ and for several acid/base pairs. Figure 10 illustrates the Bronsted–Pedersen relationship as a plot of $\log(k_{\rightarrow}/q)$ versus $\log(K_a q/p)$; the slope of the line and intercept are given by β and G_B, respectively. (A similar line for $\log(k_{\leftarrow}/q)$ versus $\log(K_a q/p)$, where the slope and intercept are given by α and G_B, is not shown in order to minimize clutter.) Included in Table 10 is the rate constraint for the hydrolysis of chlorine. In this case, reaction (50) is written so that the acid/base pair is taken as the hydronium ion, H_3O^+, and water,

$$Cl_2 + H_2O + H_2O \rightleftharpoons HOCl + Cl^- + H_3O^+. \tag{53}$$

This point has been used by the previously cited researchers to extrapolate the value for the case of the acid/base pair of water and hydroxide, i.e.,

$$Cl_2 + H_2O + OH^- \rightleftharpoons HOCl + Cl^- + H_2O. \tag{54}$$

However, the validity of the HA/A^- pairs H_3O^+/H_2O and H_2O/OH^- in the Bronsted–Pedersen relation is debatable. (The argument applies specifically for the relation as given by equations (51) and (52).) Significant departures from the linear free energy relation are not uncommon, with deviations near three orders of magnitude reported for other reactions of halogens in water [*Nagy et al.*, 1988; *Kumar and Margerum*, 1987; *Beckwith et al.*, 1996].

[83] A full discussion on the legitimacy of the species H_3O^+, H_2O and OH^- in the Bronsted–Pedersen relation is provided elsewhere [*Bell*, 1973, and references therein]. In brief, the linear free energy relation has been shown valid for catalysts of similar chemical type and charge. Some

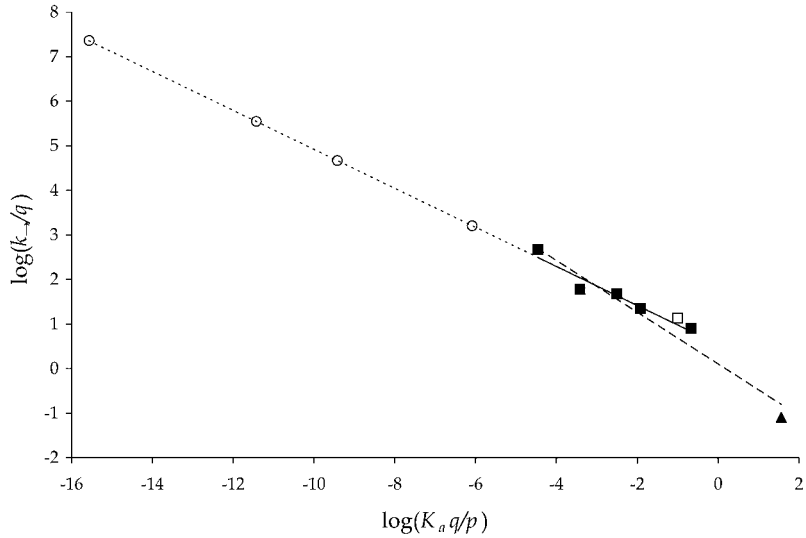

Figure 10. Bronsted–Pedersen chart for the reaction $Cl_2 + H_2O + A^- \rightleftharpoons HOCl + Cl^- + HA$ (see Table 10 for details): ■: experimental points used in original and alternate fit; □: experimental dichloroacetate point not used in either fit; ○: extrapolated points using alternate fit; ——: alternate fit; - - - -: alternate extrapolation; ▲: H_3O^+/H_2O point used in original fit; – – –: original fit by *Wang and Margerum* [1994].

curvature to the relation has been found when considering dissimilar acids and bases, always showing a tendency of lowering slope (smaller α or β values) with increasing rate constants (larger *pK* values). The curvature becomes more apparent by inclusion of H_3O^+, H_2O and OH^-; these species are of different chemical type and frequently of different charge than the other acids or bases employed in catalysis studies. As a result, the hydroxide ion and (to a lesser extent) the hydronium ion have been found to frequently exhibit a catalytic effect several orders of magnitude lower than that predicted by the Bronsted–Pedersen relation.

[84] In view of the available evidence, it is entirely conceivable that inclusion of H_2O, a neutral species and the solvent, in the analysis of halogen hydrolysis assisted by negatively charged bases could lead to erroneous predictions by Bronsted–Pedersen extrapolations to hydroxide-assisted reactions. In the case of Cl_2 hydrolysis, a detailed inspection shows that two data sets, one including and another excluding the H_3O^+/H_2O point, yield similarly high coefficients of linear correlation (r^2). However, a better fit ($\sim 3\times$) to the data—as measured by the normalized chi-square merit function (χ^2) with all points equally weighted—is obtained by neglecting the data point for H_3O^+/H_2O (see Table 10 and Figure 10). Extrapolating the better fit to reaction with OH^-, the rate constant is predicted at 6.9×10^7 M^{-1} s^{-1} at 298 K and $I = 0.5$ M. The extrapolation overestimates the rate constant for reaction with H_2O by a factor of ~ 9, as expected from previous arguments.

[85] Several studies of the specific and acid-assisted attack on the halogen of hypohalous acids by nucleophilic reagents [*Nagy et al.*, 1988; *Gerritsen and Margerum*, 1990; *Wang and Margerum*, 1994; *Beckwith et al.*, 1996], in particular halide ions, have shown that the rate constants for these reactions appear to follow the Swain–Scott relationship. However, most analyses using this linear free energy relation are based on a limited amount of experimental points (usually three) corresponding to permutations of studies of HOCl, HOBr and HOI reactions with Cl^-, Br^- and I^-. In the specific case of the reaction of HOCl with nucleophilic anions (equivalent to the acid-assisted reverse hydrolysis reaction with HA = H_2O) [*Gerritsen and Margerum*, 1990], the other nucleophiles considered, CN^- and SO_3^{2-}, have nucleophilicities so similar to Cl^- (and correspondingly similar rate constants) that an indisputable preference between the previously discussed Bronsted–Pedersen extrapolations for the reaction of Cl_2 with hydroxide cannot be established from Swain–Scott analysis of the reverse reaction.

[86] In essence, the determination of the mechanisms of chlorine hydrolysis appears tantamount to the explanation of the transition state(s). Several intermediates have been explored in order to explain the hydrolysis of chlorine in aqueous solution including Cl_2OH^-, H_2OCl_2, and H_2OCl^+ [*Bell and Gelles*, 1951; *Anbar and Taube*, 1958; *Anbar, et al.*, 1959; *Eigen and Kustin*, 1962; *Swain and Crist*, 1971; *Held et al.*, 1978; *Wang and Margerum*, 1994; *Dahl and Roeggen*, 1996; *Donaldson et al.*, 1997; *Liu et al.*, 1999]. However, a molecular-scale analysis of chlorine hydrolysis is beyond the scope of this paper.

4.2. Reaction of Dissolved Cl_2 with OH^-: Rate Constant Determination

[87] The reaction between Cl_2 and OH^- has been studied extensively, due in particular to its commercial applications in bleaching and disinfection processes. Early calculations of the rate constant of the $Cl_2 + OH^-$ reaction as 8.3×10^{12} M^{-1} s^{-1} [*Morris*, 1946] were fraught with error [*Anbar and Taube*, 1958], yielding a value that exceeds even the rate constant of proton transfer reactions ($\sim 10^{11}$ M^{-1} s^{-1}), e.g., the reaction between H_3O^+ with OH^- or SO_4^{2-} [*Benson*, 1960]. Progress was made when *Lifshitz and Perlmutter-Hayman* [1960, 1961] studied the rate of chlorine hydrolysis in pure water and in the presence of an acetate buffer at 282.5 K. Their initial studies estimated the rate constant for the reaction of Cl_2 with hydroxide at 9×10^{10} M^{-1} s^{-1}, but

Table 11. Summary of Reported Rate Constants for the Reaction $Cl_2 + OH^- \rightleftharpoons HOCl + Cl^-$ [a]

Year	Method	$k_{\rightarrow}$, M^{-1} s^{-1}	$\log(k_{\rightarrow})$	Reference
1946	Estimate	8.3×10^{12}	12.92	*Morris* [1946]
1961	Estimate	9.0×10^{10}	10.95	*Lifshitz and Perlmutter-Hayman* [1961]
1962a	Estimate	1.0×10^{10}	10.0	*Eigen and Kustin* [1962]
1962b	Bronsted–Pedersen Extrapolation	1.0×10^{9}	9.0	*Lifshitz and Perlmutter-Hayman* [1962]
1962c	Alternative Bronsted Extrapolation	1.0×10^{8}	8.0	Alternate interpretation of above data
1962d	Measurement	1.0×10^{6}	6.0	*Spalding* [1962]
1981	Measurement	2.7×10^{7}	7.43	*Sandall et al.* [1981]
1994a	Bronsted–Pedersen Extrapolation	4.1×10^{9}	9.61	*Wang and Margerum* [1994]
1994b	Alternative Bronsted–Pedersen Extrapolation	6.9×10^{7}	7.84	Alternate interpretation of above data, this work
1996	Measurement	1.6×10^{9}	9.19	*Ashour et al.* [1996]
2001	Measurement	5.0×10^{8}	8.70	Gershenzon et al. (in preparation)

[a] Measurements and extrapolations are taken at different temperatures (in the range 273–298 K) and ionic strengths (in the range $I < 1$ M).

this was modified promptly [*Lifshitz and Perlmutter-Hayman*, 1962] with a value of 10^9 M^{-1} s^{-1}. The lower rate constant value was derived from extrapolation of the Bronsted–Pedersen law to OH^- after observing evidence for a general base-assisted Cl_2 hydrolysis mechanism. The Bronsted–Pedersen parameters used in the extrapolation were obtained using only "the two most reliable" points, CH_3COO^-/CH_3COOH and $CH_2ClCOO^-/CH_2ClCOOH$. If all the points except for H_2O/H_3O^+ (questionable in the Bronsted–Pedersen relation, vide supra) and the point for $H_2PO_4^-/H_3PO_4$ (unclear due to possible parallel reactions involving $HPO_4^-/H_2PO_4^-$) are considered, the Bronsted–Pedersen extrapolation yields a value of $\sim 10^8$ M^{-1} s^{-1}. Lifshitz and Perlmutter-Hayman admit that "the extrapolation [to OH^-] is so far that it cannot be expected to be accurate. It would seem desirable to confirm the value of k_{OH^-} by additional evidence."

[88] *Eigen and Kustin* [1962] studied the kinetics of halogen hydrolysis by temperature-jump relaxation methods and estimated the rate of $Cl_2 + OH^-$ reaction at 10^{10} M^{-1} s^{-1}. This value has been widely cited although it was obtained from a mathematical analysis of experiments performed in the narrow and acidic pH range between 1 and 2.2 and involved important assumptions regarding the intermediate structures formed during hydrolysis.

[89] By analyzing chlorine absorption data in aqueous media (pH range of 1–14.2) using penetration theory, *Spalding* [1962] was able to define four distinct pH ranges (using H_2SO_4 and NaOH as buffers) that characterized Cl_2 absorption kinetics due to different hydrolysis effects. The reaction of Cl_2 with OH^- progressively governed the absorption rate as pH values increased above 10.5 until ultimately controlling the absorption rate at pH $\geq$ 12.5. Spalding estimated a rate constant for the $Cl_2 + OH^-$ reaction at 10^6 M^{-1} s^{-1}.

[90] A lack of consensus became apparent when Cl_2 absorption data obtained from a roller-drum reactor, analyzed using a surface renewal model, yielded a rate constant of 2.7×10^7 M^{-1} s^{-1} at 273 K for the chlorine hydroxide reaction [*Sandall et al.*, 1981]. No conclusion can be drawn about the room temperature rate constant as the authors did not explore this.

[91] *Wang and Margerum* [1994] examined the kinetics of reversible chlorine hydrolysis, reconciling disagreement in previously reported data by providing the temperature and ionic strength dependence of the forward and reverse reactions as well as the equilibrium constant. In addition, Wang and Margerum investigated general base assisted mechanisms for Cl_2 hydrolysis, augmenting the data of *Lifshitz and Perlmutter-Hayman* [1961, 1962] by evaluating the chlorine hydrolysis rate in the presence of sulfate and phosphate buffers using a stopped-flow method with spectrophotometric observation. The rate constants obtained were combined with those of Lifshitz and Perlmutter-Hayman for monochloroacetate, formate and acetate (after correcting for temperature and ionic strength effects) in order to obtain the parameters for the Bronsted–Pedersen equations. In doing so, the authors included the point for H_2O/H_3O^+ and extrapolated their "best fit" to the point for OH^-/H_2O obtaining a value of 4.6×10^9 M^{-1} s^{-1}. Furthermore, the authors match up their result to that of *Eigen and Kustin* [1962] by proposing that an additional direct reaction between Cl_2 and OH^- with a rate constant of 6.3×10^9 M^{-1} s^{-1} would also contribute to the formation of a Cl_2OH^- intermediate, therefore setting the overall rate constant for $Cl_2 + OH^-$ near 10^{10} M^{-1} s^{-1}.

[92] *Ashour et al.* [1996] measured the rate of Cl_2 absorption into aqueous sodium hydroxide (0.1 M NaOH) solutions in the temperature range of 293–312 K. Extrapolating the resulting temperature dependent expression, the rate constant for the reaction of $Cl_2 + OH^-$ is calculated at 1.3×10^9 M^{-1} s^{-1} at 288 K (2.9×10^9 M^{-1} s^{-1} at 298 K), below that predicted by the Bronsted–Pedersen extrapolation using H_2O/H_3O^+ but nevertheless above that predicted without using hydronium in the linear free energy relation (see Table 10 and Figure 10).

[93] In the previous section, an alternate Bronsted–Pedersen extrapolation predicted a rate constant for the reaction of Cl_2 with OH^- of 6.9×10^7 M^{-1} s^{-1} at 298 K and $I = 0.5$ M. During the preparation of this manuscript, a recent measurement of the $Cl_2 + OH^-$ rate constant at 298 K using a bubble column apparatus [*Swartz et al.*, 1997] of 5 ($\pm$2) $\times$ 10^8 M^{-1} s^{-1} was communicated to the authors (M. Gershenzon et al., Rate constant for the $Cl_{2(aq)}$ + OH^- reaction, manuscript in preparation). Table 11 summarizes reported rate constants for the reaction. These measurements and estimates illustrate that at present there is still a lack of consensus regarding one definitive and reproducible value. A rate constant of 1×10^8 M^{-1} s^{-1} (at

infinite dilution and 298 K), near the logarithmic center of the lowest and highest reported rate constants, has been chosen for MAGIC as the best compromise of the data scatter.

[94] The selection of a dissimilar value from the most recent experimental report does not imply any bias save for the indication that further studies are needed in order to reach a generally reproducible value. Model simulations adequately predict Cl_2 concentrations after the first three photolysis periods (when the aqueous-phase reaction of Cl_2 with HO_2^- predominates over the reaction with OH^-) applying the value of 5×10^8 M^{-1} s^{-1} for the chlorine hydroxide reaction rate constant and using $\gamma_s' = 2$. However, the simulations increasingly underestimate Cl_2 levels as time progress, with model calculations approaching 1/2 of the experimental measurement at the end of the simulations. Clearly, further experimental work is needed not only to better characterize the interfacial mechanism but also to better determine the rates of Cl_2 reactions in alkaline solution.

[95] The reported values in Table 11 should be viewed with the recognition that many rate constants were determined at different temperatures and ionic strengths. The inconsistency in the studies do not allow for a clear deduction of temperature effects, though it is noted that *Ashour et al.* [1996] do report a weak temperature. However, using the temperature dependence of the chlorine hydrolysis equilibrium constant, the water equilibrium product, K_w [*Whitfield*, 1975],

$$\log K_w = -4470.99/T + 6.0875 - 0.01706\ T(\text{at infinite dilution}) \tag{55}$$

and activity coefficient estimates, the following equilibrium expression

$$K = [\mathrm{HOCl}][\mathrm{Cl}^-]/[\mathrm{Cl}_2][\mathrm{OH}^-] \tag{56}$$

can be determined, with a value of 9×10^{10} at 273 K and a value of 4×10^{10} at 298 K (both at $I = 0.5$ M). At infinite dilution, the equilibrium constant increases by a factor of 1.3 while at higher ionic strengths short-range molecular interactions become important requiring individual determination of activity coefficients.

4.3. Reaction of Dissolved Cl_2 with CO_3^{2-}: Rate Constant Determination

[96] *Ashour et al.* [1996] determined an expression for the rate constant of $Cl_2 + HCO_3^- + H_2O$ in the temperature range of 293–312 K by studying potassium bicarbonate solutions (0.1 to 0.4 M initial concentration) at pH values near 8.5. Their experimental conditions were such that $[CO_3^{2-}]/[HCO_3^-] \approx 0.011$. The authors assumed in their penetration model that the rate constant for $Cl_2 + CO_3^{2-} + H_2O$ equals that of $Cl_2 + HCO_3^- + H_2O$, an assumption that both extrapolations of the Bronsted–Pedersen relation oppose. Extrapolating their results to 288 K and $I = 0.5$ M, a value for $k_{HCO_3^-}$ (and thus also for $k_{CO_3^{2-}}$) of 2.6×10^3 M^{-1} s^{-1} is computed (3.7×10^3 M^{-1} s^{-1} at 298 K). In comparison, at the same temperature and ionic strength, the Bronsted–Pedersen interpolation without H_2O/H_3O^+ yields $k_{HCO_3^-} = 3.2 \times 10^3$ M^{-1} s^{-1} and $k_{CO_3^{2-}} = 1.4 \times 10^5$ M^{-1} s^{-1} while applying the free energy relation with H_2O/H_3O^+ gives $k_{HCO_3^-} = 9.0 \times 10^3$ M^{-1} s^{-1} and $k_{CO_3^{2-}} = 1.2 \times 10^6$ M^{-1} s^{-1}. Bearing in mind the apparently erroneous assumption, $k_{HCO_3^-} = k_{CO_3^{2-}}$, the rate constant calculated by Ashour et al. is more consistent with the hydronium-less (alternate) Bronsted–Pedersen extrapolation. In view of the uncertainties, the alternate extrapolated values, even if calculated at 288 K, are included in the model.

4.4 Reactions of Dissolved Cl_2/HOCl with H_2O_2/HO_2^-: Rate Constant Determination

[97] In the model simulations, concentrations of hydrogen peroxide reach appreciable levels. In lieu of the preceding discussion, the reaction of Cl_2 with HO_2^- could be expected to follow a base-assisted mechanism, but there is evidence leading to another predominant reaction pathway.

[98] *Connick* [1947] hypothesized that the mechanism for the reaction of chlorine in hydrogen peroxide solution could be explained by the decomposition of a chloroperoxide species, HOOCl, formed from the direct reaction of Cl_2 with H_2O_2,

$$\mathrm{Cl}_2 + \mathrm{H}_2\mathrm{O}_2 \rightleftharpoons \mathrm{HOOCl} + \mathrm{Cl}^- + \mathrm{H}^+ \tag{57}$$

$$\mathrm{HOOCl} \rightarrow \mathrm{H}^+ + \mathrm{O}_2 + \mathrm{Cl}^- \tag{58}$$

with a rate law in the form:

$$-d[\mathrm{H}_2\mathrm{O}_2]/dt = k_a[\mathrm{H}_2\mathrm{O}_2][\mathrm{Cl}_2]/(k_b/k_c)[\mathrm{H}^+][\mathrm{Cl}^-] + 1 \tag{59}$$

with $k_a = 183.3$ M^{-1} s^{-1} and $(k_b/k_c) = 2.27$ M^{-2}. This expression matched data from earlier studies [*Makower and Bray*, 1933] at high HCl concentrations and remains valid down to $[H^+][Cl^-]$ products of 10^{-5} M^2, i.e., hydrochloric acid concentrations >0.003 M. *Davies and Kustin* [1973] obtained $k_a = 192$ M^{-1} s^{-1} and $k_b/k_c = 1.6$ M^{-2} from a least squares analysis of Connick's data, a small difference due possibly to different values of the Cl_2 hydrolysis equilibrium constant.

[99] At $[H^+][Cl^-]$ products below 10^{-8} M^2 (hydrochloric acid concentrations below 10^{-4} M, alternatively), HOCl becomes the main chlorine species in solution and the rate of H_2O_2 decay observed by Connick is much greater than could be explained by Expression 59. The rate law for the new reaction path detected by Connick is given by

$$-d[\mathrm{H}_2\mathrm{O}_2]/dt = k[\mathrm{H}_2\mathrm{O}_2][\mathrm{HOCl}]/[\mathrm{H}^+] \tag{60}$$

with $k \approx 10^{-4}$ M^{-1} s^{-1}. Connick also proposed that the decay of HOCl in H_2O_2 solution could be better explained by a hypochlorite pathway described by

$$\mathrm{HOCl} \rightleftharpoons \mathrm{H}^+ + \mathrm{ClO}^- \tag{61}$$

$$\mathrm{ClO}^- + \mathrm{H}_2\mathrm{O}_2 \rightarrow \mathrm{Cl}^- + \mathrm{O}_2 + \mathrm{H}_2\mathrm{O} \tag{62}$$

instead of a HO_2^- pathway

$$\mathrm{H}_2\mathrm{O}_2 \rightleftharpoons \mathrm{H}^+ + \mathrm{H}_2\mathrm{O}^- \tag{63}$$

$$\mathrm{HOCl} + \mathrm{H}_2\mathrm{O}^- \rightarrow \mathrm{Cl}^- + \mathrm{O}_2 + \mathrm{H}_2\mathrm{O} \tag{64}$$

on grounds that the Arrhenius constant of the latter pathway appeared "too great." Connick also observed evidence for a third reaction pathway in the region where $10^{-5} > [H^+][Cl^-] > 10^{-8}$ but was unable to provide a corresponding rate law.

[100] *Cahill and Taube* [1952] performed experiments on the oxidation, reduction and catalytic decomposition of H_2O_2 using heavy oxygen, O^{18}, as a tracer. They found that the O_2 liberated during the oxidation of H_2O_2 was derived "cleanly" from H_2O_2. The H–O bonds rather than the O–O bond were cleaved, leading to the conclusion that oxidation proceeded by removal of electrons from H_2O_2, thus strengthening the O–O bond. Cahill and Taube's finding supported the high acid range mechanism of Connick and the formation of an HOOCl intermediate,

$$Cl_2 + HO^*O^*H \rightleftharpoons HO^*O^*Cl + Cl^- + H^+ \quad (65)$$

$$HO^*O^*Cl \rightarrow H^+ + O^*_2 + Cl^- \quad (66)$$

but favored the alternative mechanism proposed for the low acid concentration range. An activated complex, $HOOClOH^-$, was proposed, consistent with a mechanism given by

$$HO^*O^*H \rightleftharpoons H^+ + {}^-O^*O^*H \quad (67)$$

$${}^-HOCl^+ + {}^-O^*O^*H \rightarrow HO^*O^{*-+}ClOH^- \quad (68)$$

$$HO^*O^*ClOH^- \rightarrow HO^*O^*Cl + OH^- \quad (69)$$

$$HO^*O^*Cl \rightarrow H^+ + O^*_2 + Cl^- \quad (70)$$

$$H^+ + OH^- \rightleftharpoons H_2O \quad (71)$$

[101] Further studies showed that the molecular oxygen formed during the decomposition of hydrogen peroxide and sodium hypochlorite to be in the electronically excited $^1\Delta_g$ state, recognized by its distinctive dimol chemiluminescence at 633.4 and 762.0 nm [*Khan and Kasha*, 1963, 1970]. Chemiluminescence measurements identified either the $HOCl/HO_2^-$ or the ClO^-/H_2O_2 reactions as the source of the singlet oxygen, but were only able to discard likelihood of a mechanism involving hydride ion transfer from HO_2^- to ClO^- [*Kajiwara and Kearns*, 1973]. *Held et al.* [1978] determined that the least energetically demanding path would be attack by the strongly nucleophilic HO_2^- ion on the electropositive chlorine atom of HOCl to form the HOOCl intermediate, supporting the mechanism of *Cahill and Taube* [1958], with a rate constant of 4.4×10^7 M^{-1} s^{-1}. Held et al. also found evidence for an "intermediate pH" reaction pathway for reactions of Cl_2/HOCl in solutions of hydrogen peroxide. Intriguingly, the rate law observed in this range, $10^{-5} > [H^+][Cl^-] > 10^{-8}$, coincided with the rate law and kinetics measured for the reverse chlorine hydrolysis reaction, $k[HOCl][Cl^-][H^+]$. The authors provide a detail analysis in support of a reaction between a Cl_2 hydrolysis intermediate, H_2OCl_2, and hydrogen peroxide

$$H_2OCl_2 + H_2O_2 \rightarrow H_2O + O_2 + 2\ H^+ + 2\ Cl^-. \quad (72)$$

[102] This reaction could not be included in MAGIC primarily due to the inability of the authors to determine elementary kinetic data in accordance with the proposed mechanism and the apparent absence of later research on the reaction. However, the model evaluations of MAGIC predict that the aerosol particles will become highly alkaline thereby lessening the error due to this omission, and heightening the importance of reactions with HO_2^-.

[103] Although the HOOCl molecule has not yet been observed, the molecule has been suggested as an intermediate in gas-phase reactions and heterogeneous acid-catalyzed ice surface reactions [*Wofsy et al.*, 1988; *Lee and Rendell*, 1993; *De Haan and Birks*, 1997] and in aqueous-phase reactions of Cl_2 in basic hydrogen peroxide solutions [*Storch et al.*, 1983]. The rate constant for the reaction of Cl_2 with HO_2^- was determined from measurements of chlorine absorption into laminar liquid jets with initial concentration $[HO_2^-] = 4$ M [*Ruiz-Ibanez and Sandall*, 1991; *Davis et al.*, 1992]. A base-assisted chlorine hydrolysis mechanism cannot account for the observed singlet delta oxygen formation, $O_2(^1\Delta_g)$, observed during this reaction—the excited oxygen formation is more consistent with the formation of the HOOCl intermediate. *Davis et al.* [1992] reevaluated the earlier analysis of *Ruiz-Ibanez and Sandall* [1991] accounting for the reduction of solubility and diffusivity of Cl_2 ascribed to ion effects in the liquid phase of basic hydrogen peroxide solutions and obtained a value for the rate constant (using their temperature dependent expression) of 1.8×10^7 M^{-1} s^{-1} at 288 K and a rate constant of 1.1×10^8 M^{-1} s^{-1} extrapolating to 298 K. The possibility of a reaction between Cl_2 and OH^- affecting the results of Davis et al., can be eliminated using the recommended rate constant (section 4.2) and a calculated value of 10^{-3} M for $[OH^-]$ in the experiments. Furthermore, any contribution from a secondary base-assisted mechanism is also neglected since the resultant rate constant, using the Bronsted–Pedersen relation, is orders of magnitude less than that for the reaction leading to the HOOCl intermediate.

[104] Finally, the reaction rate of H_2O_2 with chloride ions [*Mohammad and Liefbhafsky*, 1934; *Hansen and Espenson*, 1995] is too slow to affect the system modeled by MAGIC at all.

5. Conclusion and Future Applications

[105] A model of gas-phase and aqueous-phase chemistry, MAGIC, has been developed in order to explain the production of Cl_2 from the photolysis of mixtures of ozone and deliquesced sodium chloride particles in a laboratory chamber. The *Schwartz* [1986] method is used to calculate the rate of mass transfer of soluble species considering the limitations imposed by gas-phase diffusion, mass accommodation, and aqueous-phase diffusion. Activity coefficients are calculated using the *Pitzer* [1991] ion interaction approach and the kinetic salt effect is estimated using Debye–Huckel–Bronsted equations. The model shows that within this seemingly simple system, experimental and model results cannot be reconciled on the basis of currently known gas-phase and aqueous-phase chemical reactions and mass transfer parameters.

[106] As part of a multidisciplinary research effort, collaborators have shown that chloride ions reside at the

surface of deliquesced sodium chloride particles and that these ions are expected to attract reactive gases such as $OH^{\bullet}$ and O_3 [*Knipping et al.*, 2000]. A methodological analysis of the system strongly supports a hypothesis for a mechanism of Cl_2 formation rate-determined by the reaction of chloride ions and $OH^{\bullet}$ radicals at the gas–liquid interface. A kinetic expression given for the overall mechanism matches the observed experimental data well. Sensitivity studies demonstrate that the modeling of Cl_2 production is greatly affected by the uncertainties in the rate constants for decomposition of Cl_2 in alkaline solution, in particular reaction with OH^-, HO_2^-, and CO_3^{2-}, and uncertainties in the aerosol population parameters.

[107] The reactive fate of a potential $OH\bullet\bullet\bullet Cl^{\bullet-}_{surface}$ species formed in the rate-determining interfacial reaction is still subject to further studies. For instance, it is possible that the bound complex may self-react forming Cl_2 and hydroxide ions. In an alternative, possibly parallel mechanism, the chloride–hydroxyl surface complexes may react with other surface chloride ions forming $Cl_2^{\bullet-}$. If the $Cl_2^{\bullet-}$ radical anion is stabilized at the interface, it could also recombine or react with other chloride–hydroxyl complexes hence releasing chlorine to the gas phase. Considering that the $OH\bullet\bullet\bullet Cl^{\bullet-}_{surface}$ surface complex and the species formed by OH_{aq} and Cl^- in bulk solution, $HOCl^{\bullet-}$, are most likely not the same species, molecular dynamics simulations suggest that $OH\bullet\bullet\bullet Cl^{\bullet-}_{surface}$ is sufficiently stable in order to accumulate and allow for the proposed interfacial processes to occur at significant rates. In summary, the overall phenomenological model presented herewith is founded on the results of quantum chemical calculations and molecular dynamic simulations, evidenced by experimental observations and supported by a series of kinetic modeling simulations which fit the observations within rational tolerances.

[108] It is important to address the relevance of the interfacial mechanism to conditions representative of the true tropospheric multiphase system. There are several atmospheric conditions worthy of investigation using these results, e.g., the remote marine boundary layer, polluted coastal regions, and the polar troposphere. A significant discussion on any of these topics requires a description of the formulation, chemical mechanism, input data, results, and analysis of an extensive modeling study, i.e., a level of detail falling beyond the scope of the current manuscript. However, some preliminary observations and comments are made at the present time.

[109] Hydrocarbon and DMS measurements in the marine boundary layer have been used to infer chlorine atom concentrations or its contribution to oxidation of these compounds in the marine boundary layer [*Rudolph et al.*, 1996; *Singh et al.*, 1996a, 1996b; *Wingenter et al.*, 1996, 1999; *Davis et al.*, 1999; *Ramacher et al.*, 1999]. Estimates of chlorine atom concentrations from these studies range from less than 10^3 molecule cm^{-3} up to 10^5 molecule cm^{-3}. The two order-of-magnitude concentration range appears to be highly dependent on pH and the pollutant load of the air masses. Previous estimates of chlorine atom concentrations using the interfacial mechanism show that these results can be reasonably reproduced [*Knipping et al.*, 2000]. Inference of 24-hour average $[Cl^{\bullet}]$ for the remote marine boundary layer conditions yielded 780 molecule cm^{-3} [*Wingenter et al.*, 1999]; the model predicts 980 molecule cm^{-3}. Inference of local noon instantaneous chlorine atom concentrations for relatively polluted marine air masses yielded 6.5×10^4 molecule cm^{-3} [*Wingenter et al.*, 1996]; the model estimates 3.7×10^4 molecule cm^{-3}. The contribution of the interfacial mechanism was estimated at 40% for the remote case (pH $\sim$ 4) and at 20% (pH $\sim$ 3.2) for the more polluted case, leading the authors to conclude that the interfacial mechanism may begin to govern Cl atom concentrations at aerosol pH values above 4.

[110] A few additional comments seem appropriate. First, in agreement with other modeling research (R. Sander, personal communication), the principal mechanism for chlorine atom production in the marine boundary layer for the above conditions is hydrochloric acid displacement (due to acidification of the particles by nitric, sulfuric, formic, acetic and methanesulfonic acid) and subsequent reaction with $OH^{\bullet}$ radicals. The contribution of this acid displacement-initiated mechanism decreases with increasing pH. The rate constant of the HCl + $OH^{\bullet}$ reaction is rather low. Thus, at pH values above 3, the Cl_2 release (and subsequent photolysis) due to the pH-independent interfacial mechanism can be on the same order or even more effective than the HCl-hydroxyl reaction with respect to the production of chlorine atoms. However, conditions that lead to acidification are commonly those that also lead to higher $OH^{\bullet}$ concentrations, i.e., higher pollutant loads and correspondingly higher ozone levels. Thus, even though the interfacial mechanism may dominate chlorine atom levels at higher pH, the absolute value of the concentrations may be low, particularly in pristine conditions.

[111] Second, the contribution of the interfacial mechanism to chloride deficits measured in the atmosphere [*Ayers et al.*, 1999] is minimal. Hydrochloric acid displacement remains the dominant pathway for Cl^- depletion, although there is evidence suggesting additional mechanisms [*Volpe et al.*, 1998]. In agreement with other model studies [*Sander and Crutzen*, 1996; *Erickson et al.*, 1999], fresh sea salt particles are found to drop in pH quickly in timescales an hour or less; the pH to which the particles initially equilibrate depends highly on the conditions being simulated.

[112] Finally, the implications of these finding may be explored by other laboratory and atmospheric models [*Sander and Crutzen*, 1996; *Erickson et al.*, 1999; *Herrmann et al.*, 2000; *Leriche et al.*, 2000; *Moldanova and Ljungstrom*, 2001]. For example, *Behnke et al.* [1999] performed experiments in Teflon bags containing ozone, pure wet NaCl aerosol and a combination of hydrocarbons. These mixtures were irradiated using a solar illuminator. Chlorine atom production rates were deduced from measurements of hydrocarbon degradation. In all experiments where the initial ozone was below 500 ppb, no appreciable chlorine atom production was inferred. These experiments differ from those described in this paper not only in O_3 concentrations but also in the addition of hydrocarbons, the photolysis of Cl_2, and dissimilarities in many parametric data. A detailed model study of a system comparable to the Behnke et al. experiments may provide further insight on the behavior of the proposed interfacial process and help ascertain the reasons for not deducing appreciable $Cl^{\bullet}$ levels.

[113] Modeling results for conditions typical of the Southern California Air Basin shall be presented in a forthcoming

paper (Knipping and Dabdub, in preparation). In this study we shall explore the impact chlorine chemistry, including the proposed interfacial mechanism and other heterogeneous processes. We shall also compare our results with measurements of Cl_2 in other coastal regions [*Spicer et al.*, 1998] and determine whether similar values can be reproduced.

[114] **Acknowledgments.** The authors acknowledge the other members of this collaboration: D. Tobias, P. Jungwirth, and R. B. Gerber for their work on the MD simulations and M. J. Lakin, K. L. Foster, and B. J. Finlayson-Pitts for their work with the experimental chamber and assistance in developing the interfacial reaction scheme. A special recognition is extended to B. J. Finlayson-Pitts for her encouragement and counsel. The authors are grateful to the National Science Foundation for financial support under CAREER grant ATM-9985025. E. Knipping thanks the Organization of American States and the Link Foundation for fellowship support. We thank P. Davidovits, D. Margerum, R. Sander, and all manuscript reviewers for insightful comments as well as E. Chapman, C. Berkowitz, and C. Spicer for allowing access to their gas-phase model.

References

Adams, D. J., S. Barlow, G. V. Buxton, T. M. Malone, and G. A. Salmon, Evaluation of the stability constant of Cl_2^- in neutral aqueous solution, *J. Chem. Soc. Faraday Trans.*, *91*, 3303–3305, 1995.

Alegre, M. L., M. Gerones, J. A. Rosso, S. G. Bertolotti, A. M. Braun, D. O. Martire, and M. C. Gonzalez, Kinetic study of the reactions of chlorine atoms and Cl_2^- radical anions in aqueous solutions, 1, Reaction with benzene, *J. Phys. Chem. A*, *104*, 3117–3125, 2000.

Anbar, M., and H. Taube, The exchange of hypochlorite and hypobromite ions with water, *J. Am. Chem. Soc.*, *80*, 1073–1077, 1958.

Anbar, M., S. Guttmann, and R. Rein, The isotopic exchange between hypohalites and halide ions, II, The exchange between hypochlorous acid and chloride ions, *J. Am. Chem. Soc.*, *81*, 1816–1821, 1959.

Ashour, S. S., E. B. Rinker, and O. C. Sandall, Absorption of chlorine into aqueous bicarbonate solutions and aqueous hydroxide solutions, *AIChE J.*, *42*, 671–682, 1996.

Atkinson, R., D. L. Baulch, R. A. Cox, R. F. Hampson Jr., J. A. Kerr, M. J. Rossi, and J. Troe, Evaluated kinetic and photochemical data for atmospheric chemistry: Supplement VI, IUPAC Subcommittee on Gas Kinetic Data Evaluation for Atmospheric Chemistry, *J. Phys. Chem. Ref. Data*, *26*, 1329–1499, 1997.

Atkinson, R., D. L. Baulch, R. A. Cox, R. F. Hampson Jr., J. A. Kerr, M. J. Rossi, and J. Troe, Evaluated kinetic and photochemical data for atmospheric chemistry: Supplement VII, Halogen Species, IUPAC Subcommittee on Gas Kinetic Data Evaluation for Atmospheric Chemistry, *J. Phys. Chem. Ref. Data*, *29*, 167–266, 2000.

Ayers, G. P., R. W. Gillett, J. M. Cainey, and A. L. Dick, Chloride and bromide loss from sea-salt particle in Southern Ocean air, *J. Atmos. Chem.*, *33*, 29,319, 1999.

Basco, N., and S. K. Dogra, Reactions of halogen oxides studied by flash photolysis, II, The flash photolysis of chlorine monoxide and of ClO free radical, *Proc. R. Soc. London, Ser. A*, *323*, 401–415, 1971.

Beach, M. W., and D. W. Margerum, Kinetics of oxidation of tetracyanonickelate(II) by chlorine monoxide, chlorine, and hypochlorous acid and kinetics of chlorine monoxide formation, *Inorg. Chem.*, *29*, 1225–1232, 1990.

Beckwith, R. C., T. X. Wang, and D. W. Margerum, Equilibrium and kinetics of bromine hydrolysis, *Inorg. Chem.*, *35*, 995–1000, 1996.

Behar, D., G. Czapski, and I. Duchovny, Carbonate radical in flash photolysis and pulse radiolysis of aqueous carbonate solutions, *J. Phys. Chem.*, *74*, 2206–2210, 1970.

Behnke, W., M. Elend, U. Kruger, and C. Zetzsch, The influence of NaBr/NaCl ratio on the Br^- catalysed production of halogenated radicals, *J. Atmos. Chem.*, *34*, 87–99, 1999.

Bell, R. P., *The Proton in Chemistry*, 2nd ed., Cornell Univ. Press, Ithaca, N. Y., 1973.

Bell, R. P., and E. Gelles, The halogen cations in aqueous solution, *J. Chem. Soc.*, 2734–2740, 1951.

Benson, S. W., *The Foundations of Chemical Kinetics*, McGraw-Hill, New York, 1960.

Bielski, B. H. J., Reevaluation of the spectral and kinetic properties of HO_2 and O_2^- free radicals, *Photochem. Photobiol.*, *28*, 645–649, 1978.

Bielski, B. H. J., A pulse radiolysis study of the reaction of ozone with Cl_2^- radical anion in aqueous solutions, *Radiat. Phys. Chem.*, *41*, 527–530, 1993.

Bielski, B. H. J., D. E. Cabelli, R. L. Arudi, and A. B. Ross, Reactivity of HO_2/O_2^- radicals in aqueous solution, *J. Phys. Chem. Ref. Data*, *14*, 1041–1100, 1985.

Bjergbakke, E., S. Navaratnam, and B. J. Parsons, Reactions between HO_2 and chlorine in aqueous solution, *J. Am. Chem. Soc.*, *103*, 5926–5968, 1981.

Blatchley, E. R., III, R. W. Johnson, J. E. Alleman, and W. McCoy, Effective Henry's law constant for free chlorine and free bromine, *Water Res.*, *26*, 99–106, 1992.

Boniface, J., Q. Shi, Y. Q. Li, J. L. Cheung, O. V. Rattigan, P. Davidovits, D. R. Worsnop, J. T. Jayne, and C. E. Kolb, Uptake of gas-phase SO_2, H_2S, and CO_2 by aqueous solutions, *J. Phys. Chem. A*, *104*, 7502–7510, 2000.

Bühler, R. E., J. Staehelin, and J. Hoigné, Ozone decomposition in water studied by pulse radiolysis, 1, HO_2/O_2^- and HO_3/O_3^- as intermediates, *J. Phys. Chem.*, *88*, 2464–2560, 1984.

Buxton, G. V., C. L. Greenstock, W. P. Helman, and A. B. Ross, Critical review of rate constants of hydrated electron, hydrogen atoms and hydroxyl radicals (OH/O^-) in aqueous solution, *J. Phys. Chem. Ref. Data*, *17*, 513–534, 1988.

Buxton, G. V., M. Bydder, and G. A. Salmon, Reactivity of chlorine atoms in aqueous solution, part 1, The equilibrium $Cl + Cl^-$; Cl_2^-, *J. Chem. Soc. Faraday Trans.*, *94*, 653–657, 1998.

Buxton, G. V., M. Bydder, and G. A. Salmon, Reactivity of chlorine atoms in aqueous solution, part III, The reactions of Cl with solutes, *Phys. Chem. Chem. Phys.*, *2*, 237–245, 2000.

Cahill, A. E., and H. Taube, The use of heavy oxygen in the study of reactions of hydrogen peroxide, *J. Am. Chem. Soc.*, *74*, 2312–2318, 1952.

Carslaw, K. S., T. Peter, and S. L. Clegg, Modeling the composition of liquid stratospheric aerosols, *Rev. Geophys.*, *35*, 125–154, 1997.

Clegg, S. L., and P. Brimblecombe, The solubility and activity coefficient of oxygen in salt solutions and brines, *Geochim. Comoschim. Acta*, *54*, 3315–3328, 1990.

Connick, R., The interaction of hydrogen peroxide and hypochlorous acid in acidic solutions containing chloride ion, *J. Am. Chem. Soc.*, *69*, 1509–1514, 1947.

Czapski, G., S. V. Lymar, and H. A. Schwarz, Acidity of the carbonate radical, *J. Phys. Chem. A*, *103*, 3447–3450, 1999.

Dahl, T., and I. Roeggen, An analysis of electron donor–acceptor complexes: $H_2O{\bullet}F_2$, $H_2O{\bullet}Cl_2$, and $H_2O{\bullet}ClF$, *J. Am. Chem. Soc.*, *118*, 4152–4158, 1996.

Davidovits, P., J. H. Hu, D. R. Worsnop, M. S. Zahniser, and C. E. Kolb, Entry of gas molecules into liquids, *Faraday Discuss. Chem. Soc.*, *100*, 65–81, 1995.

Davies, G., and K. Kustin, The hydrogen peroxide–chlorine reaction and its catalysis by manganese(III)–manganese(II), *Inorg. Chem.*, *12*, 961–962, 1973.

Davis, R. A., G. Ruiz-Ibanez, and O. C. Sandall, Nonisothermal analysis of the reaction kinetics for chlorine in basic hydrogen peroxide, *Ind. Eng. Chem. Res.*, *31*, 1461–1465, 1992.

Davis, M. J., H. Koizumi, G. C. Schatz, S. E. Bradforth, and D. M. Neumark, Experimental and theoretical study of the O + HCl transition state region by photodetachment of $OHCl^-$, *J. Chem. Phys.*, *101*, 4708–4721, 1994.

Davis, D., et al., Dimethyl sulfide oxidation in the equatorial Pacific: Comparison of model simulations with field observations for DMS, SO_2, H_2SO_4(g), MSA(g), and NSS, *J. Geophys. Res.*, *104*, 5765–5784, 1999.

De Haan, D. O., and J. W. Birks, Heterogeneous reactions of chlorine peroxide with halide ions, *J. Phys. Chem. A*, *101*, 8026–8034, 1997.

De Haan, D. O., T. Brauers, K. Oum, J. Stutz, T. Nordmeyer, and B. J. Finlayson-Pitts, Heterogeneous chemistry in the troposphere: Experimental approaches and applications to the chemistry of sea salt particles, *Int. Rev. Phys. Chem.*, *18*, 343–385, 1999.

Debye, P., and E. Hückel, Zur Theorie der Electrolyte I, *Phys. Z.*, *24*, 185, 1923.

DeMore, W. B., S. P. Sander, D. M. Golden, R. F. Hampson, M. J. Kurylo, C. J. Howard, A. R. Ravishankara, C. E. Kolb, and M. J. Molina, *Chemical Kinetics and Photochemical Data for Use in Stratospheric Modeling, Report 97-4*, Jet Propul. Lab., Pasadena, Calif., 1997.

Donaldson, D. J., J. A. Guest, and M. C. Goh, Evidence for adsorbed SO_2 at the aqueous–air interface, *J. Phys. Chem.*, *99*, 9313–9315, 1995.

Donaldson, D. J., A. R. Ravishankara, and D. R. Hanson, Detailed study of $HOCl + HCl \rightarrow Cl_2 + H_2O$ in sulfuric acid, *J. Phys. Chem. A*, *101*, 4717–4725, 1997.

Draganić, Z. D., A. Negrón-Mendoza, K. Sehested, S. I. Vujošević, R. Navarro-Gonzáles, M. G. Albarrán-Sanchez, and I. G. Draganic, Radiolysis of aqueous solutions of ammonium bicarbonate over a large dose range, *Radiat. Phys. Chem.*, *38*, 317–321, 1991.

Eigen, E., and K. Kustin, The kinetics of halogen hydrolysis, *J. Am. Chem. Soc.*, *84*, 1355–1361, 1962.

Elliot, A. J., A pulse radiolysis study of the temperature dependence of reaction involving H, OH and e^-_{aq} in aqueous solution, *Radiat. Phys. Chem.*, *34*, 753–758, 1989.

Elliot, A. J., and G. V. Buxton, Temperature dependence of the reaction OH + O_2^- and OH + HO_2 in water up to 200°C, *J. Chem. Soc. Faraday Trans.*, *88*, 2465–2470, 1992.

Erickson, D. J., C. Seuzaret, W. C. Keene, and S. L. Gong, A general circulation model based calculation of HCl and $ClNO_2$ production from sea salt dechlorination: Reactive chlorine emissions inventory, *J. Geophys. Res.*, *104*, 8347–8372, 1999.

Finlayson-Pitts, B. J., Chlorine atoms as a potential tropospheric oxidant in the marine boundary layer, *Res. Chem. Intermed.*, *19*, 235–249, 1993.

Finlayson-Pitts, B. J., and J. C. Hemminger, Physical chemistry of airborne sea salt particles and their components, *J. Phys. Chem. A*, *104*, 11,463–11,477, 2001.

Finlayson-Pitts, B. J. and J. N. Pitts Jr., *Chemistry of the Upper and Lower Atmosphere: Theory, Experiments and Applications*, Academic, San Diego, Calif., 2000.

Fridlind, A. M., and M. Z. Jacobson, A study of gas–aerosol equilibrium and aerosol pH in the remote marine boundary layer during the First Aerosol Characterization Experiment (ACE 1), *J. Geophys. Res.*, *105*, 17,325–17,340, 2000.

Fuchs, N. A. and G. A. Sutugin, High-dispersed aerosols, in *Topics in Current Aerosol Research*, edited by G. M. Hidy and J. R. Brock, Pergamon, New York, 1971.

Gerritsen, C. M., and D. W. Margerum, Non-metal redox kinetics: Hypochlorite and hypochlorous acid reactions with cyanide, *Inorg. Chem.*, *29*, 2757–2762, 1990.

Gonzalez, M. C., and D. O. Martire, Kinetics of O^- and $O3^-$ in alkaline aqueous solutions of hydrogen peroxide, *Int. J. Chem. Kinet.*, *29*, 589–597, 1997.

Graedel, T. E., and K. I. Goldberg, Kinetic studies of raindrop chemistry, 1, Inorganic and organic processes, *J. Geophys. Res.*, *88*, 10,865–10,882, 1983.

Grigor'ev, A. E., I. E. Makarov, and A. K. Pikaev, Formation of Cl_2^- in the bulk solution during the radiolysis of concentrated solutions of chlorides, *High Energy Chem.*, *21*, 99–102, 1987.

Hansen, P. J., and J. H. Espenson, Oxidation of chloride ions by hydrogen peroxide, catalyzed by methylrhenium trioxide, *Inorg. Chem.*, *34*, 5839–5844, 1995.

Hanson, D. R., Surface-specific reactions on liquids, *J. Phys. Chem. B*, *101*, 4998–5001, 1997.

Hanson, D. R., J. B. Burkholder, C. J. Howard, and A. R. Ravishankara, Measurement of OH and HO_2 radical uptake coefficients on water and sulfuric acid surfaces, *J. Phys. Chem.*, *96*, 4979–4985, 1992.

Held, A. M., D. J. Haiko, and J. K. Hurst, Mechanisms of chlorine oxidation of hydrogen peroxide, *J. Am. Chem. Soc.*, *100*, 5732–5740, 1978.

Herrmann, H., B. Ervens, H.-W. Jacobi, R. Wolke, P. Nowacki, and R. Zellner, CAPRAM2.3: A chemical aqueous-phase radical mechanism for tropospheric chemistry, *J. Atmos. Chem.*, *36*, 231–284, 2000.

Holcman, J., K. Sehested, E. Bjergbakke, and E. J. Hart, Formation of ozone in the reaction between the ozonide radical, O_3^-, and the carbonate radical anion, CO_3^-, in aqueous alkaline solutions, *J. Phys. Chem.*, *86*, 2069–2072, 1982.

Hu, J. H., Q. Shi, P. Davidovits, D. R. Worsnop, M. S. Zahniser, and C. E. Kolb, Reactive uptake of $Cl_{2(g)}$ and $Br_{2(g)}$ by aqueous surfaces as a function of Br^- and I^- ion concentration: The effect of chemical reaction at the interface, *J. Phys. Chem.*, *99*, 8768–8776, 1995.

Huie, R. E., and C. L. Clifton, Temperature dependence of the rate constants for reactions of the sulfate radical, SO_4^-, with anions, *J. Phys. Chem.*, *94*, 8561–8567, 1990.

Huthwelker, T., Th. Peter, B. P. Luo, S. L. Clegg, K. S. Carslaw, and P. Brimblecombe, Solubility of HOCl in water and aqueous H_2SO_4 to stratospheric temperatures, *J. Atmos. Chem.*, *21*, 81–95, 1995.

Jacob, D. J., Chemistry of OH in remote clouds and its role in the production of formic acid and peroxymonosulfate, *J. Geophys. Res.*, *91*, 9807–9826, 1986.

Jacob, D., Heterogeneous chemistry and tropospheric ozone, *Atmos. Environ.*, *34*, 2131–2159, 2000.

Jacobi, H.-W., H. Herrmann, and R. Zellner, A laser flash photolysis study of the decay of Cl^- atoms and Cl_2^- radical anions in aqueous solution at 298 K, *Ber. Bunsenges. Phys. Chem.*, *101*, 1909–1913, 1997.

Jacobi, H.-W., F. Wicktor, H. Herrmann, and R. Zellner, A laser flash photolysis kinetic study of reactions of the Cl_2^- radical anion with oxygenated hydrocarbons in aqueous solution, *Int. J. Chem. Kinet.*, *31*, 169–181, 1999.

Jayne, J. T., P. Davidovits, D. R. Worsnop, M. S. Zahniser, and C. E. Kolb, Uptake of $SO_{2(g)}$ by aqueous surfaces as a function of pH: The effect of chemical reaction at the interface, *J. Phys. Chem.*, *94*, 6041–6048, 1990.

Jayson, G. G., B. J. Parsons, and A. J. Swallow, Some simple, highly reactive, inorganic chlorine derivatives in aqueous solution, *J. Chem. Soc. Faraday Trans. 1*, *69*, 1597–1607, 1973.

Johnsson, K., A. Engdahl, P. Ouis, and B. Nelander, A matrix isolation study of the water complexes of Cl_2, ClOCl, OClO and HOCl and their photochemistry, *J. Mol. Struct.*, *293*, 137–142, 1993.

Jungwirth, P., and D. J. Tobias, Surface effects of aqueous ionic solvation: A molecular dynamics simulation study of NaCl at the air/water interface from infinite dilution to saturation, *J. Phys. Chem. B*, *104*, 7702–7706, 2000.

Kajiwara, T., and D. R. Kearns, Direct spectroscopic evidence for a deuterium solvent effect on the lifetime of singlet oxygen in water, *J. Am. Chem. Soc.*, *95*, 5886–5890, 1973.

Keene, W. C., and D. L. Savoie, The pH of deliquesced sea-salt aerosol in polluted marine air, *Geophys. Res. Lett.*, *25*, 2181–2184, 1998.

Keene, W. C., and D. L. Savoie, Correction to "The pH of deliquesced sea-salt aerosol in polluted marine air", *Geophys. Res. Lett.*, *26*, 1315–1316, 1999.

Keene, W. C., A. A. P. Pszenny, D. J. Jacob, R. A. Duce, J. N. Galloway, J. J. Schultz-Tokos, H. Sievering, and J. F. Boatman, The geochemical cycling of reactive chlorine through the marine troposphere, *Glob. Biogeochem. Cycles*, *4*, 407–430, 1990.

Keene, W. C., D. J. Jacob, and S. M. Fan, Reactive chlorine: A potential sink for dimethylsulfide and hydrocarbons in the marine boundary layer, *Atmos. Environ.*, *30*, i–iii, 1996.

Keene, W. C., R. Sander, A. A. P. Pszenny, R. Vogt, P. J. Crutzen, and J. N. Galloway, Aerosol pH in the marine boundary layer: A review and model evaluation, *J. Aerosol Sci.*, *29*, 339–356, 1998.

Khan, A. U., and M. Kasha, Red chemiluminescence of molecular oxygen in aqueous solution, *J. Chem. Phys.*, *39*, 2105–2106, 1963.

Khan, A. U., and M. Kasha, Chemiluminescence arising from simultaneous transitions in pairs of singlet oxygen molecules, *J. Am. Chem. Soc.*, *92*, 3293–3300, 1970.

Kim, Y. P., J. H. Seinfeld, and P. Saxena, Atmospheric gas–aerosol equilibrium, I, Thermodynamic model, *Aerosol Sci. Technol.*, *19*, 157–181, 1993.

Klaening, U. K., K. Sehested, and T. Wolff, Ozone formation in laser flash photolysis of oxoacids and oxoanions of chlorine and bromine, *J. Chem. Soc. Faraday Trans. 1*, *80*, 2969–2979, 1984.

Kozac-Channing, L. F., and G. R. Heltz, Solubility of ozone in aqueous solutions of 0–0.6 M ionic strength at 5–30°C, *Environ. Sci. Technol.*, *17*, 145–149, 1983.

Knauth, H.-D., H. Alberti, and H. Clausen, Equilibrium constant of the gas reaction $Cl_2O + H_2O = 2$ HOCl and the ultraviolet spectrum of HOCl, *J. Phys. Chem.*, *83*, 1604–1612, 1979.

Knipping, E. M., M. J. Lakin, K. L. Foster, P. Jungwirth, D. J. Tobias, R. B. Gerber, D. Dabdub, and B. J. Finlayson-Pitts, Experiments and simulations of ion-enhanced interfacial chemistry on aqueous NaCl aerosols, *Science*, *288*, 301–306, 2000.

Kumar, S., The characteristic time to achieve interfacial phase equilibrium in cloud drops, *Atmos. Environ.*, *23*, 2299–2304, 1989.

Kumar, K., and D. W. Margerum, Kinetics and mechanism of general-acid-assisted oxidation of bromide by hypochlorite and hypochlorous acid, *Inorg. Chem.*, *26*, 2706–2711, 1987.

Kumar, K., R. A. Day, and D. W. Margerum, Atom-transfer kinetics: General acid-assisted oxidation of iodide by chloramines and hypochlorite, *Inorg. Chem.*, *25*, 4344–4350, 1986.

Langer, S., R. S. Pemberton, and B. J. Finlayson-Pitts, Diffuse reflectance infrared studies of the reaction of synthetic sea salt mixtures with NO_2: A key role for hydrates in the kinetics and the mechanism, *J. Phys. Chem. A*, *101*, 1277–1286, 1997.

Lee, T. M., and A. P. Rendell, Ab initio characterization of ClOOH: Implications for atmospheric chemistry, *J. Phys. Chem.*, *97*, 6999–7002, 1993.

Lelieveld, J., and P. J. Crutzen, The role of clouds in tropospheric photochemistry, *J. Atmos. Chem.*, *12*, 229–267, 1991.

Leriche, M., D. Voisin, N. Chaumerliac, A. Monod, and B. Aumont, A model for tropospheric multiphase chemistry: Application to one cloudy event during the CIME experiment, *Atmos. Environ.*, *34*, 5015–5036, 2000.

Levanov, A. V., A. R. Gromov, E. E. Antipenko, A. V. Zosimov, and V. V. Lunin, Chlorine emission during the interaction of ozone–carbon dioxide mixtures with sodium chloride solutions, *Russ. J. Phys Chem.*, *74*, 2097–2098, 2000.

Lide, D. R., (Ed.), *CRC Handbook of Chemistry and Physics*, 79th edition, CRC Press, Boca Raton, Fla., 1998.

Lifshitz, A., and B. Perlmutter-Hayman, The kinetics of the hydrolysis of chlorine, I, Reinvestigation of the hydrolysis in pure water, *J. Am. Chem. Soc.*, *64*, 1663–1665, 1960.

Lifshitz, A., and B. Perlmutter-Hayman, The kinetics of the hydrolysis of chlorine, II, Hydrolysis in the presence of acetate, *J. Am. Chem. Soc.*, *65*, 753–757, 1961.

Lifshitz, A., and B. Perlmutter-Hayman, The kinetics of the hydrolysis of chlorine, III, Reaction in the presence of various bases, and a discussion of the mechanism, *J. Am. Chem. Soc.*, *66*, 701–705, 1962.

Lind, J. A., and G. L. Kok, Correction to "Henry's law determinations for aqueous solutions of hydrogen peroxide, methylhydroperoxide, and peroxyacetic acid" by John A. Lind and Gregory L. Kok, *J. Geophys. Res.*, *99*, 21,119, 1994.

Liu, Z. F., C. K. Siu, and J. S. Tse, Ab initio molecular dynamics study on the hydrolysis of molecular chlorine, *Chem. Phys. Lett.*, *311*, 93–101, 1999.

Long, C. A., and B. H. J. Bielski, Rate of reaction of superoxide radical with chloride-containing species, *J. Phys. Chem.*, *84*, 555–557, 1980.

Madronich, S., Photodissociation in the atmosphere, 1, Actinic flux and the effects of ground reflections and clouds, *J. Geophys. Res.*, *92*, 9740–9752, 1987.

Makower, B., and W. C. Bray, The rate of oxidation of hydrogen peroxide by chlorine in the presence of hydrochloric acid, *J. Am. Chem. Soc.*, *55*, 4765–4776, 1933.

Marsh, A. R. W., and W. J. McElroy, The dissociation constant and Henry's law constant of HCl in aqueous solution, *Atmos. Environ.*, *19*, 1075–1080, 1985.

Massucci, M., S. L. Clegg, and P. Brimblecombe, Equilibrium partial pressures, thermodynamic properties of aqueous and solid phases, and Cl_2 production from aqueous HCl and HNO_3 and their mixtures, *J. Phys. Chem. A*, *103*, 4209–4226, 1999.

McElroy, W. J., A laser photolysis study of the reaction of SO_4^- with Cl^- and the subsequent decay of Cl_2^- in aqueous solution, *J. Phys. Chem.*, *94*, 2435–2441, 1990.

Mertens, R., and C. von Sonntag, Photolysis (λ = 254 nm) of tetrachloroethene in aqueous solutions, *J. Photochem. Photobiol. A Chem.*, *85*, 1–9, 1995.

Mohammad, A., and H. A. Liebhafsky, The kinetics of the reduction of hydrogen peroxide by the halides, *J. Am. Chem. Soc.*, *56*, 1680–1685, 1934.

Moldanova, J., and E. Ljungstrom, Sea-salt aerosol chemistry in coastal areas: A model study, *J. Geophys. Res.*, *106*, 1271–1296, 2001.

Morris, J. C., The mechanism of the hydrolysis of chlorine, *J. Am. Chem. Soc.*, *68*, 1692–1694, 1946.

Nagy, J. C., K. Kumar, and D. W. Margerum, Non-metal redox kinetics: Oxidation of iodide by hypochlorous acid and by nitrogen trichloride measured by the pulsed-accelerated-flow method, *Inorg. Chem.*, *27*, 2773–2780, 1988.

Navaratnam, S., B. J. Parsons, and A. J. Swallow, Some reactions of the dichlorine anion radical, *Radiat. Phys. Chem.*, *15*, 159–161, 1980.

Nemes, A., I. Fabian, and R. van Eldik, Kinetics and mechanism of the carbonate ion inhibited aqueous ozone decomposition, *J. Phys. Chem.*, 7995–8000, 2000.

Neta, P., R. E. Huie, and A. B. Ross, Rate constants for reactions of inorganic radicals in aqueous solution, *J. Phys. Chem. Ref. Data*, *17*, 1027–1228, 1988.

Oum, K. W., M. J. Lakin, D. O. De Haan, T. Brauers, and B. J. Finlayson-Pitts, Formation of molecular chlorine from the photolysis of ozone and aqueous sea salt particles, *Science*, *279*, 74–77, 1998.

Perlmutter-Hayman, B., The primary kinetic salt effect in aqueous solution, *Prog. React. Kinet.*, *6*, 239–267, 1971.

Pethybridge, A. D., and J. E. Prue, Kinetic salt effects and the specific influence of ions on rate constants, *Prog. Inorg. Chem.*, *17*, 327–390, 1972.

Pitzer, K. S., Ion interaction approach: Theory and data correlation, in *Activity Coefficients in Electrolyte Solutions*, 2nd edition, edited by K. S. Pitzer, CRC Press, Boca Raton, Fla., 1991.

Pruppacher, H. R. and J. D. Klett, *Microphysics of Clouds and Precipitation, 2nd Ed.*, Kluwer Acad., Norwell, Mass., 1997.

Pszenny, A. A. P., W. C. Keene, D. J. Jacob, S. Fan, J. R. Maben, M. P. Zetwo, M. Springer-Young, and J. N. Galloway, Evidence of chlorine gases other than hydrogen chloride in marine surface air, *Geophys. Res. Lett.*, *20*, 699–702, 1993.

Ramacher, B., J. Rudolph, and R. Koppmann, Hydrocarbon measurements during tropospheric ozone depletion events: Evidence for halogen atom chemistry, *J. Geophys. Res.*, *104*, 3633–3653, 1999.

Ravishankara, A. R., Heterogeneous and multiphase chemistry in the troposphere, *Science*, *276*, 1058–1065, 1997.

Regimbal, J. M., and M. Mozurkewich, Kinetics of peroxynitric acid reactions with halides at low pH, *J. Phys. Chem. A*, *104*, 6580–6589, 2000.

Rochester, C. H., Salt and medium effects on reaction rates in concentrated solutions of acids and bases, *Prog. React. Kinet.*, *6*, 143–192, 1971.

Ross, A. B., W. G. Mallard, W. P. Helman, G. V. Buxton, R. E. Huie, and P. Neta, *NDRL-NIST Solution Kinetics Database: Ver. 3*, Notre Dame Radiat. Lab., Notre Dame, IN and NIST Stand. Ref. Data, Gaithersburg, MD, 1998.

Rudolph, J., R. Koppmann, and C. H. Plass-Dulmer, The budgets of ethane and tetrachloroethene: Is there evidence for an impact of reactions with chlorine atoms in the troposphere?, *Atmos. Environ.*, *30*, 1887–1894, 1996.

Ruiz-Ibanez, G., and O. C. Sandall, Kinetics for the reaction between chlorine and basic hydrogen peroxide, *Ind. Eng. Chem. Res.*, *30*, 1105–1110, 1991.

Ruiz-Ibanez, G., A. Bidarian, R. A. Davis, and O. C. Sandall, Solubility of oxygen and chlorine in aqueous hydrogen peroxide solutions, *J. Chem. Eng. Data*, *36*, 459–466, 1991.

Ruggaber, A., R. Dlugi, A. Bott, R. Forkell, H. Herrmann, and H.-W. Jacobi, Modeling of radiation quantities and photolysis frequencies in the aqueous phase in the troposphere, *Atmos. Environ.*, *31*, 3137–3150, 1997.

Sandall, O. C., I. B. Goldberg, S. C. Hurlock, H. O. Laeger, and R. I. Wagner, Solubility and rate of hydrolysis of chlorine in aqueous sodium hydroxide at 273 K, *AIChE J.*, *27*, 856–859, 1981.

Sander, R., Modeling atmospheric chemistry: Interactions between gas-phase species and liquid cloud/aerosol particles, *Surv. Geophys.*, *20*, 1–31, 1999.

Sander, R., and P. J. Crutzen, Model study indicating halogen activation and ozone destruction in polluted air masses transported to the sea, *J. Geophys. Res.*, *101*, 9121–9138, 1996.

Sander, S. P. et al., *Chemical Kinetics and Photochemical Data for Use in Stratospheric Modeling, Rep. 00-3*, Jet Propul. Lab., Pasadena, Calif., 2000.

Sauer, M. C., Jr., W. G. Brown, and E. J. Hart, $O(^3P)$ atom formation by the photolysis of hydrogen peroxide in alkaline aqueous solutions, *J. Phys. Chem.*, *88*, 1398–1400, 1984.

Schmidt, K. H., Electrical conductivity techniques for studying the kinetics of radiation-induced chemical reactions in aqueous solutions, *Int. J. Radiat. Phys. Chem.*, *4*, 439–468, 1972.

Schwartz, S. E., Gas- and aqueous-phase chemistry of HO_2 in liquid water clouds, *J. Geophys. Res.*, *89*, 11,589–11,598, 1984.

Schwartz, S. E., Mass-transport considerations pertinent to aqueous-phase reactions of gases in liquid-water clouds, in *Chemistry of Multiphase Atmospheric Systems, NATO ASI Series, Vol. G6*, edited by W. Jaeschke, Springer-Verlag, New York, 1986.

Schwartz, S. E., and J. E. Freiberg, Mass-transport limitation to the rate of reaction of gases in liquid droplets: Application to oxidation of SO_2 in aqueous solutions, *Atmos. Environ.*, *15*, 1129–1144, 1981.

Sehested, K., J. Holcman, and E. J. Hart, Rate constants and products of the reactions of e^-_{aq}, O_2^-, and H with ozone in aqueous solutions, *J. Phys. Chem.*, *87*, 1951–1954, 1983.

Sehested, K., J. Holcman, E. Bjergbakke, and E. J. Hart, Formation of ozone in the reaction of OH with O_3^- and the decay of the ozonide ion radical at pH 10–13, *J. Phys. Chem.*, *88*, 269–273, 1984a.

Sehested, K., J. Holcman, E. Bjergbakke, and E. J. Hart, A pulse radiolytic study of the reaction of OH + O_3 in aqueous medium, *J. Phys. Chem.*, *88*, 4144–4147, 1984b.

Sehested, K., H. Corfitzem, J. Holcman, C. H. Fisher, and E. J. Hart, The primary reaction of ozone in acidic solutions, *Environ. Sci. Technol.*, *25*, 1589–1598, 1991.

Sehested, K., H. Corfitzen, J. Holcman, and E. J. Hart, Decomposition of ozone in aqueous acetic acid solutions (pH 0–4), *J. Phys. Chem.*, *96*, 1005–1009, 1992.

Sehested, K., H. Corfitzen, J. Holcman, and E. J. Hart, On the mechanism of the decomposition of O_3 solutions, thermally or H_2O_2-initiated, *J. Phys. Chem. A*, *102*, 2667–2672, 1998.

Sevilla, M. D., S. Summerfield, I. Eliezer, J. Rak, and M. C. R. Symons, Interaction of the chlorine atom with water: ESR and ab initio MO evidence for three-electron ($\sigma^2\sigma^{*1}$) bonding, *J. Phys. Chem. A*, *101*, 2910–2915, 1997.

Sillén, G. H. and A. E. Martell, *Stability Constants of Metal–Ion Complexes*, Special Publication 17, Chem. Soc., London, 1964.

Singh, H. B., A. N. Thakur, Y. E. Chen, and M. Kanakidou, Tetrachloroethylene as an indicator of low Cl atom concentrations in the troposphere, *Geophys. Res. Lett.*, *23*, 1529–1532, 1996a.

Singh, H. B., et al., Low ozone in the marine boundary layer of the tropical Pacific Ocean: Photochemical loss, chlorine atoms, and entrainment, *J. Geophys. Res.*, *101*, 1907, 1996b.

Smith, R. M. and A. E. Martell, *Critical Stability Constants,* Vol. 4*, Inorganic Complexes*, Plenum, New York, 1976.

Spalding, C. W., Reaction kinetics in the absorption of chlorine into aqueous media, *AIChE J.*, *8*, 685–689, 1962.

Spicer, C. W., E. G. Chapman, B. J. Finlayson-Pitts, R. A. Plastridge, J. M. Hubbe, J. D. Fast, and C. M. Berkowitz, Unexpectedly high concentrations of molecular chlorine in coastal air, *Nature*, *394*, 353–356, 1998.

Storch, D. M., C. J. Dynek, and L. P. Davis, MNDO study of the mechan-

ism of $O_2(^1\Delta)$ formation by reaction of Cl_2 with basic H_2O_2, *J. Am. Chem. Soc.*, *105*, 1765–1769, 1983.

Swain, C. G., and C. B. Scott, Quantitative correlation of relative rates: Comparison of hydroxide ion with other nucleophilic reagents toward alkyl halides, esters, epoxides and acyl halides, *J. Am. Chem. Soc.*, *75*, 141–147, 1953.

Swain, C. G., and D. R. Crist, Mechanisms of chlorination by hypochlorous acid: The last of chlorinium ion, Cl^+, *J. Am. Chem. Soc.*, *94*, 3195–3200, 1972.

Swartz, E., J. Boniface, I. Tchertkov, O. Rattigan, D. V. Robinson, P. Davidovits, D. R. Worsnop, J. T. Jayne, and C. E. Kolb, Horizontal bubble train apparatus for heterogeneous chemistry studies: Uptake of gas-phase formaldehyde, *Environ. Sci. Technol.*, *31*, 2634–2641, 1997.

Takami, A., S. Kato, A. Shimono, and S. Koda, Uptake coefficient of OH radical on aqueous surface, *Chem. Phys.*, *231*, 215–227, 1998.

Volpe, C., M. Wahlen, A. A. P. Pszenny, and A. J. Spivack, Chlorine isotopic composition of marine aerosols: Implications for the release of reactive chlorine and HCl cycling rates, *Geophys. Res. Lett.*, *25*, 3831–3834, 1998.

Vogt, R., P. J. Crutzen, and R. Sander, A mechanism for halogen release from sea-salt aerosol in the remote boundary layer, *Nature*, *383*, 327–330, 1996.

Wagner, I., J. Karthäuser, and H. Strehlow, On the decay of the dichloride anion Cl_2^- in aqueous solution, *Ber. Bunsenges. Phys. Chem.*, *90*, 861–867, 1986.

Wang, T. X., and D. W. Margerum, Kinetics of reversible chlorine hydrolysis: Temperature dependence and general acid base-assisted mechanisms, *Inorg. Chem.*, *33*, 1050–1055, 1994.

Weinstein, J., and B. H. J. Bielski, Kinetics of the interaction of HO_2 and O_2^- radicals with hydrogen peroxide: The Haber–Weiss reaction, *J. Am. Chem. Soc.*, *101*, 58–62, 1979.

Weis, D. D., and G. E. Ewing, The reaction of nitrogen dioxide with sea salt aerosol, *J. Phys. Chem. A*, *103*, 4865–4873, 1999.

Whitfield, M., in *Chemical Oceanography*, edited by J. P. Riley and Skirrow, vol. 1, 2nd ed., Academic, San Diego, Calif., 1975.

Wilhelm, E., R. Battino, and R. J. Wilcock, Low-pressure solubility of gases in liquid water, *Chem. Rev.*, *77*, 219–262, 1977.

Wingenter, W. O., M. K. Kubo, N. J. Blake, T. W. Smith Jr., D. R. Blake, and F. S. Rowland, Hydrocarbon and halocarbon measurements as photochemical and dynamical indicators of atmospheric hydroxyl, atomic chlorine, and vertical mixing obtained during Lagrangian flights, *J. Geophys. Res.*, *101*, 4331–4340, 1996.

Wingenter, W. O., D. R. Blake, N. J. Blake, B. C. Sive, F. S. Rowland, E. Atlas, and F. Flocke, Tropospheric hydroxyl and atomic chlorine concentrations, and mixing timescales determined from hydrocarbon and halocarbon measurements made over the Southern Ocean, *J. Geophys. Res.*, *104*, 21,819–21,828, 1999.

Wofsy, S. C., M. J. Molina, R. J. Salawitch, L. E. Fox, and M. B. McElroy, Interactions between HCl, NO_x, and H_2O ice in the Antarctic stratosphere: Implications for ozone, *J. Geophys. Res.*, *93*, 2442–2450, 1988.

E. M. Knipping and D. Dabdub, Department of Mechanical and Aerospace Engineering, University of California at Irvine, 4200 Engineering Gateway, Irvine, CA 92697-3975, USA. (ddabdub@uci.edu; eknippin@uci.edu)